Hybrid Organic - Inorganic Polymer Electrolyte Membranes for Low to Medium Temperature Fuel Cells

Cordova Chavez, Miguel

DOI
10.4233/uuid:72824e9e-cb4e-4161-bd80-6a665b634739

Publication date
2017

Document Version
Final published version

Citation (APA)
Cordova Chavez, M. (2017). *Hybrid Organic - Inorganic Polymer Electrolyte Membranes for Low to Medium Temperature Fuel Cells*. [Dissertation (TU Delft), Delft University of Technology].
https://doi.org/10.4233/uuid:72824e9e-cb4e-4161-bd80-6a665b634739

Important note
To cite this publication, please use the final published version (if applicable).
Please check the document version above.

Hybrid Organic - Inorganic Polymer Electrolyte Membranes for Low to Medium Temperature Fuel Cells

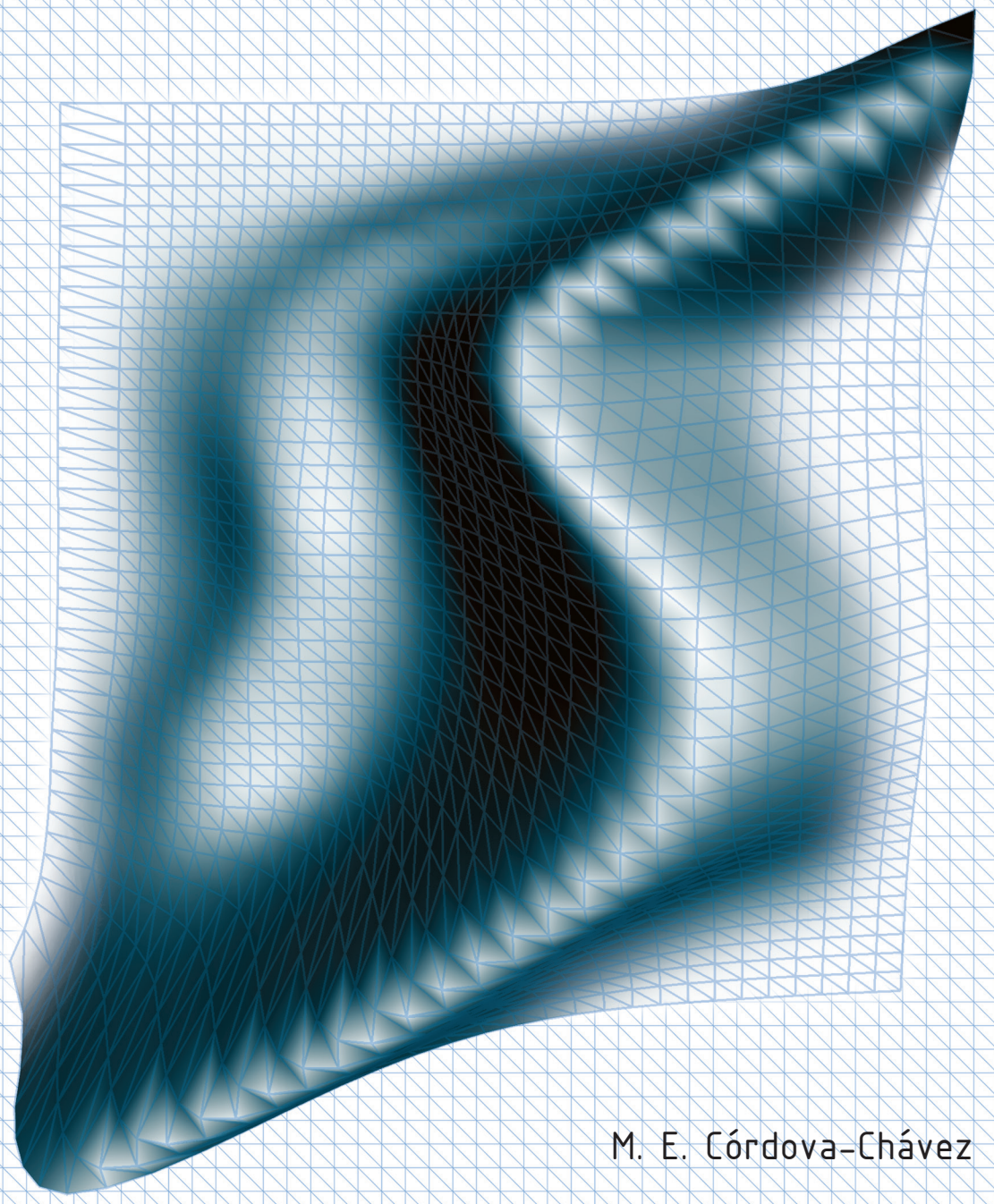

M. E. Córdova-Chávez

Hybrid Organic - Inorganic Polymer Electrolyte Membranes for Low to Medium Temperature Fuel Cells

Proefschrift

ter verkrijging van de graad van doctor
aan de Technische Universiteit Delft,
op gezag van de Rector Magnificus Prof. Ir. K.Ch.A.M. Luyben,
voorzitter van het College voor Promoties,
in het openbaar te verdedigen op donderdag 14 september 2017 om 10:00 uur

door

Miguel Ernesto Córdova-Chávez

Ingeniero de Materiales
Universidad Simón Bolívar
Magister en Ingeniería de Materiales
Universidad Simón Bolívar

geboren te Caracas, Venezuela

Dit proefschrift is goedgekeurd door de:

Promotor: Prof. dr. S. J. Pickens
Copromotor: Dr. ir. E. M. Kelder

Samenstelling promotiecomissie:

Rector Magnificus	voorzitter
Prof. dr. S. J. Pickens	Technische Universiteit Delft
Dr. ir. E. M. Kelder	Technische Universiteit Delft

Onafhankelijke leden:

Prof. dr. Theo Dingemans	University of North Carolina
Prof. dr. M.T.M. Koper	Universiteit Leiden
Prof. dr. E.J.R. Sudhölter	Technische Universiteit Delft
Prof. dr. F.M. Mulder	Technische Universiteit Delft
Dr. ing. G. J. M. Koper	Technische Universiteit Delft
Prof. dr. J.J. Smit	Technische Universiteit Delft, reservelid

Keywords: Fuel Cells, Electrolyte, sPEEK, Hybrid, BDS, Inner phase, Conductivity, $LiBPO_4$.

ISBN 978 94 028 0728 8

An electronic version of this dissertation is available at
http://repository.tudelft.nl

Hybrid Organic - Inorganic Polymer Electrolyte Membranes for Low to Medium Temperature Fuel Cells

Thesis

presented for the degree of doctor
at Delft University of Technology,
under the authority of the Vice-Chancellor, Prof. Ir. K.Ch.A.M. Luyben,
Chairman of the Board of Doctorates,
to be defended in public in the presence of a committee on
Thursday, September 14th, 2017 at 10:00 o'clock

by

Miguel Ernesto Córdova-Chávez

Bachelor Degree in Material Science
Universidad Simón Bolívar

Master in Material Engineering
Universidad Simón Bolívar

Born in Caracas, Venezuela

This thesis is approved by the promoters:

Supervisor: Prof. dr. S. J. Pickens
Copromotor: Dr. ir. E. M. Kelder

Composition of Examination Committee:

Rector Magnificus	Chairman
Prof. dr. S. J. Pickens	Technical University of Delft
Dr. ir. E. M. Kelder	Technical University of Delft

Independent Members:

Prof. dr. Theo Dingemans	University of North Carolina
Prof. dr. M.T.M. Koper	Leiden University
Prof. dr. E.J.R. Sudhölter	Technical University of Delft
Prof. dr. F.M. Mulder	Technical University of Delft
Dr. ing. G. J. M. Koper	Technical University of Delft
Prof. dr. J.J. Smit	Technical University of Delft, reserved

Keywords: Fuel Cells, Electrolyte, sPEEK, Hybrid, BDS, Inner phase, Conductivity, $LiBPO_4$.

ISBN 978 94 028 0728 8

An electronic version of this dissertation is available at
http://repository.tudelft.nl

“Here's to those who wish us well, and those who don't can go to hell.”

ELAINE BENES, Seinfeld

Table of Contents

Table of Figures

Table of Tables

Samenvatting

Ruwe olie, kolen en gas zijn momenteel de belangrijkste energiebronnen ter wereld. De World Energy Outlook beweerde in 2007 dat de belangrijkste bronnen van energie (ongeveer 84%) in 2030 nog steeds fossiele brandstoffen zijn. Indien deze voorspelling correct is, zullen de fossiele brandstofreserves van de wereld binnen enkele decennia worden verbruikt, waardoor het noodzakelijk is om een goede vervanging voor fossiele brandstoffen te hebben om in de toekomst in onze energiebehoeften te voorzien. Bovendien worden de milieueffecten van fossiele brandstoffen steeds duidelijker voor wetenschappers en overheden. Onder de bevolking groeit ook het milieubewustzijn, wat leidt tot een toename van de vraag naar energie die het milieu niet schaadt.

Brandstofcellen zijn een van de meest veelbelovende schone energietechnologieën om in de toekomst mogelijk de fossiele brandstoffen te kunnen vervangen. Ze werken als elektrochemische apparaten voor energieomzetting, vergelijkbaar met batterijen, maar behoeven niet opgeladen te worden, omdat ze gebruik maken van de aanwezigheid van brandstof om elektriciteit te blijven produceren. De meeste brandstofcellen zijn gebaseerd op het toevoegen van waterstof (anode) en zuurstof (kathode) waarbij water en elektriciteit geproduceerd worden en warmte vrijkomt. Dit proces heeft helaas enkele nadelen. De belangrijkste zijn de zeer hoge kosten, die worden veroorzaakt door het gebruik van het dure elektrolytmembraan en de katalysator.

Om de brandstofcellen verder te commercialiseren, moet het membraan verbeterd worden. Vorig onderzoek heeft aangetoond dat gesulfoneerde Poly (Ether Ether Ketone) polymeren kunnen worden gebruikt als elektrolyten voor Polymer Electrolyte Membrane Fuel Cells (PEMFC). Dit polymeer heeft een goede mechanische stabiliteit en kan water vasthouden boven 100 ° C. De membranen hebben echter een lage proton geleidbaarheid in vergelijking met Nafion® (commerciële standaard).

De PEM voor brandstofcellen moet de migratie van protonen van de ene kant van het membraan naar de andere zo efficiënt en zo snel mogelijk maken. Hierbij behandelen we het eerste sterke punt van ons onderzoek. In voorgaande onderzoeken is geen aandacht besteed aan de structuuropbouw van de binnenste fase van het membraan. In ons werk is bewezen dat het mogelijk is om de kanalen in dit membraan te ordenen. De hiervoor toegepaste procedure is gebaseerd op opeenvolgende thermische behandelingen, waardoor de kanalen in het membraan geordend worden en deze door Breedband Dielectrische Spectroscopie te volgen om dit proces zo to optimaliseren met als doel om te komen tot een optimale proton geleidbaarheid.

Ons tweede en laatste punt heeft betrekking op de manier waarop protonen mobiel zijn in dit systeem. In de meeste gevallen, zoals in sPEEK, wordt de migratie van protonen geacht plaats te vinden via de kanalen die door het water in het materiaal worden gecreëerd en door de zure zijgroepen in het polymeer worden aangedreven. Hierbij zijn essentieel de toename van water in het systeem, zonder de activiteit van de zure groepen die verantwoordelijk zijn voor de protonatie van het water te verminderen, en tevens de mechanische stabiliteit van het membraan. Deze feiten brachten onze aandacht op het gebruik van anorganische vulstoffen op de membraanmatrix als een manier om water of zure groepen te introduceren die helpen bij de protonmobiliteit. Drie nieuwe materialen werden geselecteerd op basis van de eerder genoemde eigenschappen: Lithium-base keramische materialen gebruikt voor batterij anode en elektrolyt, Gehydrateerde Zouten en Detonation Nano diamanten.

Tenslotte is ons voorstel voor een nieuwe hybride PEM om sPEEK te gebruiken, met medium/ hoge sulfonatie, als matrix gemengd met anorganische vulstoffen, om het water in de membranen te verhogen. Deze membranen gaan dan door een reeks thermische behandelingen die gericht zijn op het optimaliseren van de binnen-kanalen om de algemene geleidbaarheid te verbeteren. Het uiteindelijke doel was het bereiden van een hybride membraan met de eigenschappen om de protonen te geleiden op een vergelijkbaar niveau van Nafion® bij 100 ° C en ook om de factoren die de proton geleiding in pure en hybride PEM beïnvloeden verder te begrijpen.

De selectie van de sPEEK met een sulfoneringsgraad van 60% heeft plaatsgevonden op basis van meerdere gerapporteerde experimenten met name gepubliceerd voor graden van sulfonering die de mechanische stabiliteit van het membraan niet beïnvloeden. De capaciteit van de hierboven genoemde anorganische vulstoffen om water boven de drempel van 100 ° C op te nemen werd ook bevestigd door TGA en DSC metingen. Naar de kennis van de auteurs is er tot nu toe in de open literatuur geen publicatie aanwezig die dit belangrijke effect van deze morfologie in het membraan voor protonen geleiding beschrijft. We hebben een protocol gecreeerd die de kanalen in de gesulfoneerde clusters van sPEEK optimaliseert via thermische behandelingen van de membranen, gevolgd door DSC, EIS en BDS.

Door zijn capaciteit om het water boven 100 ° C vast te houden voor proton mobiliteit, constateerden we een hoge geleidbaarheid in ons hybride sPEEK/ $LiBPO_4$ membraan. Conductiviteiten zijn gemeten van 0,1 S/ cm bij 100 ° C en 80% R.H. (Nafion® toont een vergelijkbare waarde onder dezelfde omstandigheden). Een belangrijk voordeel van dit membraan is afhankelijk van het feit dat de productie van sPEEK en $LiBPO_4$ makkelijk naar commerciële productie kan worden opgeschaald tegen lage kosten.

We hebben aangetoond dat anorganische vulstoffen een duidelijk effect hebben op het gedrag van het materiaal. We laten dit zien via DSC en BDS. In onze studies hadden FeSO4 en DND geen effect op de geleidbaarheid, echter $LiBPO_4$ was succesvol en een voorbeeld van hoe het geaggregeerde water en de deeltjesinteracties met de matrix een grote invloed hebben op de geleidbaarheid.

Als onze algemene conclusie willen we postuleren de drie belangrijkste factoren die de proton geleidbaarheid in een PEM beïnvloeden:

• De volgorde in de binnenste fase van het membraan, welke moet worden geoptimaliseerd

• Het water in het membraan, dat moet voldoende zijn

• De zuurgroepen in het polymeer, die het water moeten kunnen protoneren en het een snel medium maken om de positieve ladingen te verplaatsen.

Deze drie hoofdfactoren moeten worden afgestemd op elk specifiek membraan dat gebruikt wordt voor PEMFC.

Met deze research geven we een voorstel voor een beproefd mechanisme om deze drie factoren aan te pakken en hoe deze kunnen worden geoptimaliseerd.

Summary

Crude oil, coal and gas are currently the main resources of energy in the world. The World Energy Outlook claimed in 2007 that the major source of energy (about 84%) would still be generated from fossil fuels in 2030. By these projections, the world's fossil fuel reserves will be consumed within a few decades, making it necessary to have a well stablished replacement for fossil fuels to fulfil our energy demands. Furthermore, the environmental impacts of fossil fuels are becoming clearer to scientists and governments. Among the population, environmental awareness is increasing as well, which leads to an increase in the demand for energy that does not harm the environment.

Fuel Cells are one of the most promising clean energy technologies, which are in clear consideration to replace fossil fuels in the future. They work as electrochemical energy conversion devices, similar to batteries, but do not require the recharging process, since they just depend on the presence of fuel to keep producing electricity. In most fuel cells, hydrogen is supplied to the anode and oxygen to the cathode, which results in production of water, heat and what is the most important, electricity. Unfortunately, several drawbacks with fuel cells have been identified. Probably the most important one is the very high cost, which is caused by use of the expensive electrolyte membrane and the catalyst.

As a way to further commercialise the fuel cells, the membrane needs to be improved. Previous research has indicated that sulfonated Poly (Ether Ether Ketone) polymers can be used as electrolytes for Polymer Electrolyte Membrane Fuel Cell's (PEMFC). This polymer has a good mechanical stability and partially retains water over 100°C. However, the membranes have a low proton conductivity in comparison to Nafion® (commercial standard).

The PEM for fuel cells needs to allow migration of protons from one side of the membrane to the other as efficient and fast as possible. Here we address the first strong point of our investigation. Generally, the structural order of the inner phase of the membrane has been overseen. In our work, it is proven that is possible, through a procedure of successive thermal treatments, to give order to these channels in the membrane, to follow this order by Broadband Dielectric Spectroscopy and to find the optimal for proton conductivity.

Our second and final point refers to the means of proton mobility. In most cases, as for example in sPEEK , the migration of protons are believed to happen through the channels that are created in the material by the water and driven by the acidic side groups in the polymer. In this sense, the increase of water in the system without diminish the acidic groups responsible of the protonation of the water or compromising the mechanical stability of it is essential. These facts brought our attention to the use of Inorganic fillers on the membrane matrix as a way to introduce water or acidic groups that helps with the proton mobility. Three novel materials were selected based on the properties mention before: Lithium-base ceramic materials used for battery anode and electrolyte, Hydrated Salts and Detonation Nano diamonds.

Finally, our proposal for a new hybrid PEM is to use sPEEK, with medium/high sulfonation, as a matrix mixed with Inorganic fillers, to increase the water in the membranes. These membranes will then go through a set of thermal treatments that will aim to optimize the inner channels to improve the overall conductivity. The final goal was to prepare a hybrid membrane capable of conduct protons at similar values of Nafion® at 100°C and also to further understand the factors that affect the proton conduction in pure and hybrid PEM.

The selection of the sPEEK with a 60% sulfonation degree was done based on multiple reported experiments published for degrees of sulfonation that will not affect the mechanical stability of the membrane. The capacity of the inorganic fillers, mentioned above, to take up water above the threshold of 100°C was also confirmed by TGA and DSC measurements.

To the knowledge of the authors, no publication had address the existence of this inner morphology, which can have a striking effects in the capacity of the membrane for proton conductivity. We created a protocol that optimizes the channels in the sulfonated clusters of sPEEK via thermal treatments of the membranes followed by DSC, EIS and BDS.

Because of its capacity to maintain the water above 100°C and its availability for proton's movement, we found high conductivity in our hybrid sPEEK/$LiBPO_4$ membrane. Conductivities of 0.1 S/cm at 100ºC and 80% R.H. (Nafion® shows a similar value under the same conditions) were measured. A major advantage of this membrane relies on the fact that the production of sPEEK and $LiBPO_4$ can be easily escalated to commercial production at a low cost.

We demonstrated that inorganic fillers have a clear effect on the behavior of the material. We showed this through DSC and BDS. For our studies, we used $FeSO_4$ and DND failure to increase conductivity and, $LiBPO_4$ success, as examples of how the aggregated water and the particles interactions with the matrix have a major effect on the conductivity.

As our global conclusion, we would like to state the three main factors we found to be affecting the proton conductivity in a PEM:

- The order in the inner phase of the membrane, that needs to be optimized
- The water in the membrane, that needs to be sufficient
- The acidic groups in the polymer, that need to be able to protonate the water and make it a fast medium to move the positive charges.

These three main factors need to be tuned for every specific membrane that wants to be used for PEMFC. We propose and prove mechanisms in this research to tackle these three factors and address how to optimize them.

Chapter 1 Introduction

Currently, there is an increasing need for more environmentally friendly energy sources and conversion systems. This chapter describes several options and explains how fuel cells have developed as a useful portable source of energy. Finally, the chapter concludes with a proposal on how to improve the electrolyte of Polymer Electrolyte Membranes Fuel Cells (PEMFC). It is proposed to optimize the PEM by using sulfonated Poly (Ether Ether Ketone) (sPEEK) as a matrix, filled with inorganic compounds, which are able to store water molecules above 100°C. Using this hybrid membrane, after an optimization of the inner structure by a thermal treatment, the proton conduction at 100°C is expected to reach values close to other commercial PEM, like Nafion®.

1.1. Introduction

Most parts of the world have become completely dependent on the availability of energy. Not only is energy necessary for travelling, charging a mobile phone or using a computer, recent studies in Europe, for example, have also shown that there is a relationship between energy consumption and economic growth.[1, 2] While most countries in Europe are trying to restore their economic growth in this times of recession, upcoming economies in Africa and China are growing with a steady annual rate of around 10%.[3] With more economies growing, the world is heading for a form of globalisation that will lead to an increase in prosperity.[4] However, this is also accompanied by an increase of the energy consumption in the next decades.

1.1.1. Energy needs and challenges overview

Crude oil, coal and gas are currently the main resources of energy in the world. The World Energy Outlook claimed already in 2007 that the major source of energy (about 84%) will still be generated from fossil fuels in 2030. Another recent study showed that the fossil fuel time depletion is calculated to be around 35, 107 and 37 years for oil, coal and gas respectively.[5] By these projections, it seems like the world could depend on fossil fuels till 2030, while some (of them) will be depleted around 2050. Nevertheless, the world's fossil fuel reserves will be consumed within a few decades, making it necessary to have a well-established replacement for fossil fuels to fulfil our energy demands.

Furthermore, the environmental impacts of fossil fuels are becoming clearer to scientists and governments. Among the population, environmental awareness is increasing as well, which leads to an increase in the demand for energy that does not harm the environment. Fossil fuels, unfortunately, do not meet the environmental standards that people are looking for nowadays and in the future. For example, combustion of fossil fuels releases CO_2 in the air. This greenhouse gas is considered as one of the reasons for climate change and has far exceeded its global limits.[6]

The above picture indicates that it is necessary to look for a source of energy that does not pollute the environment, will not be depleted in the near future and can provide the increasing demand of energy in the future.

In order to be able to achieve solutions to the environmental problems that we are facing, a long term commitment to become more conscious and efficient energy consumers needed to be reached. An important bridge in the transition to renewable energies is a more rational use of energy. The renewable energy sources usually are scattered geographically which creates a problem on their ability of matching the demands on highly populated areas. In that regard, northern European countries are characterized by an average annual solar irradiance of 150 W/m^2 which could be transformed in 20 W/m^2 taking the mean power production from a photovoltaic component at 13% conversion efficiency. For an average wind speed of 5 m/s, a micro wind turbine will produce energy at a similar order of magnitude. Now, if you take in account that a typical office building in the UK will have a demand in the order of 300 kWh/m^2 per year, this then translates into approximately 50 W/m^2 of facade, which will mean twice as much as the available renewable energies. [7] This clearly shows that there is not only a need for clean renewable energy sources, but also a need to adjust the consumption demand in order to introduce this type of energy technologies.

1.1.2. Fuel cells appearance

Fuel Cell are one of the most promising clean energy technologies which are in clear consideration to replace fossil fuels in the future. They work as an electrochemical energy conversion device, similar to batteries, but do not require the recharging process, since they only depend on the presence of fuel to keep producing electricity. In most fuel cells, hydrogen is supplied to the anode and oxygen to the cathode which results in production of water, heat and what is the most important, electricity. They have many attractive features, including high power density, rapid start-up and high efficiency, they are environmentally friendly, silent during work, (rather) safe and do not have any moving parts. It is important to realise that a single fuel cell unit can only produce a limited amount

of energy so they need to be assembled in stacks. Depending on the electrolyte used, the function of which is to separate the anode from the cathode while allowwing the proton transportation, different types of fuel cells operating under different process conditions can be identified.

The first commercial use of fuel cells was in the NASA space programs to generate power for probes, satellites and space capsules. Since then, fuel cells have been used in many other applications. Fuel cells are used for primary as well as backup power in commercial, industrial and residential buildings and in remote or inaccessible areas. They are also used to power fuel cell vehicles, including automobiles, buses, forklift trucks, airplanes, boats, motorcycles and submarines. [8]

Unfortunately several drawbacks with fuel cells have been identified, which have to be solved. Probably the most important one is very high cost which is caused by use of the expensive electrolyte membrane and the very expensive catalyst. Although many researchers are working on new polymer electrolyte membranes, the price is still very high (~800-1000 USD/m^2). By comparison, the price of the electrolyte for Li-ion batteries is around 300-500 USD/m^2.

1.1.3. The Present Approach to make sPEEK hybrid Membranes a market competitor

At the moment, Nafion® is the most common used membrane, even with the drawback that it is expensive to produce. As a way to further commercialise the fuel cells, the membrane has to be improved. This improvement can be achieved by fabricating an electrolyte of a different material that can work at higher temperatures (above 100°C) and be produced at low costs. Furthermore, membranes that work at higher temperatures have substantial reduction of CO poisoning of the catalyst at the electrodes, a higher efficiency, and a higher proton conductivity. Previous research has indicated that sulfonated sPEEK polymers can be used as electrolytes for PEMFC's. This polymer has a good mechanical stability and partially retains water over 100°C. However, sPEEK membranes have a low proton conductivity in comparison to Nafion®.

The PEM for fuel cells needs to allow migration of protons from one side of the membrane to the other as efficient and fast as possible. Here we address the first main point of our investigation. Generally, the internal structural order of the membrane has been overlooked. It is partially because of the membrane's internal structure that the protons can move easily from one side to the other. The optimisation of the percolation and orientation of the so-called water channels is important in order to maximize the proton conductivity. In our work, it is proven that it is possible, through a procedure of successive thermal treatments, to give order to these channels in the membrane, to monitor this order using Broadband Dielectric Spectroscopy, and to find the optimum treatment for proton conductivity.

Our second and final main point refers to the mechanisms allowing proton mobility. In most cases, as for example in sPEEK, the migration of protons is believed to happen through the channels that are created in the material by the water and which is assisted by the acidic side groups in the polymer. In this context, there are several possibilities acknowledged to increase the proton conductivity of sPEEK. Most of them are related to the increase of water in the system without diminishing the number of acidic groups responsible of the protonation of the water. For example, covalent or physical crosslinking of high sulfonated membranes has been proposed: crosslinking or blends of sPEEK and other simple polymers has been reported to provide have better conductivity and stability. [9] [10] Other studied paths are related to the increase in the water content and retention of it in the membrane without compromising the mechanical stability of the polymer. This brings to attention the use of Inorganic fillers in the membrane matrix as a way to introduce water or acidic groups that help with the proton mobility. This last idea caught our attention and in the next section we discuss what has been done in the literature on the topic of inorganic fillers.

1.1.4. The use of sPEEK with inorganic fillers

The possibility of preparing composite membranes containing inorganic fillers dispersed in the organic polymer network will be presented as an approach

to enhance the proton conductivity through the increase in liquid water in the membrane.

The hydration state of a polymer is a crucial factor for their electrochemical performance. Adding inorganic fillers in the polymer network allows fast retention of adsorbed water, or absorbed water on the filler and thereby leads to interesting new properties. [9]

A few examples of inorganic fillers that lead to hybrid polymers are given below with a brief description:

1. sPEEK with Silica particles [9]
    - sPEEK reacts with $SiCl_4$ to form Si-sPEEK.
    - Inorganic component is covalently linked to the organic sPEEK.
    - Good thermal stability and enhanced water uptake results in good electrochemical characteristics.
2. sPEEK with BPO_4 [11]
    - BPO_4 fine powder is incorporated in partly sulfonated PEEK.
    - Conductivity of the membrane increased, but did not increase as much as predicted by the theory.
3. sPEEK with sulfonated Silica [12]
    - Sulfonated silica's are used as fillers for the sPEEK membrane
    - The membrane prepared using silica with sulfonated Hydroxytelechelic containing 1,3,4-oxadiazole units, showed an increase in conductivity at temperatures between 40°C and 140°C compared to a pure sPEEK membrane.
4. sPEEK with silica sulphuric acid (SSA) nanoparticles [13]

- SSA was obtained by treating SiO_2 nanoparticles with SO_2Cl_2
- SiO_2 has good organic compatibility and can therefore be dispersed in the organic matrix of sPEEK more uniformly.
- Water retention ability and conductivity of the SSA-sPEEK membrane improved compared to pure sPEEK.

5. sPEEK with a Zirconia-supported Pt Catalyst (Pt-SZ) [14]
    - The SZ particle is a solid-state acid with a high proton conductivity.
    - Pt-SZ catalyst with 2% Pt was synthesised by impregnation of sulfonated zirconia with an H_2PtCl_6 solution (solution-casting method).
    - Conductivity of membrane increased, because of the acid property of Pt-SZ particles and its assistance effect on proton transfer by bridging between clusters.

With the knowledge of the membranes mentioned above, we focus on finding an inorganic filler able to increase the water content in the membrane, while also enhancing the mechanical, and gas permeation properties of the matrix.

Our goal was to prepare a hybrid membrane, with sPEEK with a medium/high level of sulfonation as the matrix, which could be able to reach, at least, the same proton conductivity as Nafion®. We wanted this conductivity to remain at least at 100°C which, as it has been explained before, allows us to get rid of water overflow in the cell, preventing the poisoning of the platinum particles, among other advantages. We looked for materials that were able to bond with water and hold it at temperatures above 100°C. Three novel materials were selected: Lithium-based ceramic materials that are normally used for Li-ion battery anodes and electrolytes, Hydrated Salts and Detonation Nano Diamonds.

1.1.5. Lithium-doped BPO_4: ceramic materials $Li_{3x}B_{1-x}PO_4$

$Li_{3x}B_{1-x}PO_4$ is a white, inexpensive ion conducting solid electrolyte initially suggested as solid electrolyte for lithium ion batteries. It can be synthesized using

a very simple method from easily available precursor compounds. Moreover, BPO_4 is known as an analogue of quartz (SiO_2) (see figure 1.1). That is why it is assumed that it shows silica-gel properties, hence, keeping the water in its structure. It is also hygroscopic which results in formation of hydrates. When Li^+ are introduced to the BPO_4 structure, more water can be adsorbed, and this water can only be released from the structure above 200°C.[15]

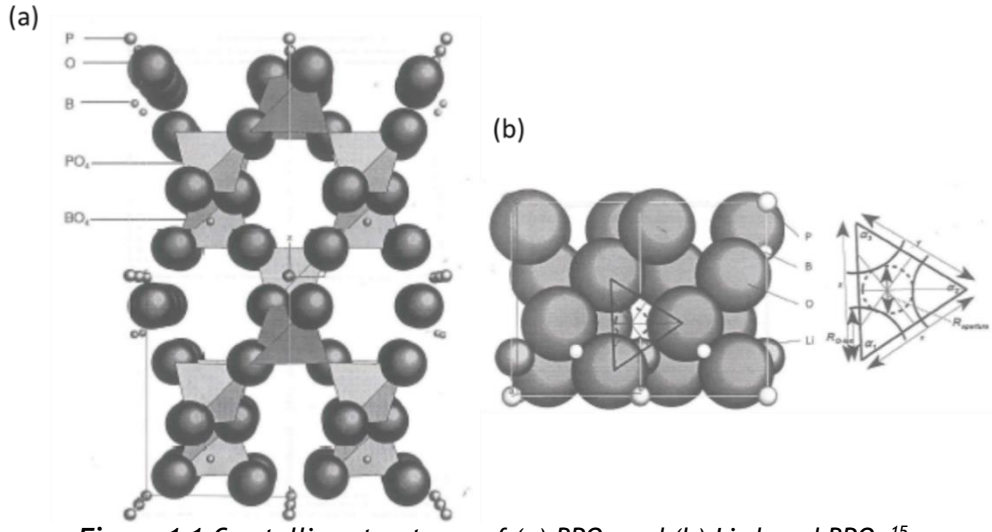

Figure 1.1 *Crystalline structures of (a) BPO_4 and (b) Li-doped BPO_4.*[15]

1.1.6. Hydrated Salts: $FeSO_4$. $7H_2O$

Hydrated Salts are inorganic compound that are able to bond water molecules in their crystalline state, incorporating the water molecules into its structure (see figure 1.2). This crystalline water is quite well bonded to the salts, and as a consequence, the energy needed to remove the water into the gas phase is higher, causing the dehydration process to occur at temperatures well above 100°C. Iron (II) sulphate hepta-hydrate ($FeSO_4.7H_2O$) is an example of this type of salt-hydrate. It is a blue-green, crystalline solid, under normal conditions of temperature and pressure. It is generated as a by-product of the pickling of steel or as a by-product during manufacturing of titanium dioxide (TiO_2). For this reason it is a very inexpensive compound.

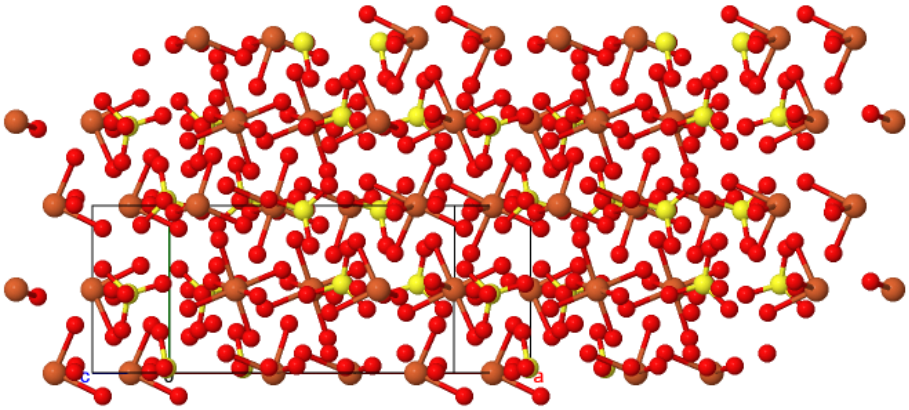

Figure 1.2 *Crystalline structure of $FeSO_4$ x $7H_2O$.*[16]

1.1.7. Nano Diamonds Prepared by Detonation (DND)

This particular material was obtained from an oxygen deficient explosive mixture of TNT/RDF. [17] The Nano diamonds obtained by this method differs from the typically obtained nano diamonds. Even though the size obtained is between 4-6 nm, the powder is a mix of aggregates (100 nm measures by Dynamic Light Scattering) of diamonds, raw carbon and impurities (N, O, H) with different reactive groups on the surface (see figure 1.3). [17] These surface groups are able to retain the water inside the polymer matrix.

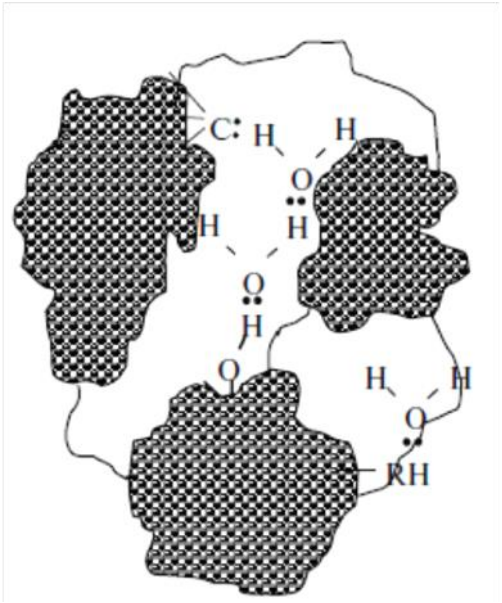

Figure 1.3 *Structures developed by detonation Nano Diamonds.*[17]

The introduction of Inorganic fillers in a polymer matrix has been proven to be a path to increase the proton conductivity as it was show before. Nevertheless, it is important to notice that, even though it is clear that there is an increase in the water content of the membrane, the mechanism, by which the inorganic particles increase the proton conductivity in the membranes, is still not fully understood. We will use characterization techniques for polymers in our research, that are capable of elucidate the interactions between the particles and the matrix by examining the interfaces, as a way to understand better the role of the inorganic filler as an enhancer of the proton conduction.

Finally, our proposal for a new hybrid PEM is to use sPEEK, with medium/high sulfonation, as the polymer matrix mixed with the inorganic fillers, like Hydrated Salts, DND and $LIBPO_4$, so as to keep the water content in the membranes. These membranes will then go through a set of thermal treatments that will aim to optimize the structure of the internal water channels, where the water will be located under hydrated conditions, so as to improve the overall proton conductivity. The final goal is to prepare a hybrid membrane capable of conducting protons at similar values of Nafion®, at 100°C and also to further understand the factors that affect the proton conduction in pure and hybrid PEM.

1.2. Dissertation Overview

The main objective of our research is focus on the development of new polymer electrolytes. The new PEM should be able to have a conductivity similar to the ones shown by the commercial membranes, at least up to 100°C under a standard relative humidity. Finally, it should also be viable in principle to make our materials at a commercial level, thereby reducing the cost of the PEM.

Our specific objectives then are focussing on studying the inner structure of the sPEEK membranes; see how they can influence the proton conductivity of the membrane, for instance by affecting the structure of the water channels that are

required for the protons to move from one side of the membrane to the other efficiently.

In addition, as way to improve the conductivity of the membrane at temperatures above 100°C, we are introducing selected inorganic fillers in the matrix of sPEEK, in order to increase the water content and trap the water in the membrane at high temperatures. In this way, water will be available for the protons to move and the conductivity should increase.

For the chapters to come, in chapter 2 we will discuss the theoretical background of our research. There are many studies on the potential of sPEEK for proton mobility, and on the use of inorganic fillers as a way to increase the properties of the PEM by enhancing the mechanical properties, conductivity and permeability to gases.

In chapter 3, we focus on the methodologies we followed for the preparation of the polymer and two of the fillers we used, that we had to synthetize beforehand. We go through the sulfonation procedure used and the characterization done on the membrane to ensure the required degree of sulfonation and stability. We explain the methodology used for the preparation of the membranes. We also address the multiple set ups created and used to try to measure the conductivity of the membrane, under ideal conditions, with stable values, and discuss the final setup selected. We also provide an overview of all the used characterization techniques.

Chapter 4 explains the way we found to optimize the membranes, through thermal treatments, and how we were able to follow the optimization process by investigating the changes in the internal structure by BDS. We present a model for the clusters of sulfonic groups in the sPEEK, and how the treatment creates alignment in the channels, making them more efficient for proton mobility.

Chapter 5 focuses on the preparation of the sPEEK 60% with $LiBPO_4$ as an inorganic filler, how the amount of inorganic filler was selected and how, through the thermal treatment, we were able to optimize the membrane for ideal proton

conduction. It also presents a model of the clusters including the inorganic filler in the structure.

Chapter 6 present the results for the other inorganic fillers used, $FeSO_4.7H_2O$ and DND, which were intended to increase the water in the membranes but after optimizations via thermal treatments were not successful in achieving a good conductivity. In some cases, they even decrease the capacity of the sPEEK to transport protons.

Chapter 7 finally focuses on explaining, based on the results of DSC and BDS, how the inorganic particles used in this study interact with the sPEEK, how this interaction can actually affect the conductivity and, based on these results, what are the parameters that need to be taken in account when we think of designing a new PEM with inorganic fillers.

Chapter 8 is a compilation of all the various conclusions from the previous chapters and, based on these conclusions, suggestions are made on the possible paths to follow next in the research of hybrid PEMs for medium temperature fuel-cells.

1.3. Bibliography

1 Pirlogea, C. & Cicea, C. Econometric perspective of the energy consumption and economic growth relation in European Union. *Renewable and Sustainable Energy Reviews* **16**, 5718-5726 (2012).

2 Acaravci, A. & Ozturk, I. On the relationship between energy consumption, CO_2 emissions and economic growth in Europe. *Energy* **35**, 5412-5420 (2010).

3 Group, T. W. B. (ed The World Bank Group).

4 McCloskey, D. *The Bourgeois Virtues: ethics in an age of commerce*. (University of Chicago Press, 2007).

5 Shafiee, S. & Topal, E. When will fossil fuel reserves be diminished? *Energy Policy* **37**, 181-189 (2009).

6 Röckstrom, J. A safe operating space for humanity. *Nature* **461**, 472-475 (2009).

7 Falkners, H. The UK Energy Efficiency Best Practice Program Lessons Learned *Energy Efficiency Improvements in Electronic Motors and Drives*, 483-497 (2000).

8 Basu, S. *Recent Trends in Fuel Cell Science and Technology*. First Ed. edn, (Springer, 2007).
9 Di Vona, M., Marani, D., Epifanio, A., Traversa, E., Trombetta, M., Licoccia, S. A covalent organic/inorganic hybrid proton exchange polymeric membrane: synthesis and characterization. *Polymer* **46**, 1754-1758 (2005).
10 Şengül, E. *et al*. Effects of sulfonated polyether-etherketone (SPEEK) and composite membranes on the proton exchange membrane fuel cell (PEMFC) performance *International Journal of Hydrogen Energy* **34**, 4645 - 4652 (2009).
11 Mikhailenko, S., Zaidi, M. & Kaliaguine, S. Sulfonated polyether ether ketone based composite polymer electrolyte membranes. *Catal. Today* **67**, 225-236 (2001).
12 Gomes, D., Buder, I. & Nunes, S. Novel proton conductive membranes containing sulfonated silica. *Desalination* **199**, 274-276 (2006).
13 Du, L., Yan, X., He, G., Wu, X., Hu, Z. & Wang, Y. . SPEEK proton exchange membranes modified with silica sulfuric acid nanoparticles. *Int. J. Hydrogen Energ.* **37**, 11853-11861 (2012).
14 Zhang, Y., Zhang, H., Zhu, X. & Bi, C. . Promotion of PEM Self-Humidifying Effect by Nanometer-Sized Sulfated Zirconia-Supported Pt Catalyst Hybrid with Sulfonated Poly(Ether Ether Ketone). *J. Phys. Chem.* **111**, 6391-6399 (2007).
15 Jak, M. J. G. *Dynamic Compactation of Li-ion Battery Components and Batteries* PhD thesis, TUDelft, (1999).
16 Villars, P. *FeSO4·7H2O (Fe[SO4][H2O]7) Crystal Structure*, <http://materials.springer.com/isp/crystallographic/docs/sd_1713271> (2014).
17 Dolmatov, V. Polymer-Diamond Composites based on Detonation NanoDiamonds. Part 1. *J. SuperHard Mater.* **29**, 1-11 (2007).

Chapter 2 Literature Review

In this chapter, an introduction of different available energies, the different type of fuel cells and how they worked is presented. The reactions occurring at the cathode and anode will be addressed. Nafion as the main commercial electrolyte material used in fuel cells and the importance of sPEEK in the research as a serious competitor for Nafion. In that respect, will be discussed an inside on the proton conduction mechanism is explained.

2.1. Theoretical Background

There is a series of technologies in the market presented as potential green sources of energy. They cover different ranges of applications from main power sources

for cities to portable devices. A small review on these different energy options is reviewed in the next section.

2.1.1. Types of green energy sources

Different types of green energy technologies has been investigated and develop in the world, most of them targeting mass power generation, in order to be able to satisfy the needs of the mayor cities. In that regard, 40% of the energy consumption of the world is taken by buildings, the rest is spread between industries, public uses, houses and mobility.[1] Among the most develop renewable energy the following can be named:

- **Nuclear Power**: the principle behind is based on a controlled fission reaction, the heat from this reaction is used to heat up water and move a turbine that generates electricity. The issues associated with this process is related to the complex system, needed to be running, to keep the reaction constant and the temperature and pressure stable to avoid any possible problems. Although is a clean source of energy, since its by-product doesn't contribute to pollute the air or damage the ozone layer, the risk related to this type of energy are high, catastrophes like what happened in Fukushima in 2011 could lead to a contamination beyond manageable.
- **Hydroelectric Power**: is based on water stored at high levels and controlled flow of this water downstream, where it takes advantage of gravity and the natural water circle. This flow of water will move turbines and thus produce electricity. Is a very clean and efficient source of energy but it requires a huge water source, and a basin for water storage. Hence, it is necessary to build dams, which may have an environmental impact on the region and the communities that lives around.
- **Wind Power**: It takes advantage of the currents of air generated by temperature difference in the atmosphere. It harvest this wind by the use of turbines that can be used to lift water or produce electricity. It's a growing green energy but it needs significant amount of space to generate adequate amounts of energy.

- **Solar Power**: the energy source is the sun and there are different methods developed to take advantage of this kind of energy. It ranges from heating water to directly convert solar energy to electricity by photovoltaic cells. It is accessible for everybody and it can be installed everywhere. The downside relies on the fact that you need a certain amount of sun to generate a proper level of energy, which depends of the position on the globe and the weather conditions. The low efficiency that exist in the conversion of energy, which is around 12-15%, it is already attractive and with the new generation of cells this will be increased to even 30%.
- **Biomass**: is the name given to taking energy from plants and organic material. The use of wood for heat and cooking is considered biomass power but it has an impact on environment. The new approach taken to this energy is conversion of organic waste in methane generation or in methanol for fuelling cars or electric power plants.
- **Geothermal Energy**: It is based on the use of the remaining heat on the soil. The gradient of temperature in the surface of the earth is relatively constant, taking the year average, and this could be used with heat pump to heat up buildings in winter and to cool them down in summer days. The production of electricity from this source is not viable.
- **Hydrokinetic Energy**: it is harnessed from the kinetic energy of water, like tides, waves and currents, to produce electrical energy. This technology is not completely developed but it projects as an important future clean energy source. The prototypes to transform waves and currents in a electrical energy are based on turbines and piston-like elements.
- **Hydrogen and Fuel Cells**: Hydrogen is not considered a renewable energy resource but it's very abundant, available, and creates a very low pollution when it's used as a fuel. It could be burned, in most cases as fuel for vehicles, with water as the only by-product of the combustion or it could be used as a fuel for Fuel Cells to power electric motors, which also produce water as a product from the reaction. The main problems to overcome from this technology are based on cost. The cost of hydrogen production, the

storage and also the cost of the fuel cells. Research has been done in all areas and the panorama can change drastically with the new developments for hydrogen storage, fuel cells technology and hydrogen production by other renewable energies like solar cells.

2.1.2. Fuel Cells

Figure 2.1 gives an overview of how a fuel cell works. There are different kinds of fuel cells that will be discussed later on this chapter, but the general working method of all the fuel cells is the same. Hydrogen gas (H_2) enters at the anode and is split at the electrode into positive hydrogen ions (H^+) and negatively charged electrons (e^-). The electrons are drawn from the anode to the cathode through an external circuit to produce electricity. The hydrogen ions pass through an electrolyte and will subsequently combine with oxygen (O_2) to form water vapor (H_2O).

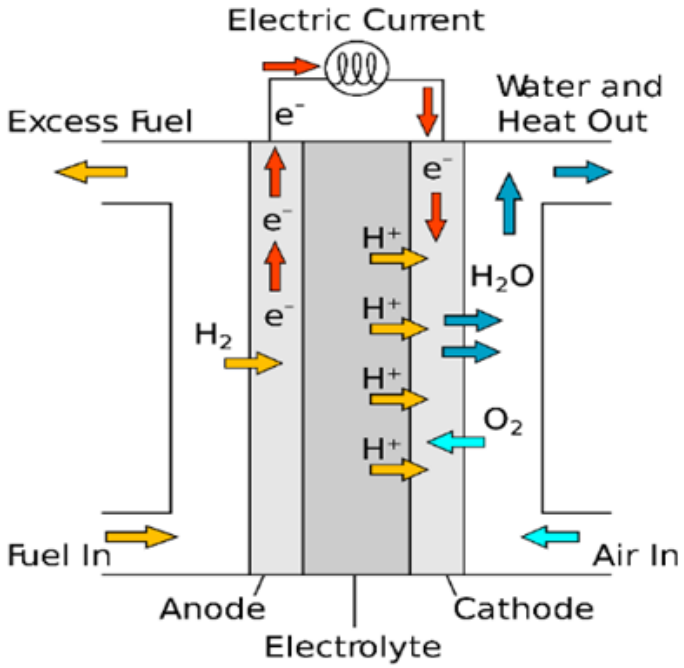

Figure 2.1. Scheme of a Fuel Cell working principle of a single cell, the electrolyte can be made of a Polymeric or Ceramic material depending on the working temperatures.

The following chemical reactions take place in a fuel cell:

Anode reaction:

$$H_2 \rightarrow 2H^+ + 2e^- \qquad \textit{Equation 2.1}$$

Cathode reaction:

$$\frac{1}{2}O_2 + 2H^+ + e^- \rightarrow H_2O \qquad \textit{Equation 2.2}$$

Overall Reaction:

$$H_2 + \frac{1}{2}O_2 \rightarrow H_2O \qquad \textit{Equation 2.3}$$

Hydrogen gas is not likely to be added in a pure form, since it comes from gasification of natural gas or wood (as shown in reactions equations 2.4 and 2.5 respectably). In both cases, CO is created as an extra product and therefore there will be a small fraction of CO in the hydrogen gas added as fuel to the fuel cell. In the case of Polymer Electrolyte Fuel Cells due to a better efficiency and CO tolerance of the platinum catalyst, the temperatures required in the fuel cell must be high, meaning at least above 80°C. [2]

H_2 from natural gas:

$$CH_4 + xO_2 \rightarrow yCO + zH_2 \qquad \textit{Equation 2.4}$$

H_2 from wood:

$$CH_{1.4}O_{0.6} + xO_2 \rightarrow yCO + zH_2 \qquad \textit{Equation 2.5}$$

There are, of course, some technical obstacles that hinder the widespread replacement of fossil fuels by FC's. These obstacles include inadequate water and heat management, the intolerance to impurities such as CO, sluggish electrochemical cathode kinetics, and their high cost. So there is a strong need to enhance the performance of current fuel cells, before it can replace fossil fuels. [3, 2]

Another important obstacle has been the hydrogen storage issue when using hydrogen based FCs. This has an especial repercussions on mobile applications. Because of its low boiling point (20.39K = -252.76°C), liquid hydrogen has to be stored in cryogenic tanks. A liquefaction process creates a large energy loss in order to cool down to very low temperature. Moreover, those tanks have to be isolated to prevent rising the temperature. This then requires additional cost. Hydrogen can also be stored as a gas, but because of its low density (0.08376 kg/m^3) [4] at ambient temperature it has to be stored in pressure cylinders. The biggest problem with compressed hydrogen is the big volume and weight of the tank. There are some other methods for hydrogen storage such as metal hydrides, organic chemical hydrides, carbon materials and silica microspheres. [4] Unfortunately, none of these methods are without problems.

2.1.3. Types of fuel cells

Different types of fuel cells can be classified based on the type of the electrolyte they use and the different application they are used for (see ***Table 2.1***). The six most common fuel cells types are:

- Alkaline Fuel Cells (AFCs)
- Phosphoric Acid Fuel Cells (PAFC)
- Molten carbonate fuel cells (MCFCs)
- Solid oxide fuel cells (SOFCs)
- Polymer Electrolyte Membrane Fuel Cells (PEMFCs)
- Direct Methanol Fuel Cells (DMFCs)

- **Alkaline fuel cells** use a solution of potassium hydroxide (KOH) in water soaked in a matrix as the electrolyte and can use multiple non-precious metals (e.g., Ni, Ag, metal oxides, spinels, and noble metals). [5] The biggest problem with this type of fuel cell is carbon monoxide (CO) and carbon dioxide (CO_2) poisoning. CO_2 in a fuel can react with KOH to form a solid carbonate, which destroys the electrolyte.

- **Phosphoric Acid Fuel Cells** use liquid phosphoric acid as an electrolyte. Because of the Pt catalyst it uses, they have to work at high temperatures to avoid CO poisoning. It was the first type of fuel cell which was used commercially.
- In **Molten carbonate Fuel Cells** the electrolyte is usually a combination of alkali carbonates suspended in a lithium aluminium oxide ($LiAlO_2$) matrix. This fuel cell operates from 600°C to 700°C and noble metals as catalyst are not required. The big advantage of this type of fuel cell is that there is no need of fuel reforming. Due to the high temperature, fuel is converted to hydrogen in a process called internal reforming, which reduces the cost.
- **Solid oxide Fuel Cells** use solid, non-porous metal oxide as the electrolyte. The most commonly used is Y_2O_3-stabilized ZrO_2. Like MCFCs it can use a non-precious metal catalyst and because of the extremely high working temperature, there is no need for an external reformer to purify the fuel.
- **Direct Methanol Fuel Cells** is a Polymer Electrolyte Membrane Fuel Cells type as described below, with the difference that instead of hydrogen, it uses methanol as a fuel. The main advantage of using methanol instead of hydrogen, is the ease to store and transport the fuel. Since the efficiency of DMFCs is quite low (up to 40%), they are used especially in portable applications, such as 3G mobile phones, personal digital assistant (PDA) or navigation systems. [7]
- **Polymer Electrolyte Membrane Fuel Cells (Hydrogen and Methanol)** are the most promising type of fuel cells. They use a solid polymer electrolyte (fluorinated sulfonic acid polymer or other similar polymers) and porous carbon electrodes coated witch a Pt catalyst. As it was mentioned earlier, PEMFCs use hydrogen as a fuel. The purity of the fuel is very important because there is a possibility of catalyst poisoning and membrane degradation when there are impurities present. PEMFCs can be divided into two groups: low temperature PEMFC (LT-PEMFC's) which usually work between 60-80°C and high temperature PEMFC's (HT-PEMFC's) which work above 100°C. [2]

Table 2.1 *Characteristics of Operation of Different types of Fuel Cells taken from the Data Center Handbook*[6]

Fuel Cell Type	Common Electrolyte	Operating Temperature	Efficiency	Applications	Advantages	Disadvantages
Polymer Electrolyte Membrane (PEM)	Perfluoro-sulfonic acid	50-100ºC Typically 80ºC	60% transportation 35% stationary	Backup power, Portable power and Transportation	Solid electrolyte reduces corrosion and electrolyte management problem, it works at a low temperature and has a quick start-up	Expensive catalyst, Sensitive to fuel impurities and Low temperature waste heat
Alkaline (AFC)	Aqueous solution of potassium hydroxide soaked in a matrix	90-100ºC	60%	Military and Space	Cathode reaction faster in alkaline electrolyte, leads to high performance and low cost component	Sensitive to CO_2 in fuel and air and it requires electrolyte management
Phosphoric Acid (PAFC)	Phosphoric acid soaked in a matrix	150-200ºC	40%	Distributed Generation	Increased tolerance to fuel impurities	Pt catalyst, long start-up time and low current and power
Molten Carbonate (MCFC)	Solution of lithium, sodium and/or potassium carbonates, soaked in a matrix	600-700ºC	45-50%	Electric utility and Distributed Generation	High efficiency, fuel flexibility and can use a variety of catalysts	High temperature corrosion and breakdown of cell components, low power density and long star-up time
Solid Oxide (SOFC)	Yttria stabilized zirconia	700-1000ºC	60%	Auxiliary power, Electric Utility and Distributed Generation	High efficiency, Fuel flexibility, a variety of catalysts can be use and it uses a solid electrolyte	High temperature operation requires long star-up time and limits and High temperature corrosion and breakdown of cell components

The PEM is the most crucial component of the fuel cell. It has two functions. Firstly, it has to provide ionic conduction between the cathode and the anode. The ions may only be protons, in order to avoid unwanted side-reaction or even short circuiting. Secondly, it serves as a separator for the gaseous reactants. Unfortunately, there are still drawbacks in PEM fuel cells which needs to be solved. The most important issue is very high cost which is caused by use of expensive electrolyte membrane and catalyst. Although many researchers are working on new polymer electrolyte membranes, the price is still very high (~800-1000 USD/m^2).

The most commonly used membrane in polymer electrolyte membrane fuel cells is Nafion®. It was discovered in 1967 by Walther Grot of DuPont®. It is a graft polymer with the backbone formed of Polytetrafluoroethylene (PTFE) chains (commonly known as Teflon®) ending with Sulfuric Acid HSO_3 groups **(***Figure 2.2***).** When the membrane becomes hydrated, protons from HSO_3 groups become mobile by bonding to the water molecules and moving between successive sulfonic acid groups. [8]

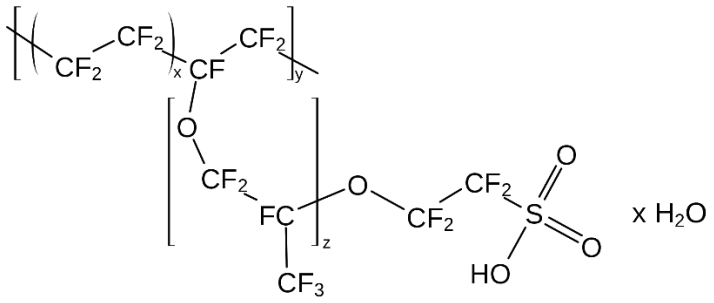

Figure 2.2.*Chemical Structure of Nafion® by DuPont*

However, the perfluorinated polymers have some major drawbacks: very high costs and loss of conductivity at high temperature (>80°C), what may limit their further application. That is why a number of possible candidates were developed. [9, 10, 11, 12, 13, 14]

Direct Methanol Fuel Cell are based on the same technology as the PEMFC, but in this particular form of fuel cell, hydrogen gas is not needed and the power

of the fuel cell is generated by direct conversion of liquid methanol to hydrogen ions. [15] The reactions that take place in the fuel cell are given below.

Anode reaction:

$$CH_3OH + H_2O \rightarrow 6H^+ + 6e^- + CO_2 \qquad \textit{Equation 2.6}$$

Cathode reaction:

$$1.5O_2 + 6H^+ + 6e^- \rightarrow 3H_2O \qquad \textit{Equation 2.7}$$

Overall Reaction:

$$CH_3OH + 1.5O_2 \rightarrow 2H_2O + CO_2 \qquad \textit{Equation 2.8}$$

The reaction at the anode is slow and therefore the same amount of catalyst is necessary at the anode and the cathode. Another difference of the DMFC compared to the PEMFC is the type of catalyst used for the reaction. A DMFC uses a high surface area (50:50%) Pt/Ru alloy as anode catalyst to overcome the slow reaction, which is more expensive than the Pt catalyst used with a PEMFC. The MEA consists of the same components as the PEMFC. Another difference between the two types of fuel cells is that with the PEMFC, flooding is undesirable and gas has to be drawn in, to constantly remove the water formed from the cathode, while with the DMFC, CO_2 must be removed, but flooding is actually required by a methanol/water mixture.

The operating temperature of the DFMC lies between 50°C and 120°C. DMFC's have many advantages, for example, liquid fuel, high energy density and no membrane humidification. However, disadvantages, as fuel crossover, safety concerns and low power density also have to be taken into account.

2.2. Alternative to Nafion membranes

2.2.1. sPEEK Importance in PEMFC's

PEEK is a widely known and commercially produced polymer with low costs, excellent mechanical strength, thermal properties and broad chemical resistance.[15] Sulfonation of PEEK leads to an increase in its ability to conduct protons.[16, 17, 18] *Figure 2.3* shows the original structure of PEEK and the modified structure after sulfonation, the sulfonated PEEK (sPEEK).

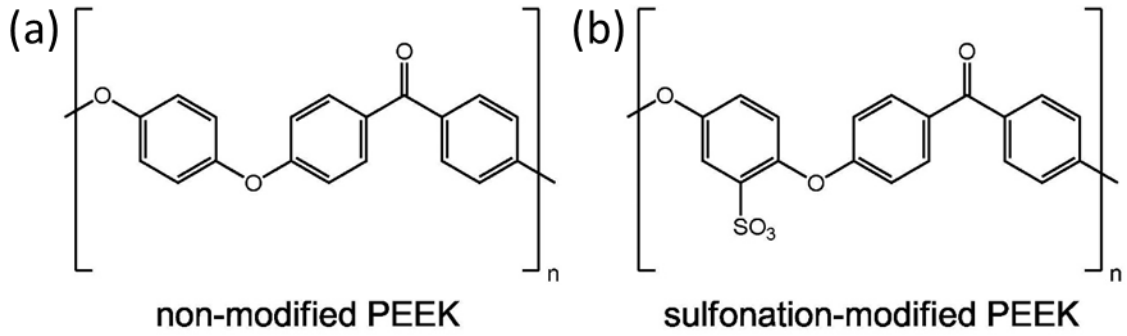

Figure 2.3.*Chemical Structures of (a) PEEK and its modified form (b) sPEEK.*

As with Nafion, the ionic functionality of sPEEK is given by the SO_3H group that is added by the sulfonation process. Sulfonation is an electrophilic substitution and reported as to be a second order reaction. The SO_3H group has multiple places at the PEEK to bond. Under normal conditions the substitution will take place at the first carbon ring, because the electron density of the other two aromatic rings in the repeating unit is relatively low. Longer reaction times or high temperatures can lead to multiple substitution on the aromatic rings of the polymer. Many synthesis reactions for PEEK sulfonation are reported in the literature. [16, 19, 17, 20, 21, 22, 23]

Some advantages of the sPEEK membrane are, low costs, improved water retention at high temperatures and good mechanical stability. With the latter allowing the make the membrane thin enough to decrease the resistance offered by the thickness of the membrane. However, there are some problems that need

to be solved, before sPEEK can replace Nafion commercially in fuel cells. At the moment, the mechanical properties get worse as the sulfonation degree increases and the high proton conductivity is achieved. The key issue that needs to be considered is increasing the protonic conductivity of sPEEK membranes.

2.2.1. Proton Movement Dynamics and Water medium

One of the main difficulties in the development of new polymer electrolyte membranes is that the proton conductivity mechanism has not been fully understood. The most general approach is that the conduction happens through a Hopping Mechanism (e.g. Grotthuss transport [24]) or Diffusion (e.g. through water [25]). This implies difficulties for creating accurate models as to develop new materials. However, various studies using a series of relationships of the materials characteristics and its ability to conduct protons has been encounter and, with this as a guide it is possible to use that as a start to design an appropriate material able to efficiently conduct protons.

The main factor that drives the proton conductivity in the polymer membrane is the degree of hydration. This degree can be controlled by different approaches, e.g. the degree of sulfonation in the sPEEK polymer. There is a compromise in this case, since more sulfonic groups will increase the conductivity because of the addition of water, but the mechanical properties of the membrane will drop for the same reason. In that regard, partially sulfonated sPEEK can give an optimum of these properties but in the end its proton conduction seems to be still too low for a fuel cell application.

A study presented by Ma *et al.* [26] showed that actually the real differences between the sulfonated aromatic polymers was the microstructure. This was obtained by creating different sulfonated polymers, with comparable equivalent weight, which presented similar conductivities at different water contents. This proof that the there is only a low or even non-existent correlation between the degree of sulfonation and the water uptake. This concept has been addressed and confirm earlier by Kreuer, [27] who gave more importance to the phase formation and inner structure in ionomer conducting membranes.

The kinetics of the water adsorption/desorption has also been addressed in recent studies. Tosto *et al.*[28] compared curves of adsorption and desorption for sPEEK membranes modified with different percentages of silylation (25 and 50% molar). They found that the near surface diffusion coefficient D_s was the same for different membranes. This implies that the mechanism for the water entering the surface of the membrane is also deciding the rate as the limiting step for diffusion. Another study on the impact of water in the membrane is presented by Di Vona *et al.*[29] They calculated the minimum amount of humidity needed in the membrane for the Grotthuss mechanism to occur, by comparing sPEEK/Silylite membranes and Nafion®. The results were given by λ numbers, which represent the number of water molecules bond per sulfonic acid group, and through energy calculations they found that for the hybrid sPEEK membranes the change between vehicular movement of protons through the sulfonic groups and the hopping movement through water was λ≈4 while in Nafion λ≈5.

Finally, the activation energy for the proton conductivity is measured by creating an Arrhenius plot of Conductivity vs. Temperature. The energy needed for the proton conduction to occur has been linked to the flexibility of the structure in the polymer. Typically this flexibility is being characterized by the glass transition temperature *Tg*, hence this is linked to the free volume presented by the polymer. A higher rigidity in the polymer will be related to a high free volume, which will be represented by a high T_g value and vice versa. It is believed that a lower rigidity will mean a lower energy required for proton conductivity.[29] As a clear objective of this thesis, a new model taking these issues into account is presented. Common polymers used for PEM are formed by two phases. A hydrophilic and a hydrophobic phase. Initially this inner structure and its order has been accepted as one of the main variable for an optimal proton conduction before. [25-27] In the model presented, this phase separation, in the case of the sPEEK, leads to an apparent and significant lower T_g values (during the time of the operation in a test or fuel cell). The water in the membrane swells the hydrophilic phase, plasticizing the polymer and changing the inner structure. Notice that the analysis done for proton conductivity and its relationship with the T_g values cannot

be determined using the common values obtained for the polymers through DSC or other common techniques.

2.2.2. Inner structures in Nafion and sPEEK

Cathion exchange membranes operate by transport proton through their hydrated structure. This structure is linked by negative-charged groups fixed along the backbone of the conducting path. These side groups can be sulfonate, phosphonate or carboxylate ion groups among others. *Figure 2.4* shows models representing the difference between the inner structure of Nafion® and sPEEKK. The capacity of conduction of this paths can be improved by the aid of water molecules into the membrane or as it will be shown further on by different treatments of the polymer in a controlled way.

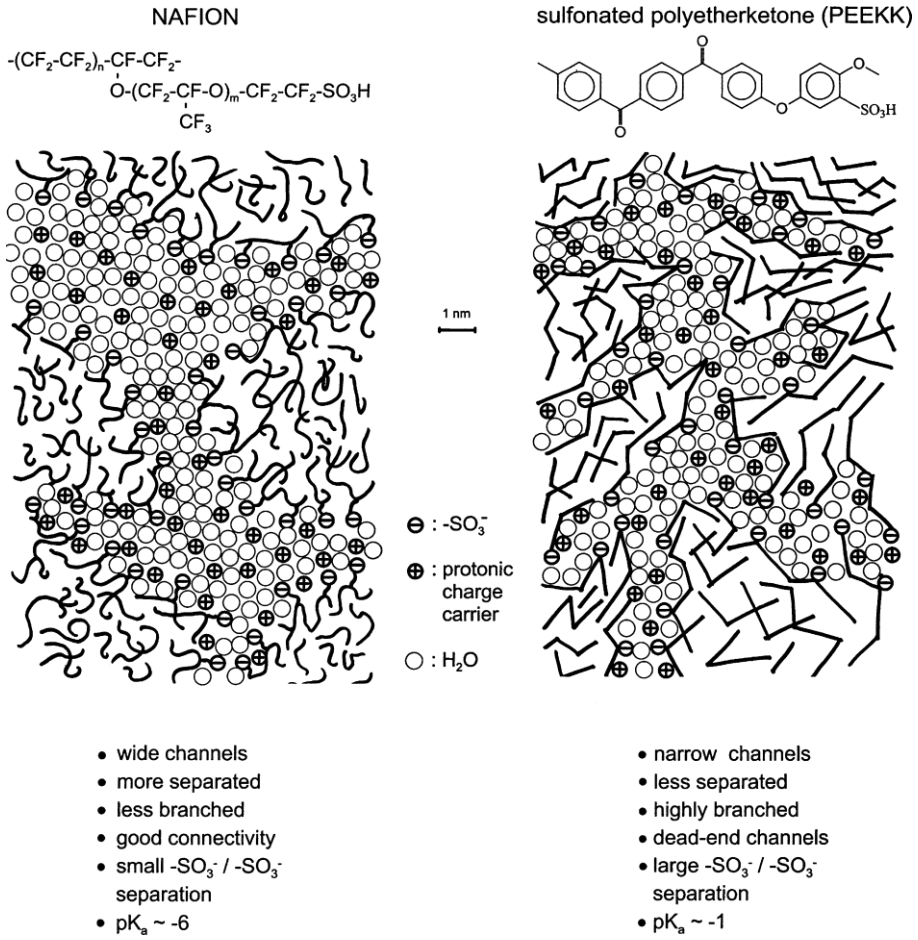

Figure 2.4 *Inner structure models for Nafion and sPEEKK reported Kreuer et al.[25] depicted from SAXS experiments.*

2.3. Bibliography

1 Scientists, U. o. C. (ed Union of Concerned Scientists).

2 Bose, S. *et al*. Polymer membranes for high temperature proton exchange memebrane fuel cell: recent advances and challenges. *Prog. Polym. Sci.* **36**, 813-843 (2011).

3 Zhang, J. *et al*. High temperature PEM fuel cells. *Journal of power sources* **160**, 872-891 (2006).

4 Gupta, R. B. *Hydrogen fuel. Production, transport and storage*. (CRC Press, 2008).

5 E. G. & G. Services - Parsen Inc. , S. *Fuel Cells : A Handbook*. 5th Edition edn, (E. G. & G. Services - Parsen Inc., 2000).

6 Geng, H. *Data Center Handbook*. Vol. 30 (John Wiley & Sons, 2014).

7 Larminie, J., Dicks, A. . *Fuel Cell Systems Explained*. 2nd Edition edn, (Wiley, 2003).

8 ECS. *Proton Exchange Membrane Fuel Cells 9*. Vol. 25 (ECS, 2009).

9 Liu, F., Yi, B., Xing, D., Yu, J. & Zhang, H. Nafion/PTFE composite membranes for fuel cell applications. *J. Membr. Sci.* **212**, 213-223 (2003).

10 Kongkachuichay, P. & Pimprom, S. Nafion/Analcime and Nafion/Faujasite composite membranes for polymer electrolyte membrane fuel cells. *Chem. Eng. Research and Design* **88**, 496-500 (2010).

11 Matos, B. *et al*. Nafion-based composite electrolytes for proton exchange membrane fuel cells operating above 120 °C with titania nanoparticles and nanotubes as fillers. *J. Power Sources* **196**, 1061-1068 (2011).

12 Lee, J.-R., Kim, N.-Y., Lee, M.-S. & Lee, S.-Y. SiO2-coated polyimide nonwoven/Nafion composite membranes for proton exchange membrane fuel cells. *J. Membr. Sci.* **367**, 265-272 (2011).

13 Amjadi, M., Rowshanzamir, S., Peighambardoust, S.J., Hosseinic, M.G., Eikanid, M.H. . Investigation of physical properties and cell performance of Nafion/TiO_2 nanocomposite membranes for high temperature PEM fuel cells. *Int. J. Hydrogen Energ.* **35**, 9252 - 9260 (2010).

14 Peighambardoust, S., Rowshanzamir, S. & Amjadi, M. Review of the proton exchange membranes for fuel cell applications. *Int. J. Hydrogen Energ.* **35**, 9349-9384 (2010).

15 Basu, S. *Recent Trends in Fuel Cell Science and Technology*. First Ed. edn, (Springer, 2007).

16 Mikhailenko, S., Zaidi, M. & Kaliaguine, S. Sulfonated polyether ether ketone based composite polymer electrolyte membranes. *Catal. Today* **67**, 225-236 (2001).

17 Huang, R., Shao, P., Burns, C. & Feng, X. Sulfonation of Poly(Ether Ether Ketone)(PEEK): Kinetic Study and Characterization. *J. Appl. Polym. Sci.* **82**, 2651-2660 (2001).

18 Di Vona, M., Marani, D., Epifanio, A., Traversa, E., Trombetta, M., Licoccia, S. A covalent organic/inorganic hybrid proton exchange polymeric membrane: synthesis and characterization. *Polymer* **46**, 1754-1758 (2005).

19 Zaidi, S. M. J., Mikhailenko, S. D., Robertson, G. P., Guiver, M. D. & Kaliaguine, S. Proton conducting composite membranes from polyether ether ketone and heteropolyacids for fuel cell applications *Journal of Membrane Science* **173**, 17-34 (2000).
20 Xing, P. *et al*. Synthesis and characterization of sulfonated poly(ether ether ketone) for proton exchange membranes *Journal of Membrane Science* **229**, 95 - 106 (2004).
21 Gil, M. *et al*. Direct synthesis of sulfonated aromatic poly(ether ether ketone) proton exchange membranes for fuel cell applications *Journal of Membrane Science* **234**, 75 - 81 (2004).
22 Zhao, C. *et al*. Synthesis of the block sulfonated poly(ether ether ketone)s (S-PEEKs) materials for proton exchange membrane *Journal of Membrane Science* **280**, 643 - 650 (2006).
23 Di, Y. *et al*. Preparation and characterization of continuous carbon nanofiber-supported SPEEK composite membranes for fuel cell application. *RSC Adv*. **4**, 52001-52007 (2014).
24 Pourcelly, G., Gavach, C., . *Perfluorinated Membrane*. 294 - 310 (Cambridge University Press, 1992).
25 Kreuer, K. D. On the development of proton conducting polymer membranes for hydrogen and methanol fuel cells. *J. Membr. Sci*. **185**, 29-39 (2001).
26 Ma, C., Zhang, L., Mukerjee, S., Ofer, D., Nair, B. An investigation of proton conduction in select PEM's and reaction layer interfaces-designed for elevated temperature operation. *J. Membr. Sci*. **219**, 123-136 (2003).
27 Kreuer, K. D. On the complexity of proton conduction phenomena. *Solid State Ionics* **136-137**, 149-160 (2000).
28 Tosto, S. K., Philippe; Di Vona, Maria Luisa. Water Adsorption/desorption in proton-conducting ionomer membranes: The model case of sulfonated and silylated poly-ether-ether-ketone. *Solid State Ionics* **209-210**, 9-14 (2012).
29 Di Vona, M. L. M., D.; D'Epifanio, A. D.; Licoccia, S.; Beurroies, I.; Denoyel, R.; Knauth, P. Hybrid materials for polymer electrolyte membrane fuel cells: Water uptake, mechanical and transport properties. *J. Membr. Sci*. **304**, 76-81 (2007).

Chapter 3 Materials, Sample Preparation and Characterization Techniques

This chapter describes the modification of PEEK into sulfonated PEEK. It further discusses the synthesis of certain fillers based on BPO_4, such as $Li_{3x}B_{1-x}PO_4$, and the addition of them to the membrane. Besides these, detonation Nano Diamonds (DND) and iron sulfate ($FeSO_4 \times 7H_2O$) were used as fillers. It introduces the various thermal treatments applied, the use of solvent and prepared solutions to cast and activate the membranes and also gives an inside in the characterization techniques used throughout the other chapters.

3.1. Introduction

SPEEK is a commonly used polymer electrolyte for fuel cells, its synthesis has been review in many different publications and its capacity for mechanical and proton conductivity improvment by inorganic fillers has also been extensibly research. The metodologies followed to produces this membranes are able to affect and change their performance. Mostly by changes in the inner phase created by the water on the membrane. The water phase structures in sPEEK are small and not easy to observe by common imaging techniques.[1, 2] Thus, the development of a new methodology was required in order to understand better the behaviour of this water phase. This methodology needed to be based on the ability to probe internal structural modifications that may occur in the material during thermal treatment, with and without water channels, and that these changes can be examined via a fast and simple characterization technique.

3.2. Materials Modifications and Synthesis

The base materials used to create our electrolytes where modified, synthetize and characterized completely in order to control all the variables in the process of creating the membranes. The procedures used are the following.

3.2.1. PEEK modification into sPEEK

Sulfonation of PEEK was carried out following a procedure reported in the literature. [3] PEEK (Vitrex 450 PF Mw: 39200) powder (50 g) was slowly added into vigorously mechanically stirred 758 ml of H_2SO_4 (95-98% Sigma Aldrich) (95/5 in weight %) in a three-neck reactor at room temperature under nitrogen atmosphere (Figure 3.1). After complete dissolution of PEEK (~19 hours, left overnight), the flask was heated in a silicon oil bath at 55°C for the desired time (5 hours). The time was chosen to lead to a 60% sulfonation (hereafter referred to as sPEEK0.6). There is a significant amount of publications related to sPEEK sulfonation including

different degrees of sulfonation.[3, 4, 5] It turns out that, 60% is considered to be the lower limit of sulfonation, increasing the water content and conductivity but not compromising the swelling of the membrane or destroying its mechanical properties.[2] In order to stop the sulfonation reaction, the solution was cooled down to room temperature and precipitated into a large excess of ice-cold demineralized water under mechanical stirring. The polymer was filtered and washed several times with demineralized water until the pH was found to be neutral. The obtained polymer was then dissolved in acetone and left for 3 days inside the fume hood, allowing the acetone to evaporate. The resulting sPEEK0.6 was dried at 80°C in a vacuum oven for one week (see Figure 3.2). The modification was also checked by TGA and DSC measurements (see figure 3.3 and 3.4) since the incorporation of sulfonic groups will change the degradation behavior of the polymer, the crystallinity will be suppress and the *Tg* modified.

Figure 3.1 *Experimental setup with the reaction vessel for sulfonation of PEEK to form sPEEK0.6.*

Figure 3.2 *The resulting sPEEK0.6 from the process: on the right is the sPEEK0.6 recovered from the acetone drying and on the left is the ground polymer used for preparing the membranes because it dissolved faster.*

To determine the degree of sulfonation, a back titration method was used.[3, 5, 6] A sample of about 0.5g was placed in 200 ml of 0.01 M NaOH for 3 days. Then a diluted sulfuric acid solution (0.0045 M) was used to back titrate the solution using phenolphthalein as indicator. It is stressed that the synthesis of the polymers and the back titration was done twice for each sample, so as to be sure that the results were reproducible (see table 3.1).

Table 3.1 *Results obtained from the back titration performed on the sPEEK 0.6*

Sample	Yield
sPEEK 0.6 (1)	63%
sPEEK 0.6 (2)	58%

The sulfonation of PEEK above 60% suppress the crystallization in the PEEK. In figure 3.3a, a standard cooling and heating DSC from PEEK are shown and in figure 3.3b the modified polymer only presents the *Tg* which value is modified form the PEEK (aprox. 140°C).

TGA also shows difference between PEEK and the sulfonated PEEK. The hydrophilicity of the sulfonic groups make that water is store inside the membrane, which it can be seen in figure 3.4 as the first fall on the weight. The second fall is refer to the degradation of the sulfonic groups and the third, which is also presence in the PEEK is the degradation of the carbon chains.

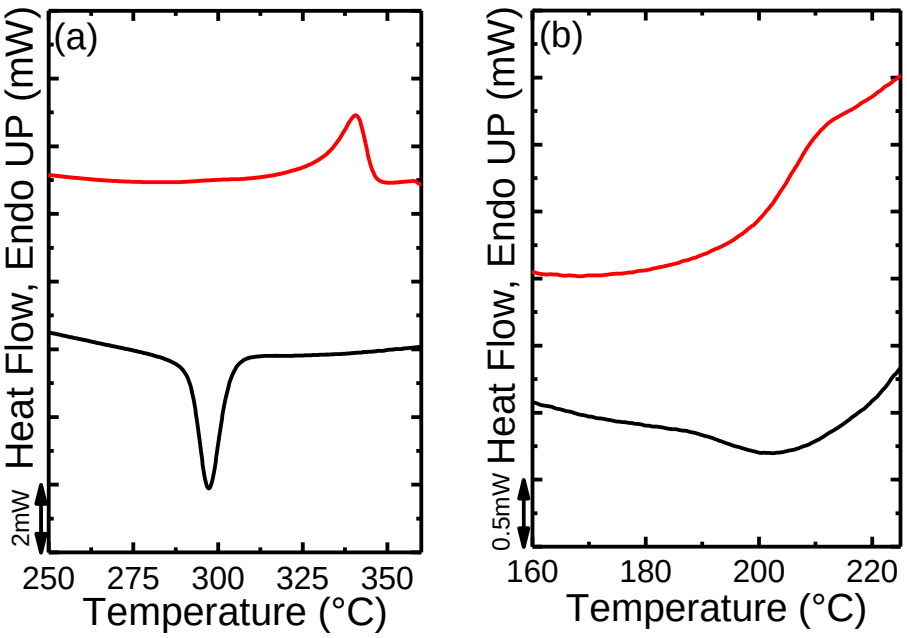

Figure 3.3 *Standard cooling and heating dynamic DSC of (a) PEEK showing the crystallization and melting and (b) sulfonated PEEK showing only the modified glass transition.*

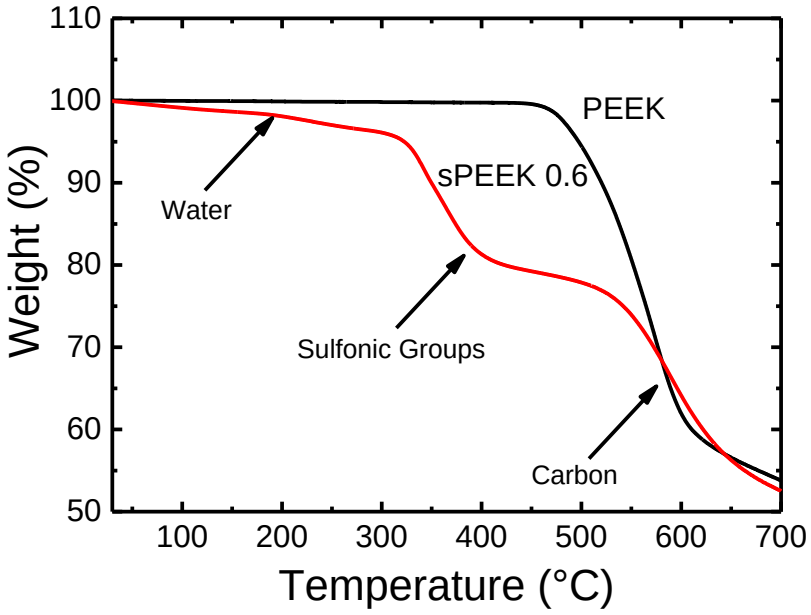

Figure 3.4 *Thermal Gravimetrical Analysis of the PEEK and sulfonated PEEK showing the typical changes in the degradation temperatures of the polymer.*

3.2.2. Synthesis of BPO_4

The synthesis of BPO_4 was done following the procedure reported by Jak.[7] The reaction was carried out using Boric Acid (H_3BO_3) and Phosphoric Acid

(H_3PO_4) in equal molar proportions in a beaker with demineralized water. The reaction is presented below:

$$H_3BO_3 + H_3PO_4 \rightarrow BPO_4 + 3H_2O \qquad \textit{Equation 3.1}$$

A white precipitate was formed. The water was left for evaporation and the powder collected from the beaker and used as one of the fillers for the membranes base on the works reported by Krishnan *et al.*[5]

3.2.3. Synthesis of $Li_{3x}B_{1-x}PO_4$

The synthesis of $Li_{3x}B_{1-x}PO_4$ ($0.0<x<0.30$) was carried out by the same procedure as reported by M.J.G. Jak. [7] Two different synthesis were reported in the dissertation in order to make $Li_{3x}B_{1-x}PO_4$. Here, Ammonium phosphate ($H_2NH_4PO_4$), boric acid (H_3BO_3) and lithium hydroxide mono hydrate ($LiOH.H_2O$) were mixed in a beaker in order to synthesize $Li_{3x}B_{3-x}PO_4$ with x=0.1. The reaction can be written as follows:

$$H_2NH_4PO_4+(1-x)\ H_3BO_3+3xLiOH\cdot H_2O \leftrightarrow Li_{3x}B_{1-x}PO_4\cdot {}^{1}/_{2}\,H_2O+\left(3+1\,{}^{1}/_{2}\,x\right)H_2O+\ NH_3 \qquad \textit{Equation 3.2}$$

The beaker was covered with aluminum foil containing a small hole to release reaction gasses, while CO_2-free demineralized water was added until a white homogeneous paste was formed. The mixture was heated in air in a programmed furnace using the temperature program given below:

1. Heating from room temperature to 110°C at 2°C/min,
2. Keeping the sample for 2 hours at 110°C,
3. Heating from 110°C to 600°C at 4°C/min,
4. Keeping the sample for 10 hours at 600°C (reaction temperature),
5. Cooling down the sample in the furnace to room temperature.

According to the previous reported work by Jak, this should lead to a ceramic foam with spherical agglomerates of about 2µm. The primary particle size is around 50 nm. The structure was confirmed by XRD (see Figure 3.5) and for simplicity we will refer $Li_{0.3}B_{2.9}PO_4$ as Li-BPO_4.

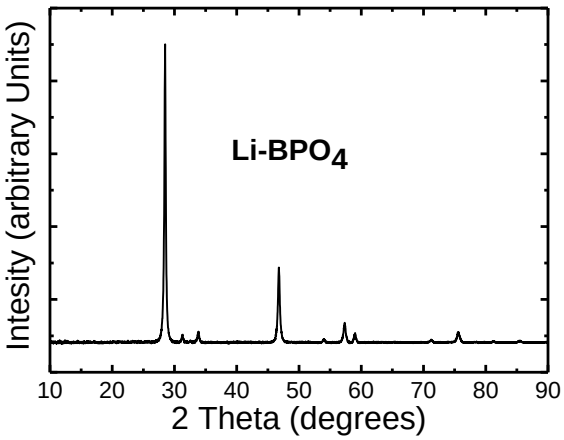

Figure 3.5 *XRD refraction for Li-BPO_4 which is in concordance with the results presented by Jak.*[7]

3.3. Membrane preparation

This section will respectively describe the preparation of sPEEK0.6 and hybrid membranes of Li-BPO_4, $FeSO_4 \cdot 7H_2O$, Detonation Nano Diamonds (DND), and BPO_4.

The inorganic compounds were ground with mortar and pestle and sieved with metallic sifters to a particle size of 45 micrometers.

15 ml of *N,N*-dimethylacetamide (DMAc, Sigma-Aldrich, Anhydrous 99.8%) was heated to 120°C under continuous stirring. When the DMAc reached the desired temperature, sPEEK0.6 was added and dissolved at constant temperature (this takes between 15 and 60 minutes). After the sPEEK0.6 was fully dissolved, the inorganic compound was added to the solution. Table 3.2 gathers the full list of samples prepared including the various weight percentages. A homogeneous suspension is desired and this will take between 30 and 60 minutes. Afterwards, the solution was casted onto a Petri dish in a fume hood and left at 55°C for 24-48 hours. The membrane was removed from the petri dish using demineralized water and then dried at 55°C in a vacuum oven for 24 hour (see Figure 3.6). Finally the optimal thermal treatment obtained by Broadband Dielectric Spectroscopy was

applied. This will be further explained in Chapter 4. The thickness of all the membranes was between 150-250 µm.

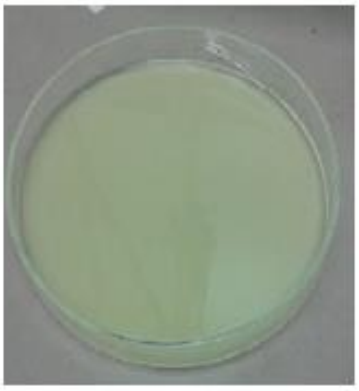

Figure 3.6 *Petri dish containing a sPEEK0.6/ 25% Li-BPO_4 membrane (Li-$BPO_4$25).*

Table 3.2 *Base polymer and Hybrid samples, with different weight compositions prepared to run the different test and find the optimal compositions and fillers.*

Sample Name	Inorganic Filler	sPEEK0.6 % (wt.)	Filler % (wt.)
sPEEK0.6	-	100	-
Li-$BPO_4$15	$LiBPO_4$	85	15
Li-$BPO_4$20		80	20
Li-$BPO_4$25		75	25
Li-$BPO_4$30		70	30
$FeSO_4$6	$FeSO_4$+7H_2O	94	6
$FeSO_4$9		91	9
$FeSO_4$12		88	12
DND1	DND	99	1
DND1.5		98.5	1.5
DND2		98	2
$BPO_4$30	BPO_4	70	30 [a]

[a] This % was chosen based on the publication of Krishnan *et al.*[5]

3.4. Characterization Techniques and Sample preparation

Every characterization technique requires different sample preparations. Hence, the membranes were cut in different parts and sizes and taken through different treatments, so as to make the results reliable. It is however stressed that these treatments are important to be taken into account to reach proper results, since a specific treatments may influence the outcome of a specific parameter to be analyzed. A review on the techniques them self is also presented.

3.4.1. Broadband Dielectric Spectroscopy

Dielectric spectroscopy (DS) is a very powerful characterization tool for studying the molecular dynamics in polymers, due to its broad dynamical range. Modern DS equipment can measure between 10^{-6} up to 10^{12} Hz and from -170 to +500°C. Therefore, the motional processes that take place in polymeric systems on extremely different time scales, can be studied in a broad frequency and temperature range. Because the motional processes depend on the morphology and microstructure of the system under investigation, information on the structural state of the material can be extracted by taking the molecular mobility as a probe for the structure. This method is sensitive to molecular fluctuation of dipoles within the system and these fluctuations are related to the molecular mobility of groups, segments or whole polymer chains which present themselves as different relaxation processes.

Types of polarization induced in the material

In DS, an external electric field ($\vec{E}$) is applied, this generates a polarization of the material from which different possible responses are originated: 1. atomic polarization due to small displacements of atoms or groups of atoms on the macromolecule; 2. electronic polarization that causes induced dipoles due to the distortion of the electron cloud of each atom with respect to the positive nucleus; and 3. an orientational polarization, which corresponds to the reorientation of the permanent dipoles in the direction of the applied electric field.

The atomic and electronic polarizations have a characteristic instant response (lower than 10^{-13} s), which is independent on the temperature. Based on this, and taking into account the frequency window employed in BS, the orientational polarization should be responsible for the observed relaxation behavior. [8]

Types of Orientational Polarization in Polymers

As it was explained before, polymers responding to an applied electric field, are highly affected by the type of dipoles that are associated to the chain bonds. For macromolecules, different possibilities for the orientation of a molecular dipole vector in respect to the polymer backbone are possible (see Figure 3.7). [8] Polymers with molecular dipoles fixed parallel to the backbone are called Type A, when the dipole moment is rigidly attached perpendicular to the chain backbone it's a Type B Polymer, and if the chain molecules have the dipoles in a more or less flexible side chain these are then called Type C.

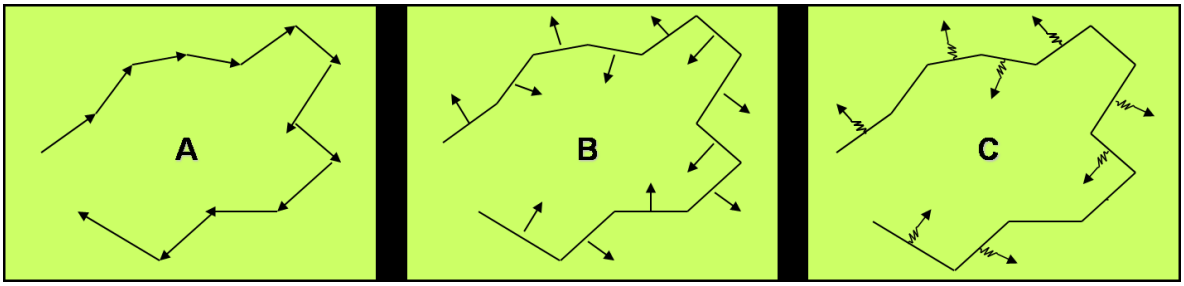

Figure 3.7 *Schematic representation of the different types of dipoles associated to the polymer chain.*[8]

Relaxation Processes in Polymers

Molecular motions in polymers are controlled by clearly differentiated time and length scales. Different parts of the total dipole moment can be affected by a particular motional process. This motional processes can be localized to some bonds or to a short side chain, giving rise to local relaxations and, on a larger and longer spatial and time scale for temperatures above the glass transition, the so called segmental mode or α-relaxation, which involves a cooperative relaxation of segments in the polymer chain. At even longer times and more extended length

scale, for A-type polymers, an additional process can be observed referred to as normal-mode relaxation. [8, 9]

Models Used to Describe the Relaxation Processes

As soon as an electric field is applied, the dipoles orientational distribution changes and align to it. To arrive at the new equilibrium state, a finite time is required, this is a consequence of the hindering intermolecular forces of the units that contribute to dipoles. For interacting dipoles, this rearrangement to an equilibrium is characterized by a distribution of relaxation times. Only when enough time is given, after the application of an electric field for the orientation to attain equilibrium, a maximum in the polarization (highest observable dielectric constant) will be obtained in the material. This is called the static dielectric constant, ε_s. Now, if the polarization is measured instantly after the field is applied, and no time for dipole orientation to take place is given, then the observed instantaneous dielectric constant, denoted ε_∞ will be low and only is a consequence of the deformation of the molecules. The total response of a measurement will be a dispersion from the highest (ε_s) to a lowest dielectric constant (ε_∞).

To obtain this dispersion, consider the application of an alternating electric field $\vec{E}$, amplitude $\vec{E}_0$ and angular frequency $\omega(\omega = 2\pi f)$, across a dielectric material:

$$\vec{\mathrm{E}} = \overrightarrow{\mathrm{E_0}}\ cos\,\omega\mathrm{t} \qquad \textit{Equation 3.1}$$

A polarization which alternates in direction will be created, and, if the frequency is high enough, the orientation of any dipoles will present inevitably a lag behind the applied field. Mathematically, this can be summarize as a phase lag in the electric displacement:

$$\vec{\mathrm{D}} = \overrightarrow{\mathrm{D_0}}\ cos(\omega\mathrm{t} - \delta) \qquad \textit{Equation 3.2}$$

Which could be written as

$$\vec{D} = \overrightarrow{D_1}\ cos\,\omega t + \overrightarrow{D_2}\ sin\,\omega t \qquad \textit{Equation 3.3}$$

Where

$$\overrightarrow{D_1} = \overrightarrow{D_0}\ cos\,\delta \quad \text{and} \quad \overrightarrow{D_2} = \overrightarrow{D_0}\ sin\,\delta \qquad \textit{Equation 3.4}$$

From where two dielectric constants are obtained:

$$\varepsilon' = \frac{\overrightarrow{D_1}}{\varepsilon_0 \vec{E}_0} \quad and \quad \varepsilon'' = \frac{\overrightarrow{D_2}}{\varepsilon_0 \vec{E}_0} \qquad \textit{Equation 3.5}$$

And these two can be combine into a complex dielectric constant of relative permittivity:

$$\varepsilon^*(\omega) = \varepsilon' - i\varepsilon'' \qquad \textit{Equation 3.6}$$

The complex permittivity ε^* of a given sample can be calculated from the measurement of the complex impedance Z^* given by equation (3.7):[8]

$$Z^*(\omega) = \frac{U^*(\omega)}{I^*(\omega)} \qquad \textit{Equation 3.7}$$

Where U^* and I^* are the voltage and current circulating through the sample at a certain angular frequency ω. Once the impedance has been measured, ε^* can be calculated by means of equation (3.8):[10]

$$\varepsilon^*(\omega) = \varepsilon' - i\varepsilon'' = \frac{1}{i\omega Z^*(\omega) C_0} \qquad \textit{Equation 3.8}$$

Where ε' and ε'' are the real and imaginary part of the complex permittivity and C_0 corresponds to the capacity of the empty sample holder. The complex permittivity is measured over a frequency window and in a certain temperature range.

The imaginary part of the obtained dielectric permittivity is analyzed by the phenomenological Havriliak-Negami (HN) function as shown in equation (3.9):[11]

$$\varepsilon^*(\omega) = \varepsilon_\infty + \frac{\Delta\varepsilon}{[1+(i\omega\tau_{HN})^b]^c} \qquad \textit{Equation 3.9}$$

Where $\Delta\varepsilon = \varepsilon_S - \varepsilon_\infty$; ε_∞ and ε_S are the unrelaxed and relaxed values of the dielectric constant and τ_{HN} is the characteristic relaxation time. Here, b and c are shape parameters ($0 < b,\ c \leq 1$) which describe the symmetric and the asymmetric broadening of the equivalent relaxation time distribution function.

Equation (3.10) shows how the average relaxation time (τ_{max}) can be obtained from the H-N fitting parameters:[11]

$$\tau_{max} = \frac{1}{2\pi F_{max}} = \tau_{HN}\left[sin\frac{b\pi}{2+2c}\right]^{\frac{-1}{b}}\left[sin\frac{bc\pi}{2+2c}\right]^{\frac{1}{b}} \qquad \textit{Equation 3.10}$$

The corresponding τ_{max} values could follow a Vogel-Fulcher-Tammann-Hess (VFTH) dependence with the reciprocal temperature as shown in equation (3.10):[11,12]

$$-log_{10}(\tau_{Max}) = -log_{10}(\tau_0) - \left(\frac{1}{ln\,10}\right)\left(\frac{B}{T-T_0}\right);\ T_0 < T_g \qquad \textit{Equation 3.11}$$

From B and using equation 3.11 one can calculate the activation energy E_{vft}:[12]

$$B = \frac{(E_{vft}\left(1-\frac{T_0}{T}\right)^2)}{R} \qquad \textit{Equation 3.12}$$

The dynamic glass transition temperature can be determined from equation 3.13:[12]

$$T_g^{BDS} = \frac{B}{ln(100)} - T_0 \qquad \textit{Equation 3.13}$$

The time 100s is commonly used as it refers to the temperature, within narrow limits, at which the heat capacity jump characteristic of the glass transition (when heating rate for the sample is 10°C/min) starts.[13]

The samples size used are related to the electrodes. The samples were disks of 15mm diameter punched from the membranes, to be used with electrodes of 10mm. The thermal treatment used for the samples will be explained in detail in Chapter 4. While the sample was going through the thermal treatment, to ensure the sample was kept flat, it was placed in between two stainless steel mesh electrodes.

3.4.2. Electrochemical Impedance Spectroscopy

EIS is a powerful tool to investigate fuel cell properties and performance. EIS measures the frequency dependence of the electrical impedance of a fuel cell upon a small sinusoidal Alternating Current (AC) voltage and measuring the current response.

EIS data are most often represented in Nyquist (complex plane – Figure 3.8) and Bode (impedance magnitude and phase angle as a function of frequency) plots. These complementary plots can give information to the capacitive and inductive character of the cell, and, through an equivalent circuit model, can provide the electrical properties of the system being studied.[14]

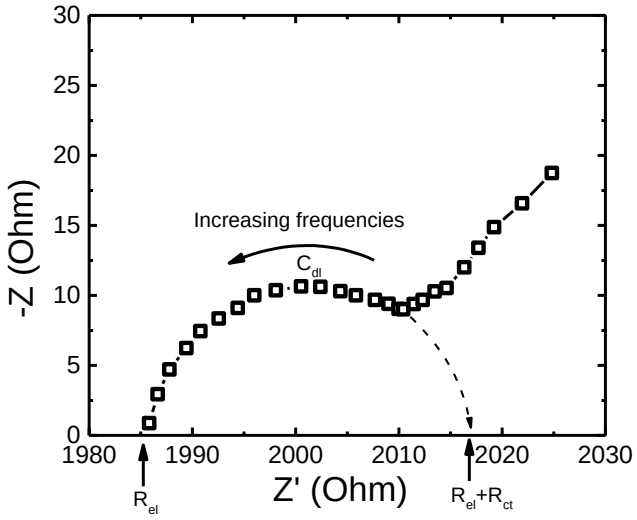

Figure 3.8 *Nyquist plot of EIS for the sPEEK0.6/30% BPO_4 sample at 90°C 80% R.H.*

The equivalent circuit, combination of resistances, capacitances and inductances, should reflect a physical model of the charge carriers' migration and are hence prefer to be as simple as possible. In Figure 3.9, an example of an equivalent circuit of an electrochemical cell is shown, where R_{el} represent the electrolyte (membrane) resistance, usually observed at the high-frequency intercept. C_{dl} is the capacity related to the double layer of the electrode/electrolyte interface. R_{ct} is a charge transfer resistance, which in combination with Warburg impedance (W) describes the mass transfer in the electrode/electrolyte interface. [15] A Warburg element is a diffusion circuit

element commonly used to model semi-infinite linear diffusion, that is, unrestricted diffusion to a large planar electrode. A Warburg impedance element is nearly always associated with a charge-transfer resistance and a double layer capacitance.

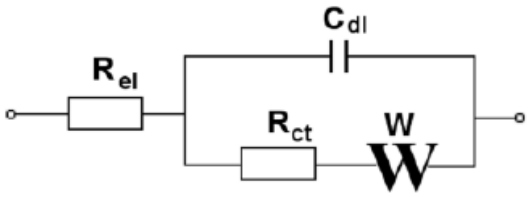

Figure 3.9 *Equivalent circuit of a typical electrochemical cell.*

Operation conditions such as temperature, pressure, fuel and oxidant flow rates and humidity can affect the fuel cell performance. When using a proper cell, it is possible to operate the measurement in a controlled environment and under fixed conditions. [15]

Proton transport in polymer electrolyte membranes can occur in two directions, through and across the membrane. That is why there are different methods to measure the conductivities. [16] It is possible to carry out the measurement with either the 2- or 4-probe method. The 4-probe method gives more stable results but is more complicated than that the 2-probe method. Therefore, the 2-probe method is used more often. Figure 3.10 shows schematics for the in plane 4-point-probe measurement.

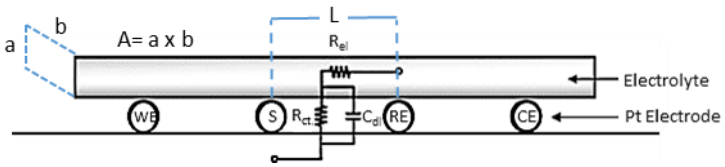

Figure 3.10 *In plane 4-point probe scheme for electrolyte conductivity measurements. A simple equivalent circuit has been added to show the position of the various individual elements.*[16]

From the measured membrane resistance, its conductivity (σ) can be calculated using the equation:[15]

$$\sigma = \frac{L}{(R_{el} * A)}$$ *Equation 3.14*

Where, L is the distance between the electrodes in cm, R_{el} is the proton conduction resistance in Ω and A is the electrode area in cm^2

The cells used to measure the samples in EIS are particularly problematic. Many variables can affect the measures since it's quite sensitive to different factors. From sample preparation to connections, parameters and cell configuration. Many different setups were tried to measure the EIS of the samples (see figure 3.11). Ideally, one should measure the conductivity in the closest conditions to the normal working fuel cell as possible. This would mean using electrodes, humidity, pressure and a through plane conductivity measurement.

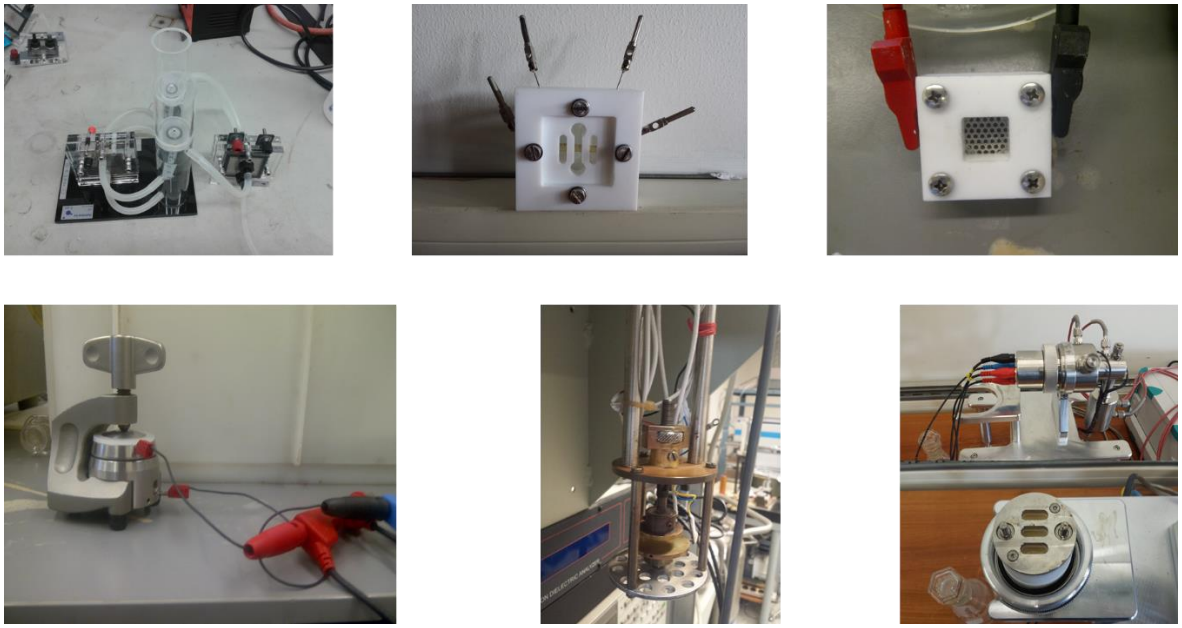

Figure 3.11 *Different set ups and cells developed trying to achieve a reliable electrochemical impedance spectroscopy measurement from the samples tested.*

Every elements in this step presents its own issue to be addressed at the moment of conducting the measurement using EIS. The electrodes present a new interface in the impedance, where this interface affects the effective active area size, since it depends on the dispersion and compatibility of the electrodes and

the electrolyte. It is emphasized that besides an interface arise between the electrode and electrolyte, this may also lead to the formation of an actual new phase between those, also referred to as an interphase, and should not be confused with the interface. The pressure needs to be kept constant and can influence the values of the conductivity. Humidity has to be present since the water phase in the membrane needs to be hydrated to be able to conduct protons, but the condensation process that usually occurs in the membrane by humidity in air can lead to new interphases and misleading values of the proton conductivity by creating alternative paths for the protons to move. Finally the through plane measurements present a complicate geometry since you need to have the humidity reaching the whole membrane without condensation, while you have to have electrodes covering part of the surfaces and also, usually, needs to be measure using a two point probe measurement, even when the 4 point probe is a more stable measurement in EIS.

All these different problems were presented in the different cell configuration used. The biggest problems were related to maintain adequate contact between the probes and the electrodes. If they are not properly connected and isolated from external disturbances, they will create noise in the measurement.

Finally we got a commercial cell for the measurements. This commercial cell tackle most of the issues that has been discussed before. The connections with the probes were stable, isolated and the electrodes used were made out of Pt. The humidity was controlled by a humidity chamber and three different temperature regulators that were able to set the values for different part of the cell within 0.01 °C error. The measurement was done in an in plane, 4 point probe geometry, which allows the humidity to reach the membrane evenly. As a safety precaution the relative humidity was kept at 80% in the sample, so no condensation would occur.

The samples for EIS depended of the cell size used to measure the conductivity. In this case, an in plane 4 point probe was used, which requires rectangle samples of 1.5 by 4 cm x cm, which were simply cut from the membrane,

before testing. The membranes were put in acidic water (1M H_2SO_4) for 24 hours in order to activate the conduction mechanism.[17] The sample was then washed with demineralized water and mounted in the cell for 2 hours at the lowest measuring temperature, which was 80°C. The measurements were done 20 times, with a 2 minutes intervals between every run, for every sample, until stability was reached. The procedure was repeated for every temperature. The thickness of the sample was measured at the end of the essays in order to calculate the specific conductivity. Every sample was at least measured twice to obtain the same conductivity. The voltage used for the EIS was 20mV. However, also test were done at 10mV and 30 mV, giving the same values for the measurement, which assures that the voltage was not affecting the measurement.

3.4.3. Differential Scanning Calorimetry

Differential Scanning Calorimetry is a thermo-analytical technique, in which the heat flux in a sample is monitored dynamically throughout temperature and time, and the difference in heat flux between the sample and an empty reference sample holder is monitored. For polymers, DSC is mainly used to determine glass transition temperatures (T_g), melting points (T_m) and crystallization temperatures. [18] It also has different applicability in material science and chemistry, e.g. can be used for inorganic compounds, to determine thermal stability of the sample.

Samples of 10 and 20 mg were cut from the membranes ran through the thermal treatment explained in Chapter 4 and then placed in a saturated solution of Potassium Nitrate salt allowing to equilibrate at 100% R.H. and 25°C. [19] Another sample was only ran through the thermal treatment before testing them in the DSC. The 10 mg sample was put in a standard aluminum pan and the 20 mg sample in a hermetic sealed cap. The reason behind the two weights is the rate of heating, 10 and 5°C/min respectively, for the dynamic DSC. The weight changes in order to be able to compare the results between them. The difference in the samples is referred to the need of keeping the water inside the membrane, we needed sealed caps in order to study the effect of water as a plasticizer, on the T_g of the polymer. The other samples in the regular caps allowed the water to release from the

membrane while heating, and thus it is possible to monitor the difference in the standard behavior of the material and the changes caused by the thermal history.

3.4.4. Thermo-Gravimetrical Analysis

TGA is a technique to analyze the different reactions and phase transformations that are present in a sample. If they occur together with a release or incorporation of material this can be followed further by measuring the changes in the weight of the sample at constant heating rate. The use of controlled heating also give us information on the rate at which the reaction takes place.

TGA samples of 5 mg were cut from the membranes, ran through the thermal treatment explained in Chapter 4 and equilibrated in the same salt used for the DSC samples. The test was run twice for every sample. Difference on water absorption in the samples were expected after going through the thermal treatment and the presence of the inorganic compounds.

3.5. Bibliography

1 G. Gebel, Macromolecules 2013, 46, 6057.
2 D. D. Brush, Marek; Schlick, Shulamith Macromolecules 2015, 48, 637.
3 R. Huang, P. Shao, C. Burns, X. Feng, J. Appl. Polym. Sci. 2001, 82, 2651.
4 K. Roelofs, T. Hirth, T. Schiestel, J. Membr. Sci. 2010, 346, 215; G. P. Robertson, S. D. Mikhailenko, K. Wang, P. Xing, M. D. Guiver, S. Kaliaguine, J. Membr. Sci. 2003, 219, 113; I. Colicchio, D. Demco, M. Baias, H. Keul, M. Moeller, J. Membr. Sci. 2009, 337, 125.
5 P. Krishnan, J. Park, C. Kim, J. Membr. Sci. 2006, 279, 220.
6 Y. Di, W. Yang, X. Li, Z. Zhao, M. Wang, J. Dai, RSC Adv. 2014, 4, 52001.
7 M. J. G. Jak, in *Chemical Engineering*, Vol. PhD, TUDelft, The Netherlands 1999.
8 F. S. Kremer, Andreas, *Broadband Dielectric Spectroscopy*, Springer-Verlag Berlin Heidelberg, 2003.
9 A. R. Blythe, *Electrical properties of polymers*, Cambridge University Press, Oxford 1979; J. P. F. Runt, J.J., *Dielectric spectroscopy of polymeric materials. Fundamentals and applications.*, American Chemical Society, Washington, DC. 1997.
10 A. R. Blythe, *Electrical Properties of Polymers*, Cambridge University Press, Cambridge 1980.

11 M. Hernández, J. Carretero-González, R. Verdejo, T. A. Ezquerra, M. A. López-Manchado, Macromolecules 2010, 43, 643.
12 P. Atorngitjawat, R. J. Klein, J. Runt, Macromolecules 2006, 39, 1815.
13 C. A. Angell, J. Non-Cryst. Solids 1991, 131-133, 13.
14 A. J. F. Bard, Larry R., *Electrochemical Methods: Fundamentals and Applications*, Wiley, 2001.
15 X.-Z. R. S. Yuan, C.; Wang, H.; Zhang, J. , *Electrochemical Impedance Spectroscopy in PEM Fuel Cells - Fundamentals and Applications*, Springer-Verlag London, 2010.
16 C. H. Lee, H. B. Park, Y. M. Lee, R. D. Lee, Industrial & Engineering Chemistry Research 2005, 44, 7617.
17 Y. Hudiono, S. Choi, S. Shu, W. J. Koros, M. Tsapatsis, S. Nair, Micropor. Mesopor. Mat. 2009, 118, 427.
18 W. M. Groenewoud, in *Characterisation of Polymers by Thermal Analysis*, (Ed: W. M. Groenewoud), Elsevier Science B.V., Amsterdam 2001, 10.
19 O. E. inc., in *OMEGA Web Technical Temperature Reference*, Vol. 2015, 2003-2015.

Chapter 4 sPEEK0.6 Membranes Optimization through Broadband Dielectric Spectroscopy

In this research we report a novel methodology to obtain optimized sPEEK membranes based on controlled thermal treatments. The corresponding structural changes (channels created by water observed by SAXS), that allow this proton conduction to occur, have been verified by analysis of the dynamics as determined by dielectric spectroscopy. Another important result is the ability to treat the sample in such a way that the highest conductivity of the PEMs occurs at a working temperature of 100°C: this allows the PEMs to be optimized for operation conditions where managing the water in the fuel cell is easier and the poisoning of the platinum in the electrodes is reduced. This pioneering methodology will serve as the basis for the optimization of new sPEEK-based PEMs to be used in fuel cells applications.

4.1. Introduction

sPEEK is widely used in the development of new polymer electrolyte membranes for fuel cells.[1,2,3,4] Many different routes have been explored to allow sPEEK to compete with Nafion® as a commercial PEM material, taking into account the high costs that are involved with the use of the latter. Membranes of sPEEK are generally made via a solvent evaporation method, either being by doctor-blade casting from a sol-gel or casting in solution and slowly evaporating the solvent until a film is formed.

The interaction of the polymer with the solvent for casting has an effect on the capacity of the membrane to conduct protons. It has been reported by Kaliaguine *et al.*[5] that the use of different solvents hinders the availability of sulfonic groups for proton conduction by creating secondary products that then damage the polymer.[6] The membranes also have to be exposed to various thermal treatments to remove the solvent and the moisture[7, 8] before they are placed in a controlled humidity chamber for conductivity and/or fuel cell testing.

sPEEK, which is composed of a hydrophylic and a hydrophobic component,in the presences of water, behaves as a two phase polymer. Water in the membrane creates channels, and the water inside these channels is considered to be the primary driver for proton conduction.[9,10 ,11] When water, or any solvent that interacts with the sulfonic groups in the sPEEK, enters the membrane, it modifies, destroys or swells the internal structure depending on the type of interaction. In the case of water, a change in the inner structure takes place by the swelling of the sulfonated regions in the polymer, thereby creating water channels. This is similar to what happens in block copolymers and polymer blends, where the phase organization and orientation also is sensitive to thermal treatment and solvent interactions. These interactions or treatments are able to create order or disorder in the polymer depending on the affinity of the solvent and/or how far the thermal treatment is removed from any temperature-related transition(s) that may be present in the polymer, like the glass transition temperature (T_g).[12,13,14,15] These

similarities with block copolymer phases were our motivation to investigate if there is evidence for the formation of such phases in sPEEK and if the ability to control those, provides a method to get a better internal structure in the proton conducting membrane.

We propose in this study, how various thermal treatment procedures influence the order of the hydrophylic phase water channels in the polymer, and how this allows the creation of the most optimal and stable proton conducting membrane. Broadband dielectric spectroscopy (BDS) is used to investigate the dynamics of the prepared membranes during and after thermal treatment while inner structural changes in the membrane are verified by SAXS measurements.

4.2. Experimental Methodology

4.2.1.SPEEK Synthesis

The sPEEK used is the sPEEK0.6, of which the synthesis and other particularities were explained in Chapter 3 already.

4.2.2. Membrane preparation

The membranes were prepared as it was explained in Chapter 3, and the thermal procedure was the following.

Figure 4.1 shows the different steps that every sample experienced: first, the casted sample was vacuum dried at 55°C; The low temperature used was intended to remove most of the solvent without changing the internal structure signifincantly. The sample was then hydrated to create water channels in the structure in a controlled fashion. Afterwards, It was annealed at different temperatures. Finally, the sample was rehydrated to recreate the channels in the treated membrane and vacuum dried again at 55°C to assure that most of the water was extracted, while keeping the created channel structure intact.

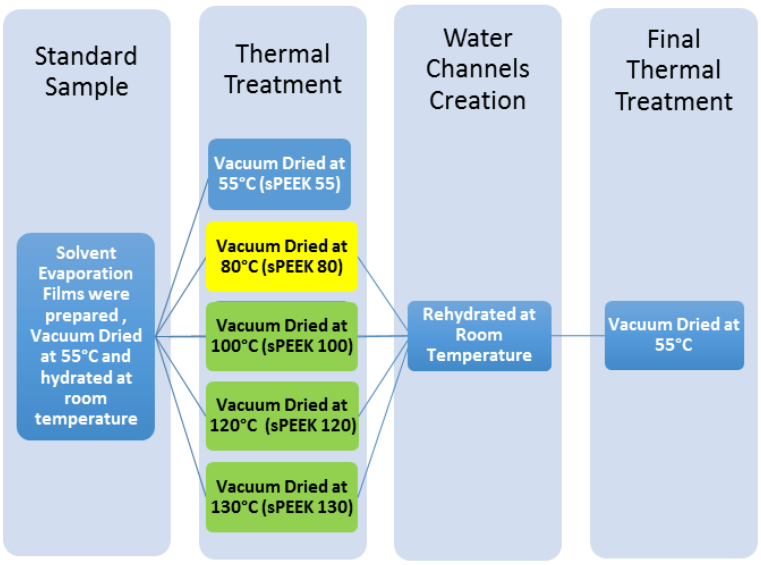

Figure 4.1 *Scheme of sample preparation. The colors indicates the degree of modification in the inner structure of the polymer.* Blue *means that there is only an extraction of the water from the membrane.* Yellow *means the extraction of the water with a level modification of the membrane because of the annealing process occurs bellows the apparent* T_g*' of the polymer.* Green *means that the water is taken out but also the structure is modify highly since the treatment is done above the apparent* T_g*' of the membrane.*

4.3. Measurements

4.3.1. Differential Scanning Calorimetry (DSC)

Dynamic heating and cooling measurements were made under inert atmosphere (pure nitrogen). The DSC was a Perkin Elmer DSC 7 and the equipment was previous calibrated using Indium and Tin standards. Measurements were performed at a constant heating and cooling rate of 5 or 10°C/min. For normal pans, 10°C/min was used as heating and cooling rate, a first heating from -5 to 235°C, followed by 5 minutes isothermal treatment, to delete thermal history of the sample was followed by a controlled cooling and heating. For the sealed pans, 5°C/min was used as heating and cooling rate, a first heating from -5 to 150°C, followed by 5 minutes isothermal treatment, to delete thermal history of the sample was followed by a controlled cooling and heating.

4.3.2. Thermal Gravimetrical Analysis (TGA)

Controlled heating at 20°C/min under an air atmosphere for every sample was done. All the samples were 5 mg, they were cut from the membranes ran through the thermal treatment explained in the Chapter 4 and then placed in a saturated solution of Potassium Nitrate salt allowing to equilibrate at 100% R.H. and 25°C.

4.3.3. Electrochemical Impedance Spectroscopy (EIS)

Conductivity measurements were done using an Autolab PGSTAT12 Impedance Spectrometer in the range of $1x10^5$ Hz to $1x10^{-1}$ Hz at 20mV, by using a temperature and humidity controlled, 4 point probe cell in plane measurement. The first resistance was taken as the value of the Proton conductivity for the membrane and transformed to conductivity using equation explained in chapter 3.

4.3.4. Broadband Dielectric Spectroscopy (BDS)

BDS measurements were performed on a BDS-40 high resolution dielectric analyzer (Novocontrol Technologies GmbH). This equipment is composed of an ALPHA type dielectric interface and a QUATRO type temperature controller. The experiments were carried out over a frequency window of $10^{-1} < f/\text{Hz} < 10^7$ (being $F = \frac{\omega}{2\pi}$ the frequency of the applied electric field and ω the corresponding angular frequency) in a temperature range from 35 to 235°C in 5°C steps. The temperature of the experiments was controlled by liquid nitrogen flow, with an error for each range of frequency of ± 0.1°C.

4.3.5. Small Angle X-ray Scattering (SAXS)

The two dimensional (2D) SAXS experiments were carried out on a GANESHA 300XL+ system from JJ X-ray. The instrument is equipped with a Pilatus 300K detector, with a pixel size of 172 µm x 172 µm. The X-ray source is a Genix 3D Microfocus Sealed Tube X-Ray Cu-source with integrated Monochromator (multilayer optic "3D version" optimized for SAXS) (30 W). The wavelength used is λ = 1.5408 Å. The detector moves within a vacuum chamber with sample-to-detector distance varied between 0.115 m and 1.47 m depending on the configuration. Calibration of scattering angle was done using silver behenate

(d_001=58.380 Å). The scattering patterns were reduced into 1D intensity vs *q* curves with SAXSGUI program. The Intensity has been normalized by the sample thickness.

4.4. Results and Discussion

An overall model based on the thermal treatments applied to the samples was developed to being able to understand better how the process in the inner structure of the membrane occurs. In Figure 4.2, several situations underlying the overall model are presented, these can be divided into situations (a) describes how the hydrated structure of the sample is, before the changes in the inner structure cluster, occurs, situation (b) shows the previous cluster structure after drying, situation (c) shows, the optimal organized cluster structure after the best thermal treatment for the sample hydrated, situation (d) is the final structure that will be tested.

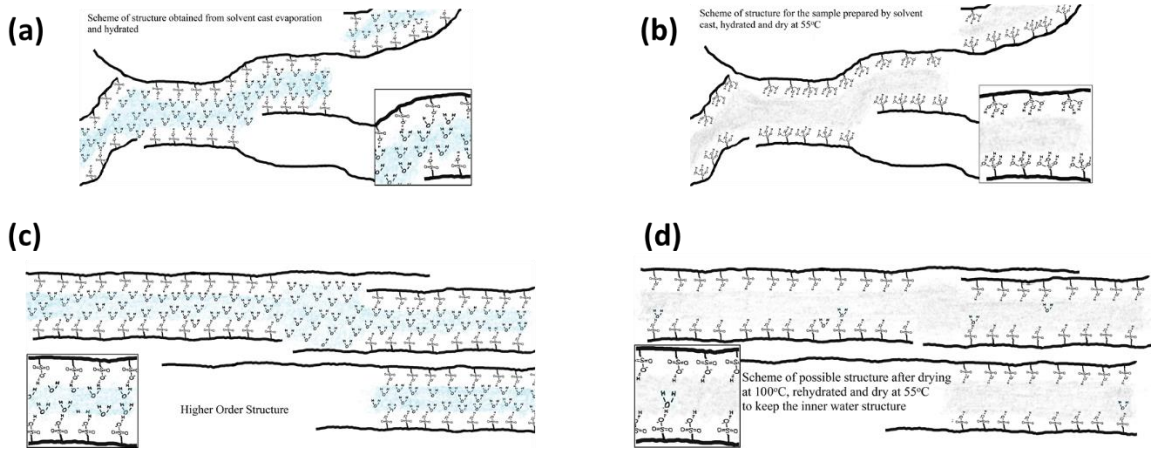

Figure 4.2 *Situation of the changes occurring in the inner cluster structure of the sPEEK0.6 membranes through the thermal treatments. See text in every situation for explanation.*

The interaction of a polymer with a solvent, depending on the degree of affinity, can lead to a depression of T_g; this depression is related to a plasticization effect of the solvent on the polymer by increasing its mobility.[16,17,18] In the

particular case of sPEEK, inter-chain interactions due to hydrogen bonding created by the addition of pendant sulfonic groups, result in an increase of T_g compared to PEEK, but these groups also increase the interaction with solvents like water as they are strongly hydrophilic. In the Figure 4.3 DSC dynamic heating for samples hydrated at different conditions, encapsulated in sealed pans, are presented. The samples shows a significant depression created by the plasticizing effect of water in the sPEEK0.6. In the sample equilibrated at the conditions normally expected in the Fuel Cell, the real T_g value during the performances of the membrane is shown.

When the sample is vacuum dried at 55°C after rehydration, following the methodology explained before, empty channels remain in the sample and the lower T_g is still observed, as the polymer inter-chain interactions are hindered due to the open space left by the channels.

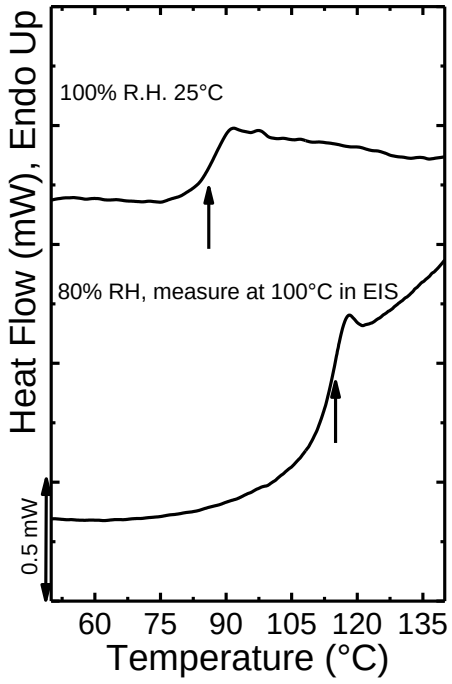

Figure 4.3 *Dynamic DSC heating runs for sPEEK0.6 samples equilibrated at different hydration conditions and encapsulated in sealed pans.*

If there is an inner phase creating empty channels in the cluster of sulfonated PEEK, and this clusters are distributed throughout the bulk sample, the distance between the sulfonated chains should be constant and it should make a signal in SAXS measurements. Figure 4.4 shows the measurements done to two samples, one where the inner phase should not be present (no water and heated to 200°C under nitrogen atmosphere) and one with a treatment were the inner gap was left via thermal treatments. This signal is typical of a lamellar structures in the bulk, not necessary a periodical phase in the polymer but the more organize and oriented the higher the intensity of the signal. The peak implies a distance of 2.8 nm, which will be the gap between the sulfonates PEEK cluster in the samples.

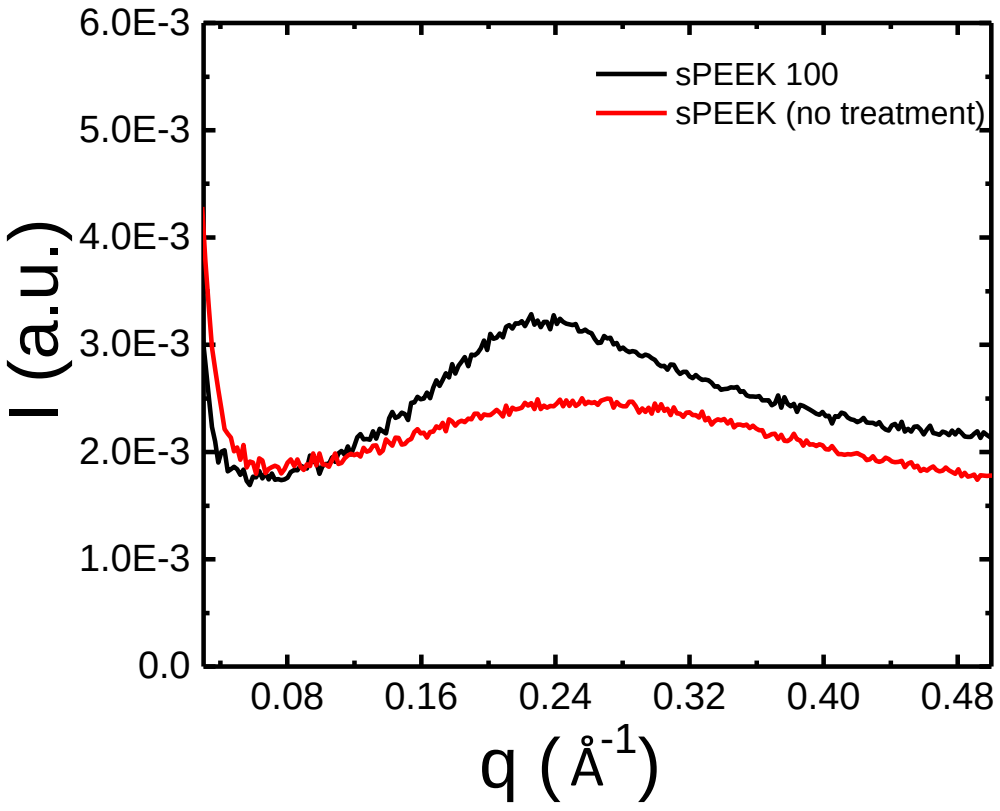

Figure 4.4 *SAXS measurement performed in a sample before the thermal treatment, with no water and heated to 200°C under nitrogen atmosphere, and later the same sample, hydrated and later on undergone a thermal treatment explained before in the chapter.*

Dynamic heating by DSC of different samples is shown in Figure 4.5. During the first heating (Figure 4.5a), clearly the occurrence of two processes can be observed. The first one is a T_g-like transition occurring at low temperatures (below 100°C), which we will refer to as T_g', followed by an endothermic process that begins at different temperatures, depending on the previous thermal treatment. It then finishes close to where the usual T_g for sPEEK is expected to be found (180-200°C).[5] The second heating (Figure 4.5b) only shows one transition, a T_g at high temperature values (around 200°C), again typically reported as the glass transition of sPEEK with 60% sulfonation. From these results, as from what it has been shown by SAXS for a similar treatment, it is possible to conclude that the 55°C thermal treatment, after rehydration, was able to preserve the channel structure created by the water in all the samples, since the T_g' can be observed in the DSC. As mentioned above, the intermediate process that occurs between the two apparent glass transitions depends on the thermal treatment that the membrane underwent before. It is believed that, the temperature of treatment, is the reason behind the change in the starting temperature of this intermediate process. It is also is not reversible since in the second heating the samples only show one T_g.

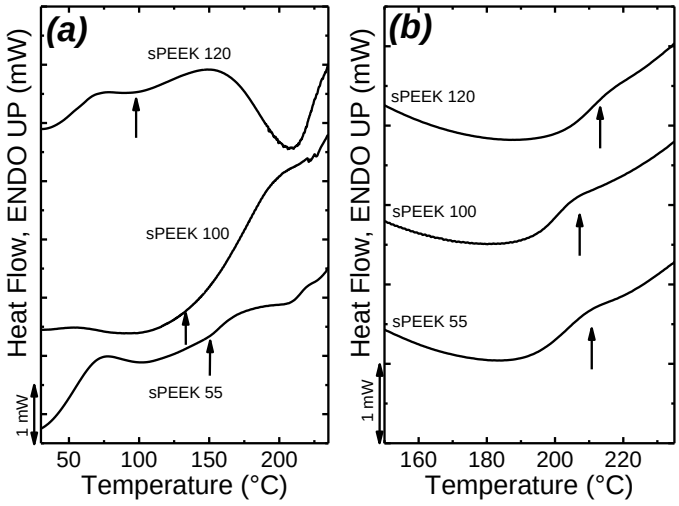

Figure 4.5 *Dynamic DSC curves from sPEEK 55, sPEEK 100, and sPEEK 120 samples. First* **(a)** *and second* **(b)** *heating at 10°C/min.*

T_g measurements in polymers can be done by different characterization techniques. For instance the α relaxation, measured by BDS in a polymer, can be related to the T_g measured by other techniques such as DSC under agreed experimental conditions.[19] BDS is a characterization method able to follow changes in the dynamics of a material. Apart from the α relaxation, it's also possible to show the dynamics of lateral groups and their phase transitions among other interactions.[20, 21] Even though it is a widely used technique for polymer characterization, it is not very well known in the field of PEMs since it is more focused on materials properties rather than on electrochemistry. Nevertheless, some studies were reported on Nafion® and sPEEK using BDS, but these were mainly focused on membrane homogeneity,[22] water plasticizing effect in Nafion® and changes on the dynamic processes depending on the degree of hydration.[23] Other electrolytes have also been studied, Singh *et al.*[24] did a dielectric relaxation research on Poly Vinyl Alcohol (PVA) with different acid groups and contents, and they observed that the acid groups decrease the relaxation times of the dynamic processes. Other techniques are also able to measure dynamic transitions, like Dynamical Mechanical Analysis (DMA). Song *et al.*[25] prepared different sPEEK samples and performed DMA, finding that the membranes presented three dynamic processes. The first was an α- process between 170 and 200°C related to the cooperative movements of the polymer (T_g), a ß- process between 20 and 60°C which they assigned to the chain segmental motions of the hydrogen bridges cross-linked network, and a α- process between -40 and -10°C which was attributed to short range molecular movements in the PEEK phase. Sgreccia *et al.*[26] studied sulfonated aromatic polymers used as electrolyte via DMA. They found that thermal treatment such as annealing, and migration of plasticizer molecules, affects the mechanical performance of the polymer, and proposed thermal treatment as a method for optimization of PEMs.

When we first run the sPEEK 55 sample, we observed a strange behavior during the heating. In the Figure 4.6 this behavior is shown using a plot of Modulus Loss, which enhance the peaks of the relaxations in the sample, and a 3D plot with contrast. This tendency was also observed in all the other samples. We decided to

process the sample under different thermal treatments to try to elucidate what was happening.

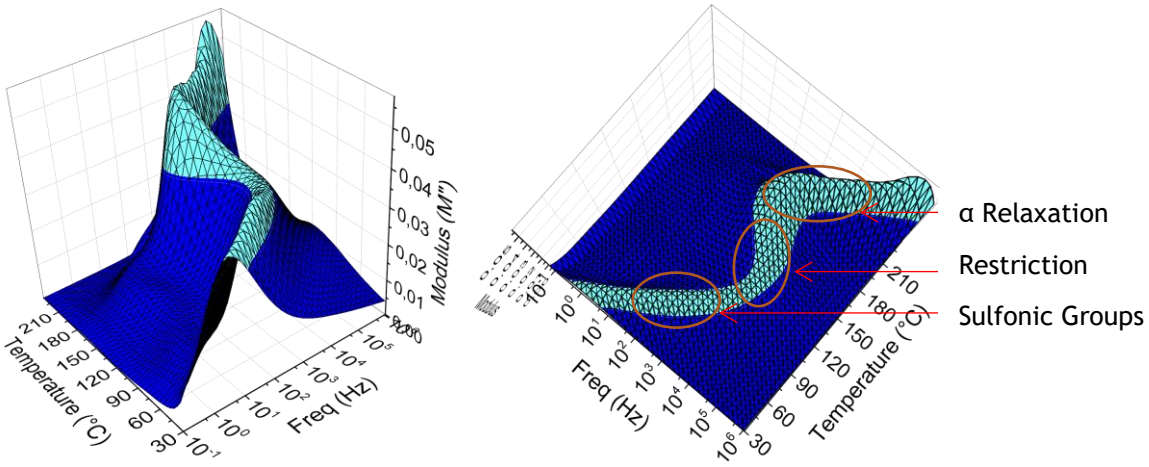

Figure 4.6 *BDS results for sPEEK 55 plotting the modulus loss as a function of the frequency and temperature.*

In Figure 4.7, the processing of our BDS measurement is presented. The intermediate curves and fitting done based on the equations explained in Chapter 3 are shown. Figure 4.8 shows, as an example, the fitting of the H-N relaxation times to the Volger-Fucher-Tammann-Hess (VFTH) equation. For all different thermal treatments, an arrangement comparing all the results, is presented in Figure 4.9 as a way to understand the effects of the different parameters on the samples. The activation plot (Figure 4.9a) shows the three relaxation processes expected based on the results obtained from DSC (Figure 4.5) and the first BDS measurement done (Figure 4.6), and also gives an additional insight in the intermediate process (herein called Dynamic Restricted Process – DRP) between the two segmental relaxations, indicated as α' (low temp.) and α (high temp.). These segmental relaxations, that are related to the T_g, are a consequence of the intrinsic structural changes produced by the water channels that are removed after treatment at elevated temperature.

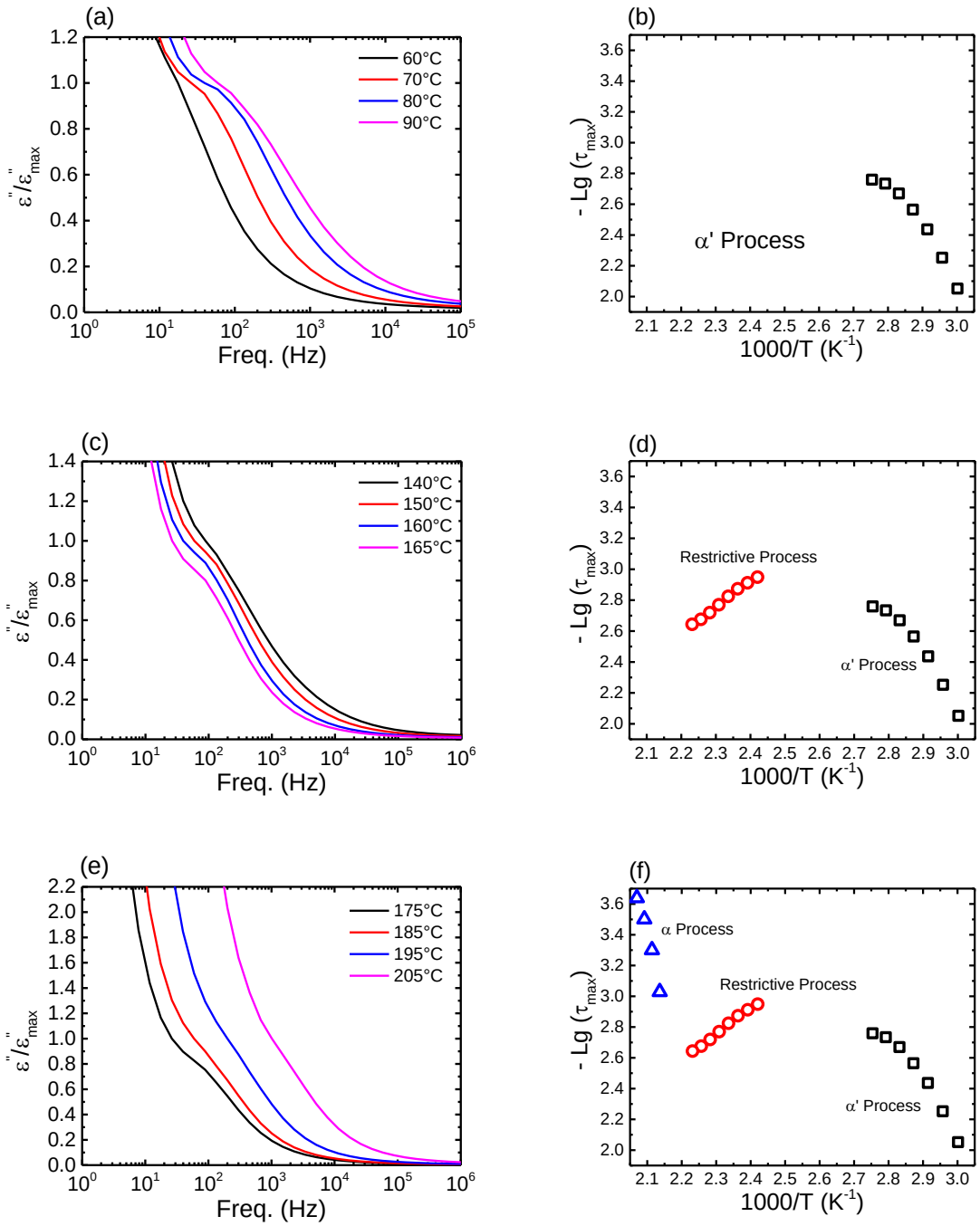

Figure 4.7 *Initial curves collected from the measurement are shown. The left panel show the normalized dielectric loss curves for the three different relaxation process presented by the sample sPEEK 55 and the right panel show the construction of the activation plot with the relaxation times calculated by the fitting with the H-N function.*

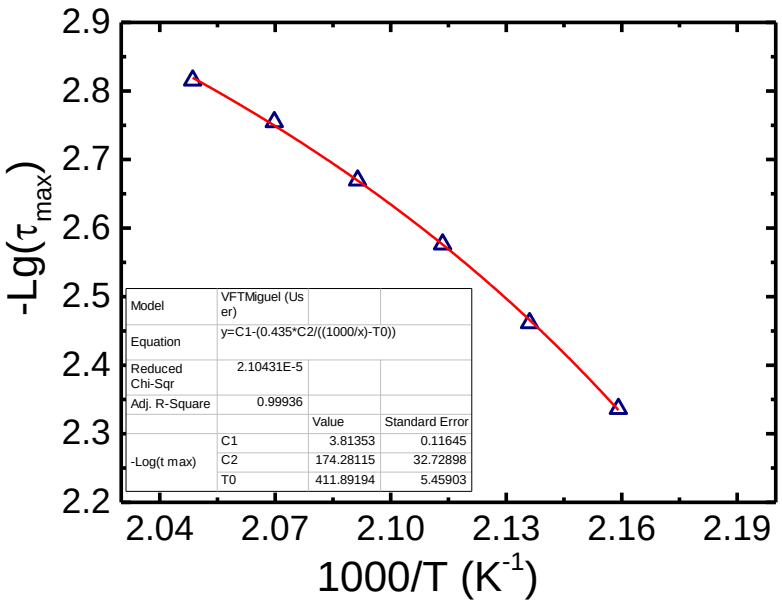

Figure 4.8 *Fitting of the VFTH equation to the relaxation time of the a'-process obtained from sample sPEEK 55.*

The mobility of the sPEEK is hindered by the inter-chain interactions of the sulfonic groups in the clusters. When hydrated, the water channels create a gap, and thereby reducing T_g. The plasticizing effect of the water also contributes to this decrease. When the sample is dried at low temperatures (55°C) this gap remains in the internal structure, causing an apparent new T_g' to be present in the material. This transition is responsible for the ability of the material to reorganize at temperatures below the T_g of sPEEK (180°C to 200°C) not undergoing a physical ageing process but an annealing. It is important to remember that this T_g' is a consequence of the thermal history of the sample, as previously found by DSC.

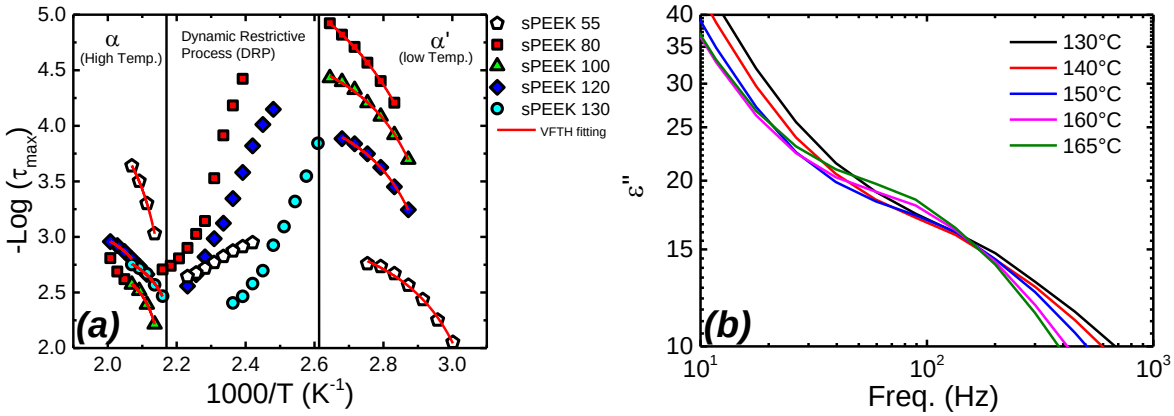

Figure 4.9 *Dynamic processes observed by BDS for sPEEK after different thermal treatments.* (a) *shows the a'- relaxation, dynamic restrictive process (DRP) and a-relaxation in order of increasing temperature and* (b) *is the imaginary part of the dielectric permittivity in the temperature range of the DRP showing the shift to lower frequencies as temperature increases for sPEEK 55 sample.*

A structural change must have happened between the α' and α relaxations. This process, the DRP, becomes more constrained as the temperature increases. The dielectric loss curves in the range of the DRP are shown in Figure 4.9b. In this model, we propose that the separation between the sulfonic groups created by the water after being taken out of the polymer is responsible for the α'-relaxation, as explained before. Then, as the temperature rises above the α', the polymer chains gain mobility and the interactions between the sulfonic groups start to recover, creating hydrogen bridges and locking the chains together again. This chain interlocking is the origin of the α-relaxation at high temperatures (see Figure 4.10). The dynamics of this process is thought to be related to how well position the sulfonated chains are, since the sulfonic groups can only lock-in when there is another sulfonic group available to them. It is believed that the thermal treatment is responsible for such rearrangement of the chains and allows positioning of the sulfonic group in front of each other.

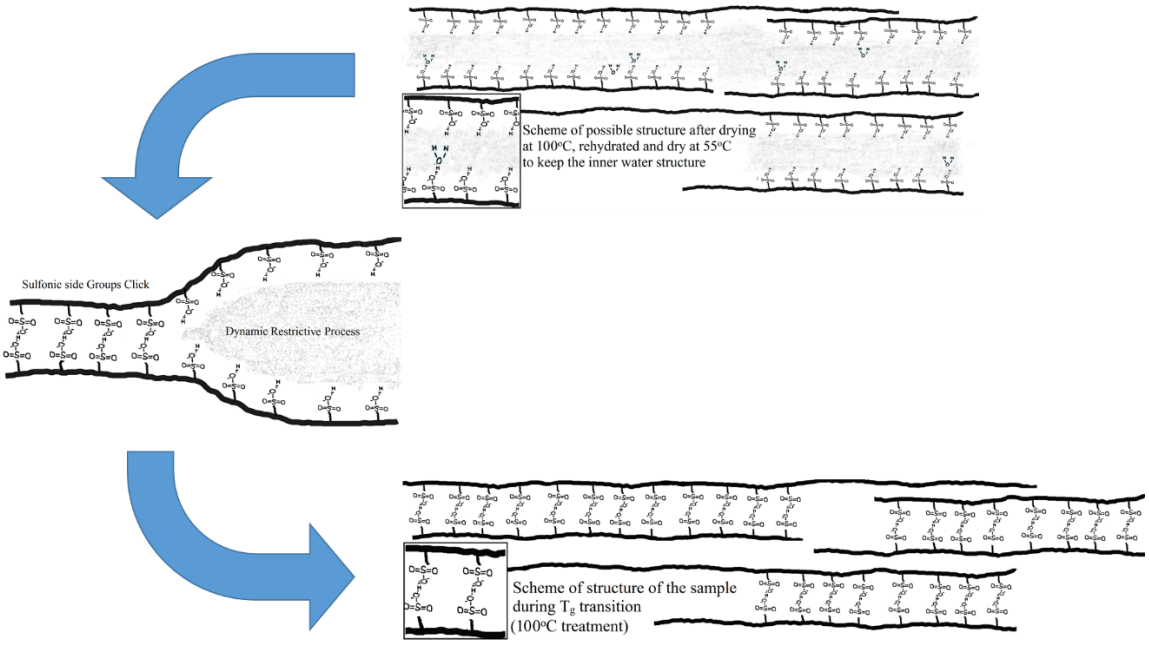

Figure 4.10 *models describing the process occurring in the sulfonated clusters during the heating of the samples after the thermal treatments.*

The α- and α'- relaxation processes times, obtained by H-N, were fitted to the (VFTH) function and the fitting parameters are given in Table 1. It is also possible to calculate an activation energy related to the α'- and α- relaxation processes at a fixed temperature; in this case we have chosen the T_g' and T_g values. For the α'-process the energy minimizes as we approach the treatment temperature range between 80 and 100°C, while for the α-process the energy maximizes in the same temperature range. This energy differential transforms into a maximum of energy between 80 and 100 ºC (see Figure 4.8a); if we believe that an rearrangement is occurring in the clusters, this temperature range should be the one at which the interlocking of the chains occurs faster and will be the one requiring more energy to jump straight from one structure to the other. It is worth mentioning that the relaxation times (τ_{max}) at 100°C for the DRP were not calculated due to their independence with temperature.

Table 4.1 *Parameters, Energies and T_g obtained from the VFTH fitting of the data derived from the H-N relaxation times.*

Thermal Treatment	α'					α				
			E_{VFTH}[(a)(b)]					E_{VFTH}[(a)(c)]		
	-Log(τ_0)	*B*	(kJ/mol)	T_0	T_g'[VFTH]	-Log(τ_0)	*B*	(kJ/mol)	T_0	T_g[VFTH]
sPEEK 55	3.4	70	266	52	67	4.6	86	441	172	209
sPEEK 80	6.3	223	99	81	130	-	-	-	-	-
sPEEK 100	5.0	79	258	67	84	2.9	23	1615	181	191
sPEEK 120	4.5	66	308	66	81	3.3	31	1207	181	194
sPEEK 130	-	-	-	-	-	2.9	8	1222	169	175

[a] The energy was calculated from *B* using the equation shown in the experimental part. The *T* reference used was the T_g' [(b)] and T_g [(c)]. Please indicate the dimensions of the all parameters

If our hypothesis is correct, we should expect an increase in the signal intensity related to the inner phase on SAXS. This would be the case if you have a more aligned phase inside the sulfonated clusters which generate a higher intensity in the scattering of the SAXS (see Figure 4.11). Our results of SAXS show a maximum in the intensity on the sample sPEEK 100. Which should mean that we have an increase of the empty channels left by the water in between the sulfonated chains in the sulfonated clusters.

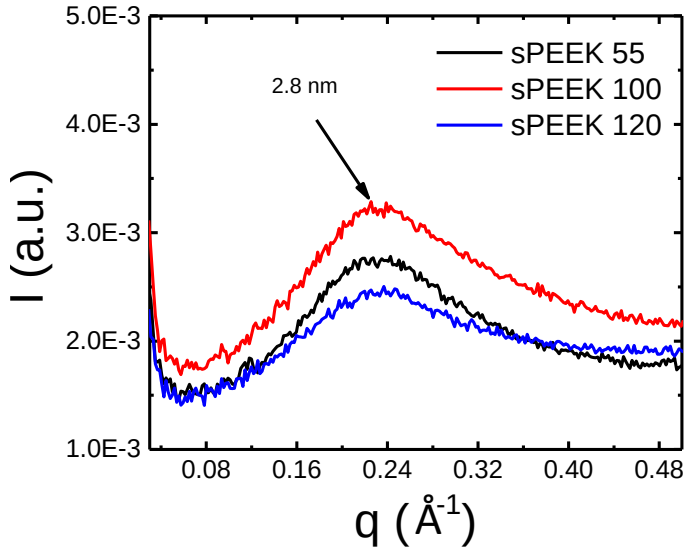

Figure 4.11 *SAXS measurements of samples that were treated with different optimization thermal treatments.*

In concordance with our model, this maximum energy range will represent the optimal conditions for the proton conduction since the pathways for the protons would be at their best percolation point in the sulfonated clusters. It's important to notice that this optimal thermal treatment can occur at any temperature below, equal or higher than the working temperature of the fuel cell since, once the structure is optimized, it won't go through any change unless we go above the working temperature of a normal PEM fuel cell, i.e. between 80 and 100°C.[9, 6] In Figure 4.12b, we show the conductivity results of samples treated at 120°C, which is the typical temperature that is used in the literature, and of our thermal treatment done at 100°C. We also show (Figure 4.9a) the distribution of the relaxation times for the different thermally treated samples at a selected temperature (T =150°C). In this graph it is possible to observe that the optimal value, *i.e.* the lowest relaxation time, lies between 80 and 100°C.

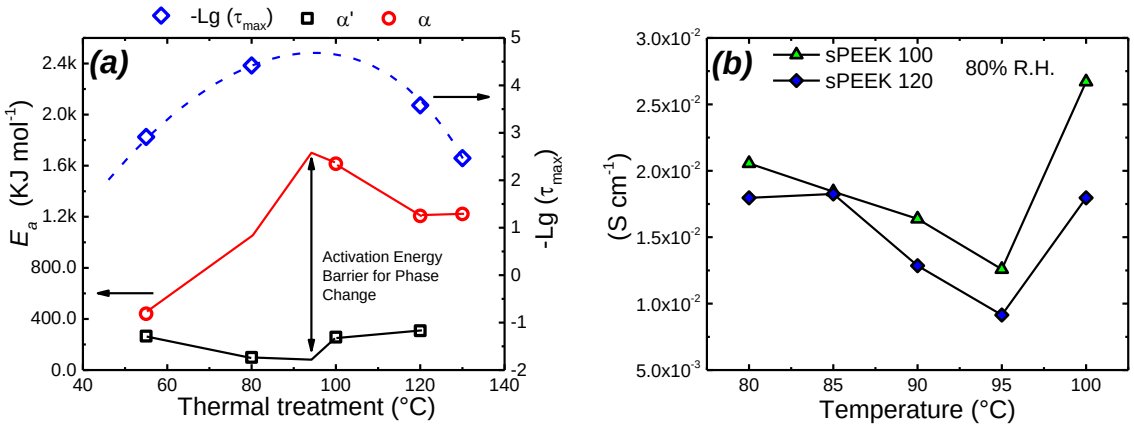

Figure 4.12 *The conductivity optimization process was based on the DRP optimal point. The optimal temperature was found by graphics like (a) where τ_{max} values corresponding to the DRP at 150°C and energies calculated from a'-process for the different thermally treated samples were plotted against the treatment temperature. The (b) plot shows the conductivity measurements obtained from EIS in a temperature and humidity controlled cell for two of the thermal treatments.*

Figure 4.12b shows a particular behavior that differs from the typical plots of the evolution of the conductivity in temperature. The difference could be related to an effect created in the sample by the thermal treatment. Since this

treatment makes changes and order in the sulfonated cluster, it is also possible that it creates partial segregation of this cluster in the polymer. This would mean that even when the sulfonated chains are more aligned inside the clusters, the percolation of this phase throughout the polymer is less connected. This is the reason why, even when higher temperatures increase the proton mobility, the loss of water in the cluster decrease the conductivity in the film. But as we reach 100°C in the measurement a change occurs, this change create a connection between all this clusters increasing significantly the conductivity of our membrane, even in the presence of lower water contents. It has been reported before that water clusters are formed in the inner phase of sPEEK and they connect better as the temperature increase.[27] The reason this happen after this temperature thresh hold can be explain by the Tg of the material being around this temperature under the plasticization effect of the water (see figure 4.3). Going over this transition gives the mobility needed to the polymer to connect the cluster and percolate the water channels in the membrane.

The optimized thermal treatment (sPEEK 100) gives higher conductivities at almost all points compared to sPEEK 120, and they are close to the highest reported value for sPEEK (usually between 1 to 2.5x10^{-2} S/cm). [6,7,9] It should be mentioned that these conductivity measurements were done at 80% relative humidity to ensure stability in the humidity chamber while most of the measurements in the literature are done at 98 to 100% relative humidity.

In order to check the possibility that the sPEEK, under working conditions like the temperature and humidity in the cell, could be able to reach the optimization point achieve by the sPEEK 100 if the sample was treated with temperatures below 100°. A measurement on the conductivity of the sPEEK 55 was done. Figure 4.13 shows the results obtained. The sample is slowly growing in conductivity reaching almost the same value obtained in the treated sample. This was not the case for the sample treated at 120°C. The structures formed at temperatures above the one needed for the optimization, creating a non-order inner phase, can't be modified at lower temperatures.

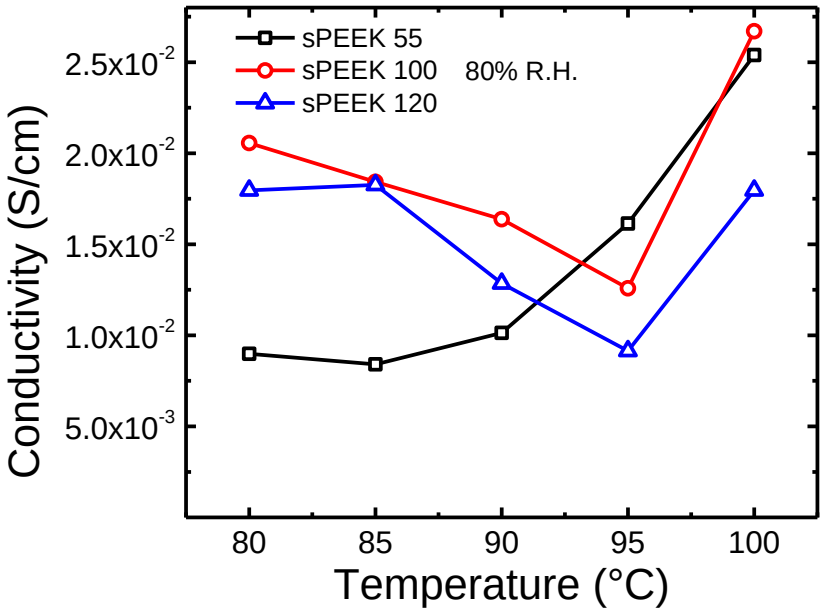

Figure 4.13 *plot showing the changes in the conductivity obtained from EIS measurements in a temperature and humidity controlled cell for three of the thermal treatments.*

Finally, measurements of the water absorption of the sPEEK with different thermal treatments are presented (see figure 4.14). TGA measurements were performed on all the samples which were previous equilibrated at 25°C 100% RH. The typical three weight drops are observed in all the samples. If we focus on the first drop, which is related to the water in the sample, two effects can be identified. sPEEK55 and sPEEK120 behaves very similar in the beginning, by drop 5% in weight before reaching 100°C. The sPEEK100 is able to keep longer the water in the system, and that's visible in the stabilization part of the heating curve around 200°C, when the curves for the sPEEK100 goes below in weight than the sPEEK55. The second important observation is that the sPEEK120 sample has approximately 2.5% more water than sPEEK100, but the conductivity is better for the sPEEK100. The reason behind this contradictory behavior lays on the fact that there is no only one factor guiding the proton conductivity in the membrane. Water

in important in the mobility of protons but also the percolation and order in the inner phase is needed and the presence of the sulfonic groups to promote the protons moving through the water. All of this factors needs to be aligned to obtain an optimal proton conduction.

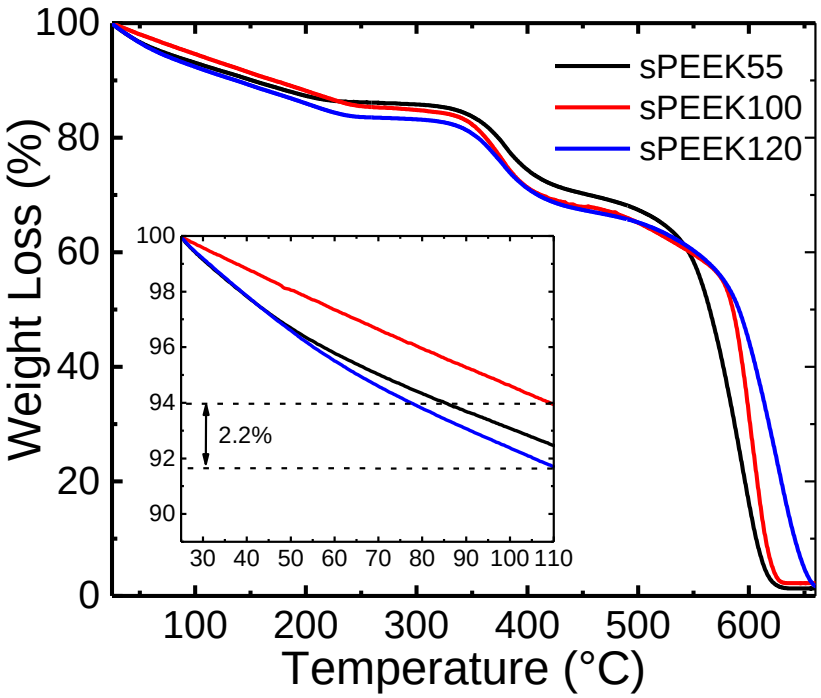

Figure 4.14 *TGA results from sPEEK samples under different thermal treatments and equilibrated in a salt at 100% RH at 25°C before testing.*

4.5. Conclusions

Our overall model presented based on the results obtained from the dielectric measurements, SAXS and DSC were confirmed by the measurements obtained for the conductivity. Every thermal treatments applied to the sample affect its performance during the proton conduction. This is a consequence of the two phases presented on the sPEEK polymer. We develop a methodology which takes in account this changes and its able to follow them and accurate predict at which point we are able to induce the most appropriate inner structure for the sulfonated clusters in the sPEEK at which, not only we will obtain the highest conductivity but also this will happen at 100°C. Which present an important advantage in a working fuel cell.

We also observe that, even when water is one of the main factors for proton conduction, there are other factors that can have a significant impact on the transport of the protons, like an optimal percolation phase. Finally, the behavior observed in the conductivity measurements, it's most likely a consequence of the thermal treatment segregating the sulfonated clusters but, as the mobility in the polymer is regain the percolation of the clusters is clear and the conductivity increase.

4.6. Bibliography

1 Huang, R. Y. M., Shao, P., Burns, C. M. & Feng, X. Sulfonation of Poly(Ether Ether Ketone)(PEEK): Kinetic Study. *J. Appl. Polym. Sci.* **82**, 2651-2660 (2001).

2 Krishnan, P., Park, J. & Kim, C. Preparation of proton-conducting sulfonated poly(ether ether ketone)/boron phosphate composite membranes by an in situ sol–gel process. *J. Membr. Sci.* **279**, 220–229 (2006).

3 Hou, H., Di Vona, M. L. & Knauth, P. Durability of Sulfonated Aromatic Polymers for Proton-Exchange-Membrane Fuel Cells. *ChemSusChem* **4**, 1526–1536 (2011).

4 Di Vona, M. L. *et al*. Analysis of temperature-promoted and solvent-assisted cross-linking in sulfonated Poly(ether ether ketone) (SPEEK) proton-conducting membranes. *J. Phys. Chem.* **113**, 7505-7512 (2009).

5 Kaliaguine, S. *et al*. Properties of SPEEK based PEMs for fuel cell application. *Catal. Today* **82**, 213-222 (2003).

6 Robertson, G. P. *et al*. Casting solvent interactions with sulfonated poly(ether ether ketone) during proton exchange membrane fabrication. *J. Membr. Sci.* **219**, 113-121 (2003).

7 Xing, P. *et al*. Synthesis and characterization of sulfonated poly(ether ether ketone) for proton exchange membranes. *J. Membr. Sci.* **229**, 95-106 (2004).

8 Zhao, C. *et al*. Synthesis of the block sulfonated poly(ether ether ketone)s (S-PEEKs) materials for proton exchange membrane. *J. Membr. Sci.* **280**, 643–650 (2006).

9 Bose, S. *et al*. Polymer membranes for high temperature proton exchange memebrane fuel cell: recent advances and challenges. *Prog. Polym. Sci.* **36**, 813-843 (2011).

10 Ye, G., Janzen, N. & Goward, G. R. Solid-State NMR study of two classic proton conducting polymers: Nafion and Sulfonated Poly(Ether Ether Ketone)s. *Macromolecules* **39**, 3283-3290 (2006).

11 Kreuer, K. & Portale, G. A critical revision of the nano-morphology of proton conducting ionomers and polyelectrolytes for fuel cells applications. *Adv. Funct. Mater.* **23**, 5390-5397 (2013).
12 Yao, Y., Hou, J., Xu, Z., Li, G. & Yang, Y. Effects of Solvent Mixtures on the Nanoscale Phase Separation in Polymer Solar Cells. *Adv. Funct. Mater.* **18**, 1783–1789 (2008).
13 Nishi, T., Wang, T. T. & Kwei, T. K. Thermally Induced Phase Separation Behavior of Compatible Polymer Mixtures. *Macromolecules* **8**, 227–234 (1975).
14 Lodge , T. P., Pudil, B. & Hanley, K. J. The Full Phase Behavior for Block Copolymers in Solvents of Varying Selectivity. *Macromolecules* **35**, 4707–4717 (2002).
15 Gupta, A. K. & Singhal, R. P. Effect of copolymerization and heat treatment on the structure and x-ray diffraction of polyacrylonitrile. *J. Polym. Sci.: Polym. Phys.* **21**, 2243–2262 (1983).
16 ten Brinke, G., Karasz, F. E. & Ellis, T. S. Depression of glass transition temperatures of polymer networks by diluents. *Macromolecules* **16**, 244–249 (1983).
17 Bizot, H. *et al.* Calorimetric evaluation of the glass transition in hydrated, linear and branched polyanhydroglucose compounds. *Carbohydr. Polym.* **32**, 33–50 (1997).
18 Blasi, P., D'Souza, S. S., Selmin, F. & DeLuca, P. P. Plasticizing effect of water on poly(lactide-co-glycolide). *J. Control Release* **108**, 1–9 (2005).
19 Atorngitjawat, P., Klein, R. J. & Runt, J. Dynamics of sulfonated polystyrene copolymer using broadband dielectric spectroscopy. *Macromolecules* **39**, 1815-1820 (2006).
20 Hernández, M., Carretero-González, J., Verdejo, R., Ezquerra, T. A. & López-Manchado, M. A. Molecular Dynamics of Natural Rubber/Layered Silicate Nanocomposites As Studied by Dielectric Relaxation Spectroscopy. *Macromolecules* **43**, 643–651 (2010).
21 Nogales, A. *et al.* Restricted dynamics in poly(ether ether ketone) as revealed by incoherent quasielastic neutron scattering and broad-band dielectric spectroscopy. *Macromolecules* **32**, 2301-2308 (1999).
22 Mikhailenko, S. D., Celso, F., Siqueira Rodrigues, M. A. & Kaliaguine, S. Dielectric measurements of polymer electrolyte based composites as a technique for evaluation of membranes homogenity. *Electrochim. Acta* **136**, 457-465 (2014).
23 Page, K. A., Rowe, B. W., Masser, K. A. & Faraone, A. The effect of water content on chain dynamics in nafion membranes measure by neutron spin echo and dielectric spectroscopy. *J. Polym. Sci.: Polym. Phys.* **52**, 624-632 (2014).
24 Singh, K. P. & Gupta, P. N. Study of dielectric relaxation in polymer electrolytes. *Eur. Polym. J.* **34**, 1023-1029 (1998).
25 Song, J., Shin, J., Sohn, J. & Nho, Y. C. Ionic aggregation characterization of sulfonated PEEK ionomers using by X-ray and DMA techniques. *Macromol. Res.* **20**, 477-483 (2012).

26 Sgreccia, E., Chailan, J., Khadhraoui, M., Di Vona, M. L. & Knauth, P. Mechanical properties of proton-conducting sulfonated aromatic polymer membranes: stress-strain test and dynamical analysis. *J. Power Sources* **195**, 7770-7775 (2010).

27 Yang, B. & Manthiram, A. Comparison of the small angle X-ray scattering study of sulfonated poly(etheretherketone) and Nafion membranes for direct methanol fuel cells. *Journal of Power Sources* **153**, 29-35, doi:http://dx.doi.org/10.1016/j.jpowsour.2005.03.185 (2006).

Chapter 5 Hybrid sPEEK 0.6/$LiBPO_4$ Membranes for Fuel Cells Working at 100°C

This chapter will focus on the development of new hybrid membranes of inorganic fillers within a matrix of sPEEK 0.6. The idea is to improve the conductivity of sPEEK by increasing the water inside the membrane. The membranes inner phase was optimized by using the methodology developed in the previous chapter and the amount of inorganic filler was optimized to the percolation point. An optimal thermal treatment was found to achieve ordering of the polymer inner phase, obtaining a membrane able to show conductivities equal to Nafion under standard working conditions of a fuel cell.

5.1. Introduction

As it was discussed in Chapters 1 and 2, the use of inorganic filler as a way to enhance different properties of the electrolyte membrane for fuel cells has been extensively studied.[1-5] In the case of increasing the proton mobility of the membrane, the inorganic fillers could be used typically via two main approaches. The first one is to have groups able to promote the proton mobility in the membrane, like acidic groups, that activate the protons in the water medium present. The second approach it is to increase the water content of the membrane to facilitate the conductivity of the protons. Under these circumstances, the particle can increase the water content at normal operative temperatures of, e.g. PEM Fuel Cell 85 to 90°C. It is even able to keep the water at higher temperatures than it is usual seen for those membranes, allowing the proton conductivity to further enhance as a results of the higher temperature in the system.[6]

In the case of the sPEEK polymer as a matrix for inorganic fillers, the necessity in the optimization of different factors in the membrane to be an optimal proton conductor was pointed out in Chapter 4 already. Three major parameters were identified as such. The first one is the presence of groups able to activate the proton mobility in the water of the membrane. In the case of the sPEEK this then are the sulfonic groups. Second, the need of percolation of the water channels formed in the polymer to allow the protons to move from one side to the other (Conductivity medium). In the case of inorganic fillers, the addition of the filler needs to reach a value in which the inorganic filler covers all this channels but does not aggregate.[7] Third, the sample has to have its inner structure organized so as to be able to allow protons to move faster and in a shorter way. This was already shown for sPEEK100 in the previous chapter.

For this study, we propose the used of $Li_{3x}B_xPO_4$, hereafter referred to as $LiBPO_4$ as a filler for the sPEEK0.6. The precursor of this filler, BPO_4, has already been proven in other studies that is able to increase the conductivity in the membrane.[8] $LiBPO_4$ has also proven to be able to adsorb water and maintain this

water above 100°C.[9] A percolation threshold for this material needs to be found in the sPEEK matrix and, for this optimal composed membrane, the methodology developed for sPEEK using different thermal treatments and BDS will be applied to check if it's possible to optimize the inner structure of the hybrid electrolyte.

5.2. Experimental

5.2.1. Sample Preparation

The preparation of the various materials does not differ from those reported in the previous chapters. In summary, the sPEEK used is the sPEEK0.6 (see Chapter 3), and the $LiBPO_4$ was prepared following the procedure explained in chapter 3.

The membranes were prepared as it was explained in Chapter 3, and the thermal procedure was the same one used in chapter 4.

5.2.2. Differential Scanning Calorimetry (DSC)

Dynamic heating and cooling measurements were made under inert atmosphere (pure nitrogen). The DSC system used was a Perkin Elmer DSC 7 and the equipment was calibrated prior to being used using indium and tin standards. Measurements were performed at a constant heating and cooling rate of 5 or 10°C/min. For normal pans, 10°C/min was used as heating and cooling rate. A first heating from -5 to 235°C, followed by 5 minutes isothermal treatment, to delete thermal history of the sample, was followed by a controlled cooling and heating. For the sealed pans, 5°C/min was used as heating and cooling rate. Here, a first heating from -5 to 150°C, followed by 5 minutes isothermal treatment, to delete thermal history of the sample, was followed by a controlled cooling and heating.

5.2.3. Thermal Gravimetrical Analysis (TGA)

TGA measurements were done with controlled heating at 20°C/min under an air atmosphere for every sample. All the samples weighted 5 mg, and were cut from the membranes which ran through the thermal treatment explained in the

Chapter 4 and then placed in a saturated solution of Potassium Nitrate salt allowing to equilibrate at 100% R.H. and 25°C.

5.2.4. Electrochemical Impedance Spectroscopy (EIS)

Conductivity measurements were done using an Autolab PGSTAT12 Impedance Spectrometer in the range of $1x10^5$ Hz to $1x10^{-1}$ Hz at 20mV, by using a temperature and humidity controlled, 4 point probe cell in plane measurement. The first resistance was taken as the value for the proton conductivity, i.e. the high frequency touch down in a Nyquist plot. The obtained resistance was then used to calculate the conductivity using equation 3.14 in chapter 3.

5.2.5. Broadband Dielectric Spectroscopy (BDS)

BDS measurements were performed on a BDS-40 high resolution dielectric analyzer (Novocontrol Technologies GmbH). This equipment is composed of an ALPHA type dielectric interface and a QUATRO type temperature controller. The experiments were carried out over a frequency window of $10^{-1} < f/\text{Hz} < 10^7$ (being $F = \frac{\omega}{2\pi}$ the frequency of the applied electric field and ω the corresponding angular frequency) in a temperature range from 35 to 235°C in 5°C steps. The temperature of the experiments was controlled by liquid nitrogen flow, with an error for each range of frequency of ± 0.1°C.

5.3. Results and Discussions

As it was shown before, the use of inorganic fillers to enhance the different properties of the PEM has been extensively studied. The mechanism behind the increment in the mechanical properties of the material is related to the interaction of the polymer with the filler. This interaction is also the reason for the enhancement of the barrier properties for gases, depending on the structure of the filler and its interaction with the polymer. The effect related to the increase of the conductivity has been separated in two, depending on the nature of the filler. The first one is the increment of water in the channels used for the proton

transport, which should increase the conductivity since there is a correlation between the conductivity and the water content in the medium responsible for the transport of the protons. Second, the presence of would be the presence of groups that donate protons to the system, like the sulfonic groups.

In our case, we tried to increase the water content of the membrane using the filler $LiBPO_4$, which is known by previous studies to adsorbed water on its surface.[9] In Figure 5.1, the results from TGA measurements are presented. As it can be seen from the shape of the curve, all of the samples show the 3 typical drops in weight, characteristic for the sPEEK, and which also has been already discussed in Chapter 3. The first drop is related to the water content of the sample, and is the one we will focus on in this discussion. As we can see from the TGA two effects are present in the samples with $LiBPO_4$.The first is that if there is an increase in the amount of inorganic filler above the threshold of 25%, instead of increasing the water content, a decrease is obtained. This could be a consequence of the material aggregation and its preference to interact with itself instead of the water inside the inner phase of the polymer and also, the fact that blockades are generated inside the membrane by the aggregation of the material. The second effect is an increase of the water content with respect to the sPEEK 100, but more precisely there is a significant increase in the water release from the membrane from room temperature until temperatures close to 100°C, which is usually the expected range of operation for fuel cells.

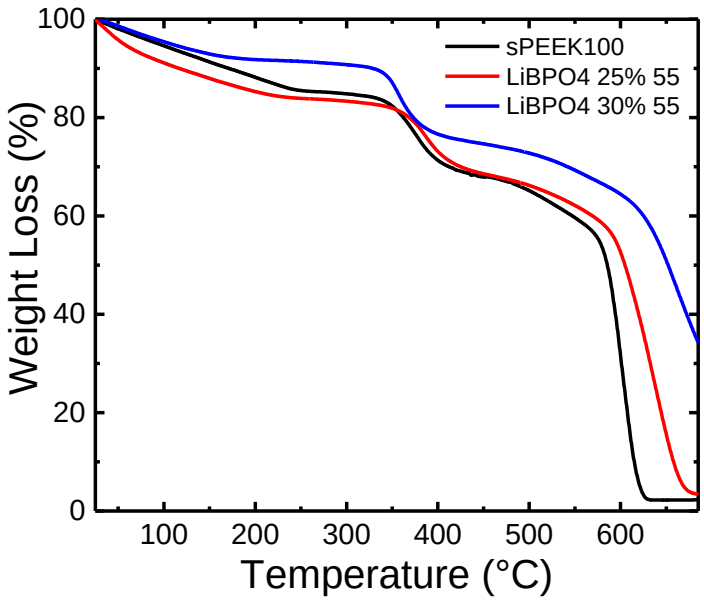

Figure 5.1 TGA result for sPEEK 100 and 25 and 30% $LiBPO_4$ 55 equilibrated at 100% RH at 25°C showing the water content and degradation temperatures of the samples.

TGA results confirms that the filler is capable of increasing the water content in the sPEEK membrane. In Chapter 4 an optimization methodology by thermal treatment was developed for sPEEK membranes. Here, a similar approach was followed for the hybrid membranes to see if it was possible to apply the same methodology towards the optimization of the inner structure of the material. In Figure 5.2, DSC measurements of the sPEEK 100, $LiBPO_4$ 25% 55 and BPO_4 30% 55 are presented. In figure 5.2a, the first heating of the sample shows the presence of the two *Tg*, as it was obtained earlier for the sPEEK in Chapter 4. Here, the *Tg'* is also followed by an endothermic process (called DRP in Chapter 4) and finally a hint of *Tg'* is observed. In Figure 5.2b the second heating only shows *Tg* proving the irreversibility of the process and the relation it has with the thermal treatment. These results are completely similar to the ones obtained in the previous chapter, except that the temperature were it occurs was different.

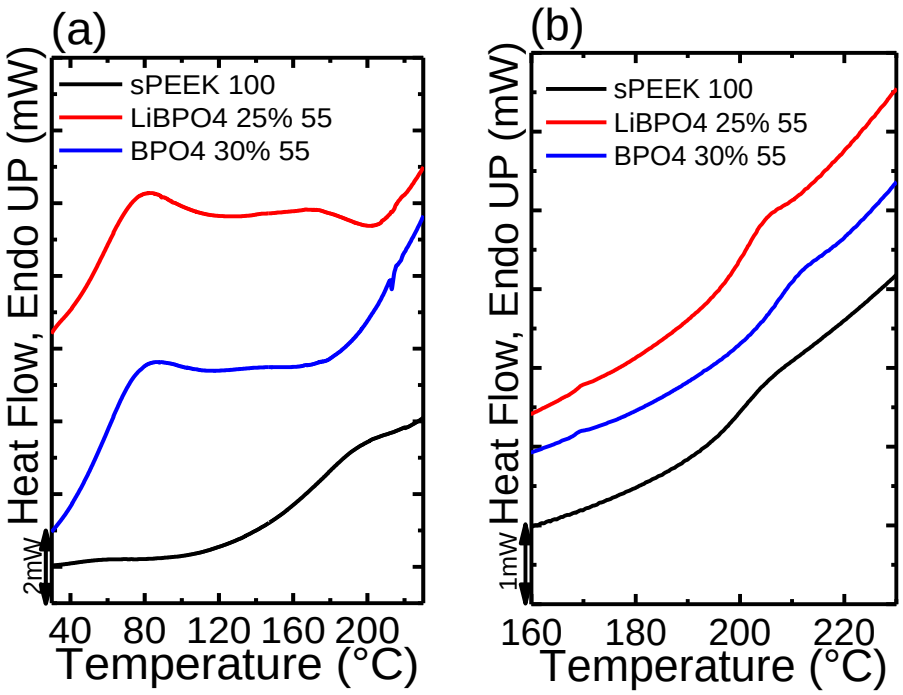

Figure 5.2 Dynamic DSC measurements of sPEEK 100, $LiBPO_4$ 25% 55 and BPO_4 30% 55 after the thermal treatment showing two glass transition temperatures (a) and the not reversible process after the first heating and cooling, on the second heating of the samples (b).

The presence of this *Tg'* at lower values was also confirmed by another DSC measurement. Figure 5.3 shows the second heating of sPEEK 100 and $LiBPO_4$ 25% 55 under different hydration conditions with measurement done in sealed pans to ensure that the water was kept in the sample. The different conditions for the sPEEK 100 shows how the *Tg* change as a consequence of highly different water contents. There isn't any observable change in the *Tg* between the sample with the $LiBPO_4$ and the sPEEK under the same conditions. The difference in the water content is not that significant as we could see from the TGA measurements, and that implies that there is not a big change in the plasticizing effect of the water in the polymer. Also it means that for hydrated membranes at low temperature, the sulfonic groups in the sPEEK interacts with the water and not with the particle. If there would have been an interaction between the particles and the sulfonic groups we would have seen a change in the *Tg* as a consequence of it.

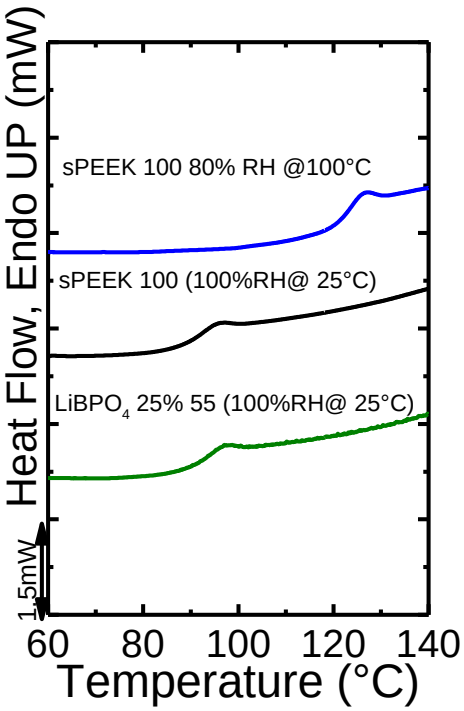

Figure 5.3 Dynamic DSC measurements for different samples using sealed pans to avoid the release of water from the membrane. Different conditions are presented and the depression of the *Tg* in the sPEEK is confirmed.

Taking the results obtained from the DSC into account, it was clear that it was possible to optimize the inner structure of the sulfonated cluster of the membranes with $LiBPO_4$ by following the methodology developed for sPEEK. In order to choose the sample to be optimized, it was assumed that a percolation threshold is required in the composition. To determine this threshold, samples were prepared and the lowest thermal treatment was used for all of them. This was done based on the fact that the organization of the inner phase of the sulfonated clusters can occur during the measurement (see Chapter 4), as long as the thermal treatment for the sample was done at temperature below the ones chosen for testing and there is water in the sample. This is the reason why 55°C was chosen as the temperature to prepare the membranes, and conductivity measurement where performed assuming that we will obtain a maximum in the conductivity for the sample closer to the percolation limit. Figure 5.4 shows the

results obtained for the different samples and it's clear that the threshold happens at 25%.

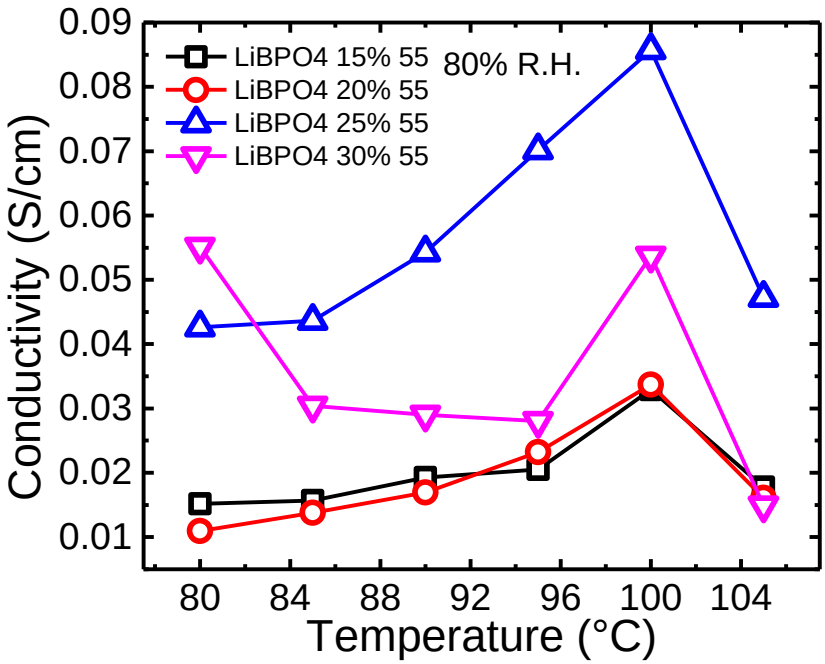

Figure 5.4 Conductivity measurements done under a controlled relative humidity and temperature for the different % of $LiBPO_4$ to obtain the percolation point of the inorganic filler.

Based on the previous result, the $LiBPO_4$ 25% sample was taken to the BDS to determine the optimal thermal treatment. Figure 5.5 shows the 3D plot of the sample with different thermal treatments using the imaginary part of the modulus to enhance the transitions of each sample throughout the temperatures. From the perspective chosen it is clear that the Dynamic Restrictive Process happens faster for the sample $LiBPO_4$ 25% 55 and as it decreases the rate at which occurs as the temperature of the thermal treatment increases.

This means that the inorganic particles affect the temperature at which the inner phase of the polymer align, which can be related to the change in the distance between the sample and the locking of the sulfonic groups, to the inorganic filler this time. The $LiBPO_4$ particles are located in between the channels created by the aligned chains of the polymer and so were able to interact with the sulfonic groups. This can be assumed by the fact that a high percentage of inorganic filler is needed to reach the threshold for percolation, and this is usually

the case for inorganic fillers and polymers that present interaction between each other.[7] Also a soft modification to higher values of *Tg* can be seen in the figure 5.2b. This modification is related to a larger free volume because of the annexation of the inorganic particles to the polymer chain for samples with no thermal history.

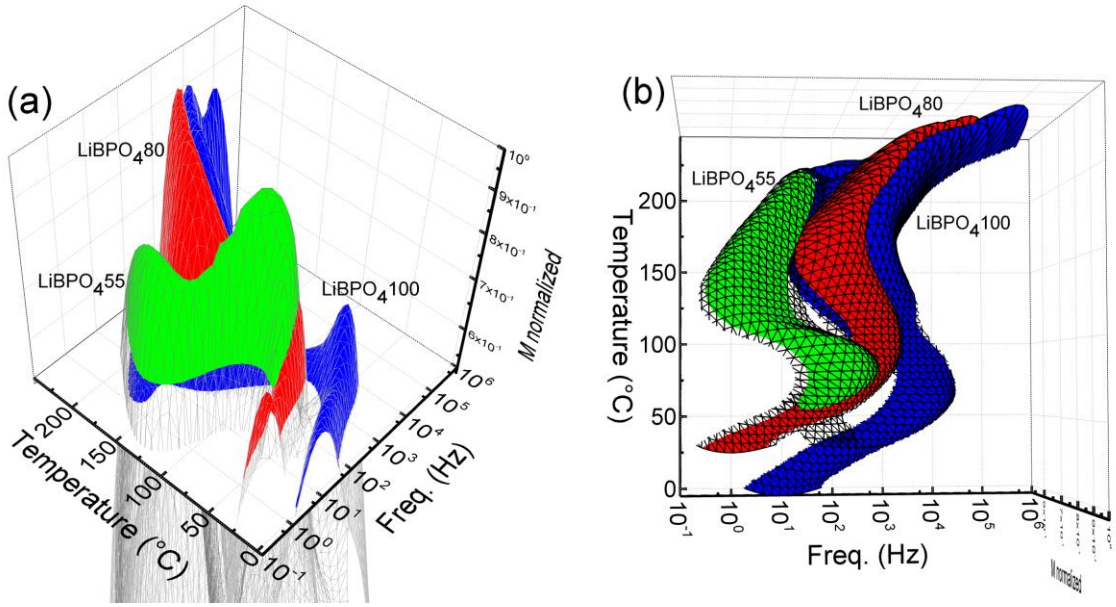

Figure 5.5 3D graph of the imaginary part of the modulus from BDS which enhances the relaxations and transitions observed for the different samples in the dielectric loss. Lateral (a) and upper view (b). The changes in the rate at which the DRP occurs in the samples with $LiBPO_4$ 25% are depicted in the graph.

The dynamic of the molecular relaxation obtained by BDS can be convert to relaxation times, from this times a clearer image of the relaxation process can be seen (Figure 5.6), from fitting the Havrielik-Negame equation to the results according to dielectric loss data derived from the BDS analysis. The times related to the relaxation process can be determined in this way and thus plotted against the temperature (see Fig. 5.6). As it was discussed in Chapter 4, three relaxation processes occur. The first and last are related to the so-called α' and α processes, a consequence of the thermal treatment, which leaves empty channels in the sample from the water extraction, separating the interaction between the sulfonic groups, and, thus, shifting the *Tg* of the polymer. The middle process, i.e. the dynamic restrictive process, is related to the change of the structure happening in

the sample as the temperature raise. The $LiBPO_4$ 25% 55 is the one with the fastest transition between the two phases, which is related to the highest alignment of the sulfonic groups, creating the fastest path for the protons in the membrane.

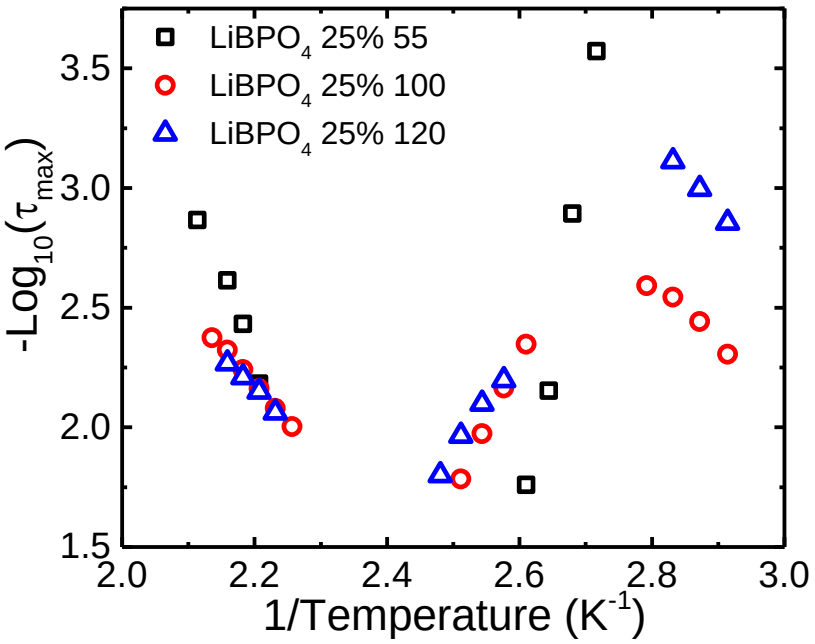

Figure 5.6 Activation plot from the $LiBPO_4$ 25% samples with different thermal treatments where is possible to observe the two alfa relaxation process and the DRP as it was presented before for the sPEEK alone (Chapter 4).

In Chapter 4, it was proven that when there is a maximum in the alignment of the sulfonic groups the DRP, which represent the transition between the two phases, occurs at its highest rate. Since the polymer is able to align itself during the measurements, under humidity and temperatures higher than the thermal treatment, a measurement of the sample treated at 100°C was done even when the results in the BDS were not the optimal under these conditions. The result of the conductivity measurement is presented in Figure 5.7. The conductivity decreases significantly as a consequence of the thermal treatment. The lack of alignment could destroy the percolation creating barriers inside the membrane, damaging the capacity of the membrane to conduct protons.

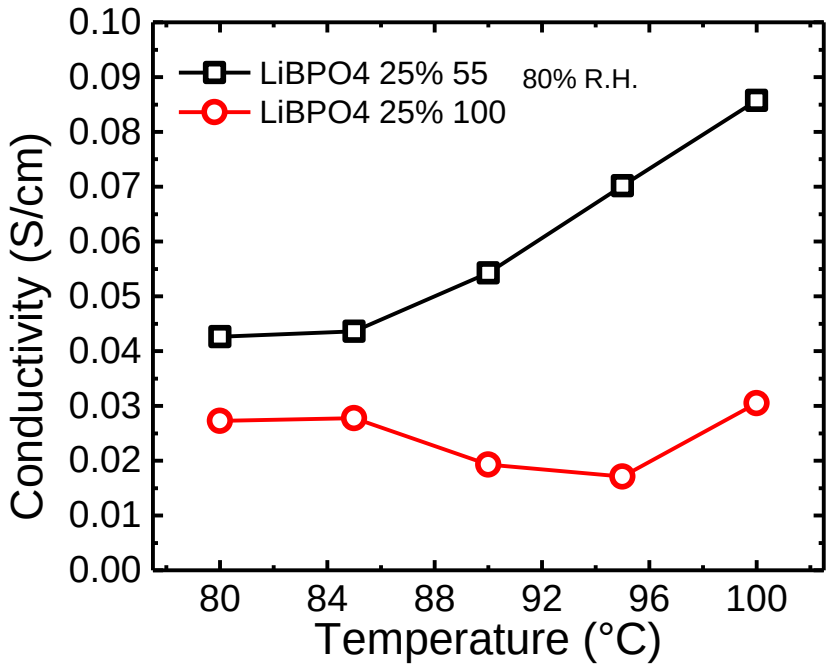

Figure 5.7 Conductivity measurements for $LiBPO_4$ 25% under two different thermal treatments to show the importance of an appropriate order in the inner phase and the capacity of the membrane for conductivity.

Another proof of the importance in the alignment of the inner structure can be concluded from Figure 5.8. Here it is observed that the water content of the $LiBPO_4$ 25% 55 is the same as in the sPEEK 120, and the conductivity of the sample with $LiBPO_4$ is significantly higher than the one presented by the sPEEK 120. The only difference between these samples, if we assume that the water is the main reason for the increase in the proton conduction, is the alignment in the inner structure. This is the same reason behind the higher conductivity presented by sPEEK 100 compared to sPEEK 120. The order in the inner phase is as important as the water content or the presence of the acidic groups to allow the protons to move in the membrane.

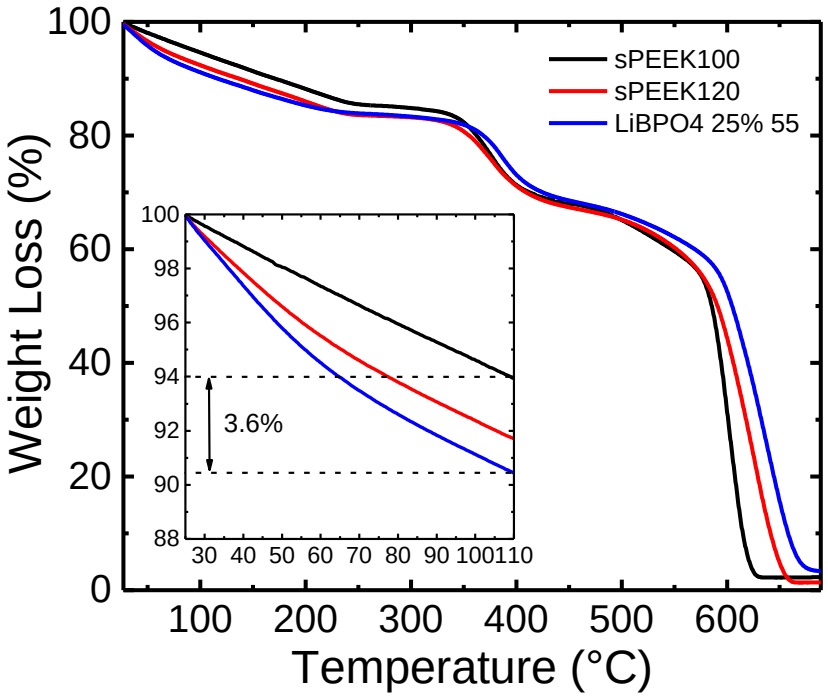

Figure 5.8 TGA measurements comparing the water contents of the different samples and between samples with different thermal treatments.

As it has been observed from all the results, there is an increase in the conductivity of the sPEEK0.6. This increase is a consequence of the presence of a higher water content, orientation of the inner structure of the membrane and the presence of the sulfonic groups free to drive the proton movement in the water through the channels. In Figure 5.9, the increase of the conductivity created by the $LiBPO_4$ is put in perspective. This was done by comparison of the conductivity of different membranes under the same conditions. In the case of the BPO_4 30% 55, the membrane was prepared based on the literature,[8] and actually the conductivity obtained in this report is higher than the one reported by the publication because of the thermal treatment. The strategy to follow for this membrane to increase the conductivity is by adding water to the system. This main reason for this is that the $LiBPO_4$ relies on the fact that the water is absorbed in the particle instead of adsorbed at the surface. The samples are compared with sPEEK 100 to show the increase in the conductivity by the addition of the filler, and to Nafion 117 to validate the measurement with the performance of a

commercial electrode under the same conditions. The increase in the conductivity presented by $LiBPO_4$ 25% 55 is comparable to the conductivity of Nafion 117 at 100°C. It is however important to realise that 100°C is a temperature at which Nafion membranes are not recommended to be used, because of the decay of its mechanical properties.

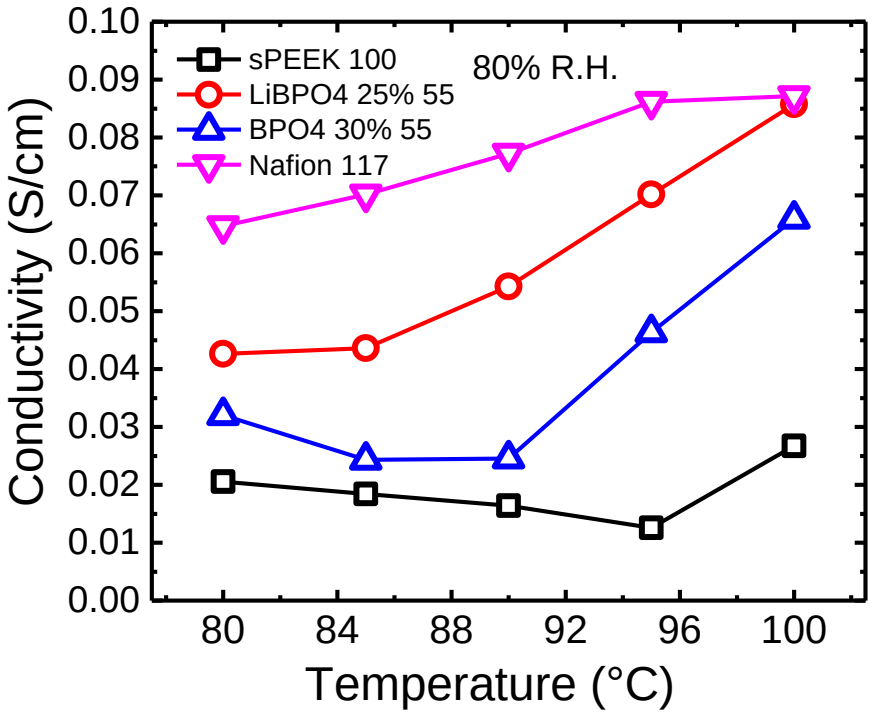

Figure 5.9 Comparison of the conductivity on the optimized sPEEK 100, $LiBPO_4$ 25% 55, BPO_4 30% 55 and Nafion 117 under the same conditions. The increase of conductivity in the sPEEK with the $LiBPO_4$ is able to reach values of conductivity close to Nafion at 100°C.

Finally, in Figure 5.10, a scheme for the inner structure of the sulfonated clusters of the material under the optimal conditions is proposed. Based on the results obtained from the DSC, BDS and conductivity, it is possible to claim that the membrane is oriented in a way that the sulfonic groups are aligned, the water in the membrane is in between the inorganic filler and the sulfonic groups and the amount of water is higher to the one obtained in sPEEK alone. Also, this higher

water content is able to stay up till temperatures of 100°C, which, as it was explained before in Chapter 4, showed to be an advantage for fuel cell operation.

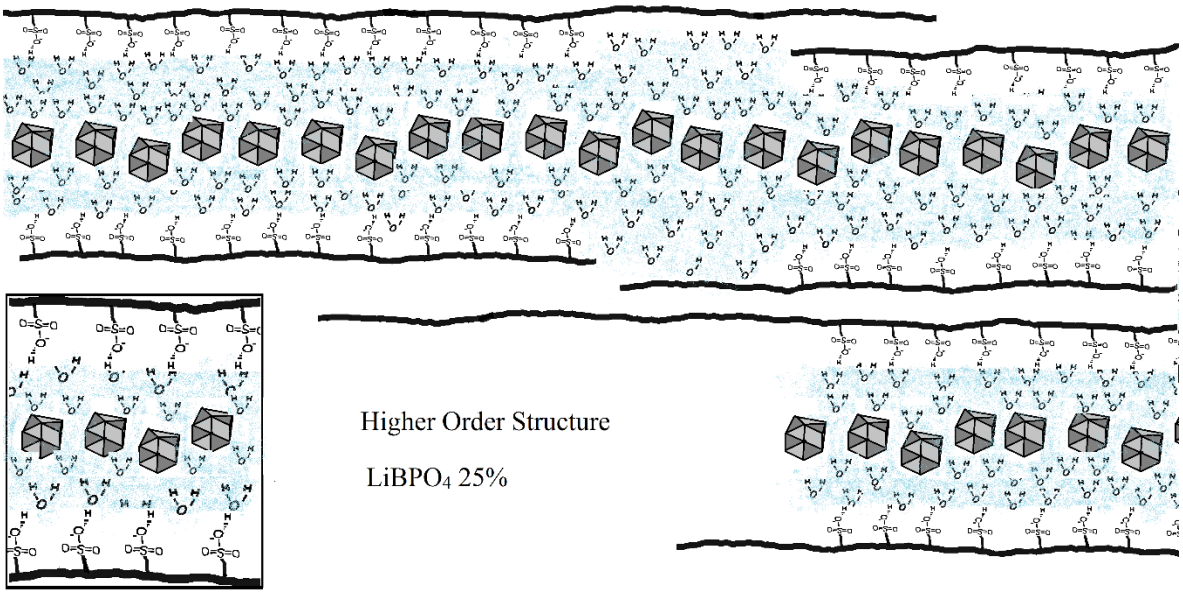

Figure 5.10 Scheme of the possible inner phase of the sulfonated clusters of the sPEEK with $LiBPO_4$ hydrated and after the optimal thermal treatment at 55°C.

5.4. Conclusions

The hybrid membrane composed of sPEEK 0.6 and $LiBPO_4$ is able to retain a higher amount of water in the electrolyte. It is further possible to optimize its inner structure of the sulfonated clusters by following the procedure developed for sPEEK. This then leads to a significant increase in the conductivity making it a competitive option for commercial electrolytes working at 100°C.

Further investigation, under more appropriated fuel cell conditions needs to be performed, but the result obtained and the specific methodology develop for the production of high conducting membranes has been proven to work for sPEEK and hybrid membranes based on it.

5.5. Bibliography

1 Di Vona, M. *et al*. SPEEK-TiO2 nanocomposite hybrid proton conductive membranes via in situ mixed sol–gel process. *J. Membr. Sci.* **296**, 156-161 (2007).

2 Mikhailenko, S., Zaidi, M. & Kaliaguine, S. Sulfonated polyether ether ketone based composite polymer electrolyte membranes. *Catal. Today* **67**, 225-236 (2001).

3 Gomes, D., Buder, I. & Nunes, S. Novel proton conductive membranes containing sulfonated silica. *Desalination* **199**, 274-276 (2006).

4 Du, L., Yan, X., He, G., Wu, X., Hu, Z. & Wang, Y. . SPEEK proton exchange membranes modified with silica sulfuric acid nanoparticles. *Int. J. Hydrogen Energ.* **37**, 11853-11861 (2012).

5 Zhang, Y., Zhang, H., Zhu, X. & Bi, C. . Promotion of PEM Self-Humidifying Effect by Nanometer-Sized Sulfated Zirconia-Supported Pt Catalyst Hybrid with Sulfonated Poly(Ether Ether Ketone). *J. Phys. Chem.* **111**, 6391-6399 (2007).

6 Tripathi, B. P. & Shahi, V. K. Organic–inorganic nanocomposite polymer electrolyte membranes for fuel cell applications. *Progress in Polymer Science* **36**, 945-979, doi:http://dx.doi.org/10.1016/j.progpolymsci.2010.12.005 (2011).

7 Kalaitzidou, K., Fukushima, H. & Drzal, L. A Route for Polymer Nanocomposites with Engineered Electrical Conductivity and Percolation Threshold. *Materials* **3**, 1089 (2010).

8 Krishnan, P., Park, J. & Kim, C. Preparation of proton-conducting sulfonated poly(ether ether ketone)/boron phosphate composite membranes by an in situ sol–gel process. *J. Membr. Sci.* **279**, 220-229 (2006).

9 Jak, M. J. G. *Dynamic Compactation of Li-ion Battery Components and Batteries* PhD thesis, TUDelft, (1999).

Chapter 6 Hybrid sPEEK0.6/Inorganic fillers membranes tested based on water retention principle

This chapter sums up the testing of two other inorganic fillers, $FeSO_4 \bullet 7H_2O$ and nano-diamond made via detonation (Detonation Nano Diamonds). Even though they are present and showing improvements of several characteristics such as an increase in the proton mobility, they were not successful in improving the performance of the sPEEK matrix electrolyte. The reasons for this failure is discussed throughout the chapter and are based on analyzing the principal factors required for conductivity. It was again proposed that not only the presence of water and the increase of its content in the membrane are enough for enhancing the proton mobility, and hence it's conductivity.

6.1. Introduction

As it was discussed in previous chapters, increasing the proton mobility of the membrane using inorganic fillers is a successful way to improve the proton conductivity.[1-3] The selection of the filler could be performed by using different approaches.[4] In our case, we focused on the increase of the water content in the membrane to facilitate the transport of the protons.

Based on this, other design characteristics in the membranes also need to be taken into account. This, as it has been presented in previous chapters, are primary twofold: the percolation of the channels of water, formed in the polymer, allowing to move the protons from one side to the other. In the case of the presence of inorganic fillers, the composition of it in the hybrid membrane needs to reach a value at which the filler is able to position throughout the water channels but does not aggregate.[5] Besides, as it was shown in Chapters 4 and 5, the sample has to have its inner structure organized so as to allow protons to migrate optimally. A poor optimized inner structure will negatively compensate for the improvement as a result of the increase in the water content.

All these characteristic are studied in this chapter for $FeSO_4 \bullet 7H_2O$ (hereafter referred to as $FeSO_4$) and Detonation Nano-Diamond (DND). Two fillers who were considered as good candidates for increasing the conductivity after showing some comparable behavior to $LiBPO_4$ and BPO_4. These fillers failed to improve the membrane and throughout the analysis we address which of the characteristics were needed for increasing the conductivity were missing in each of these hybrid membranes.

6.2. Experimental

The preparation of the various materials does not differ from those reported in the previous chapters. In summary, the sPEEK used is the sPEEK0.6 (see Chapter 3).

The membranes were prepared as it was explained in Chapter 3, and the thermal procedure was the same one used in chapter 4. The measurement of DSC, TGA, EIS and BDS were carried out following the specifications presented in chapter 5

6.3. Results and Discussions

As it was presented in the previous chapter, the characterization process for the other hybrid membranes went through the same steps than those for the ones prepared with $LiBPO_4$. The proposed strategy to increase the conductivity using these fillers, increasing the water content of the membrane and being able to keep it at high temperatures (100°C) was still followed. We would infer, that this water might be used for sharing it with the polymer matrix so as to create a pathway for proton migration.

Here, two fundamental different kind of fillers were used a first one is a hydrated salt ($FeSO_4 \bullet 7H_2O$) having water in the crystal where this water is usually referred to as crystal water, but which may be able to introduce this water in the proton conduction channels. It however, must be considered that the accessibility of this water to the proton conduction is not sure. The second filler is an anhydrous non—oxidic compound formed by detonation referred to as Detonation Nano diamond (DND). In more detail, these nano diamonds are obtained from an oxygen deficient TNT detonation of carbon. The generated high pressures and temperatures allow these nano diamonds to form. It was found that they are embedded in an amorphous carbon macro structure, then consisting of the amorphous carbon, the nano diamonds and several hydrophilic functional groups located at the surfaces of the 200 nm aggregates formed. For a deeper insight in the formation of the particles, the reader is kindly asked to see the process discussed in Chapter 3.

In order to determine the amount of water in the new hybrid membranes, TGA measurements were performed, Figure 6.1 shows the results obtained for the $FeSO_4$ 9% 55, DND 1.5% 55 and DND 2% 55. The selection of these particular compositions was done along the results of the previous chapters, by measuring the conductivities in the different compositions to find the percolation point of the specific filler. These results will be shown and discussed further in this chapter.

From the TGA measurements, it can be concluded that the increase in the water content of the membranes compared to the sPEEK is small. Only for the DND 2% 55 sample, an increment of 2% is observed. The DND 2% 55 also presented the loss of most if its water at temperatures below 100°C. In the case of the $FeSO_4$ 9% 55, the difference in the water content can only be observe at high temperatures: 240°C, where you have a fast loose of weight (arrows Figure 6.1)and where a difference in the stabilization line, before the degradation, is noticeable. These results lead us to think that the water in the case of the $FeSO_4$ is able to stay in the membrane even at relative high temperatures. For the DND 1% the change is negligible. Even with this result, it is possible that the insertion of the fillers increase the size of the channels for proton conduction, favoring the increase in the conductivity.

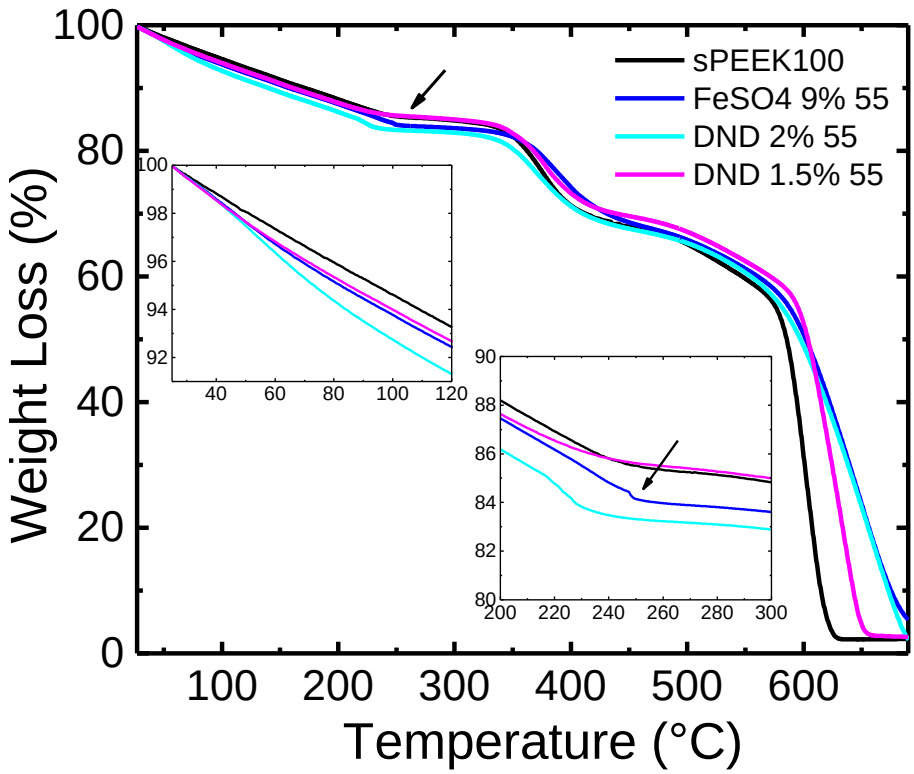

Figure 6.1 *TGA measurement of selected compositions of the hybrid membranes with $FeSO_4$ and DND and sPEEK equilibrated at 100% R.H. at 25°C.*

After TGA measurements it is possible to conclude that both inorganic fillers are capable of increase the water content in the membrane. Although, only the $FeSO_4$ 9% 55, at high temperatures (220°C), is able to reach water content close to the ones found with the $LiBPO_4$. The next step was to verify if it was possible to use the optimization strategy developed in Chapter 4. The first analysis was done using DSC measurements and trying to obtain result similar to the ones seen for the sPEEK and the $LiBPO_4$. In Figure 6.2, DSC measurements for both inorganic fillers, with different thermal treatments, are shown. The samples present both glass transitions *Tg'* at low temperature and *Tg* at high temperature, and also the endothermic process in between these glass temperatures. In the second heating the only transition observed is the expected sPEEK's *Tg*. This was expected as a result of the irreversibility of the thermal treatment process. Based on these results, an optimization process could be created following the BDS results and the different thermal treatments, as already proposed in Chapter 4.

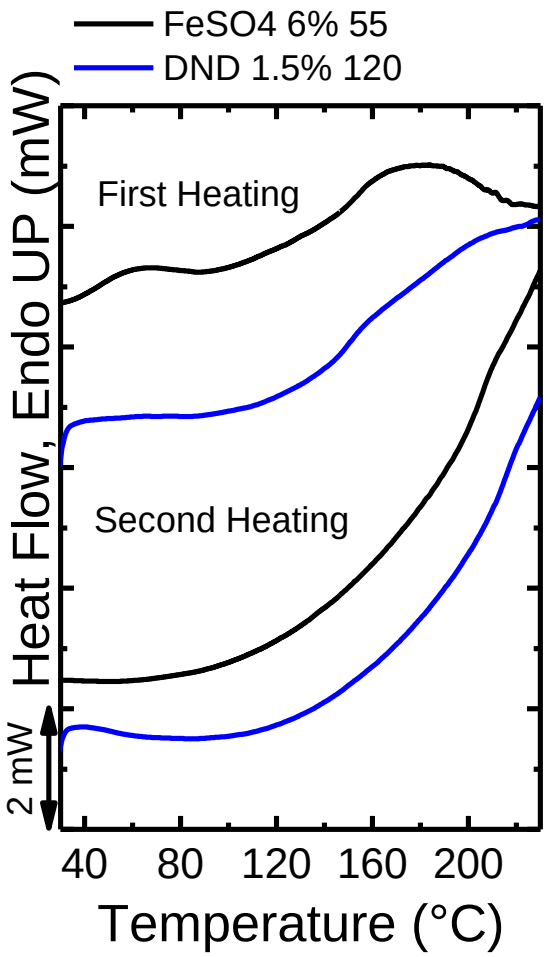

Figure 6.2 *Standard dynamic DSC measurements showing the first and second heating of the two hybrid membranes after the application of the thermal treatment explained in Chapter 4.*

6.3.1.1. Optimization for the $FeSO_4$

The optimization process for $FeSO_4$ was tried for all the different compositions. These various compositions were the measured on their conductivity so as to obtain the percolation threshold and then to make decisions which sample is the optimal one.

In Figure 6.3, two measurements were plotted in 3D, using the imaginary component of the Modulus. This variable has the advantage of enhancing the relaxation process occurring in the sample and make them more visible. Three zones can be identified in the 3D plots. The first, in the temperature range of 50

to 150 °C, its where the α' relaxation occurs, we can see the increase on the blue part section in the 3D plot to higher frequencies as the temperature increases and it reaches a plateau. The second zone is then between 150 and 200 °C and it's characterize by a sudden fall in the signal (blue surface) to lower frequencies. This is where we believe the phase change occurs in the membrane (refer to as the DRP in previous chapters). And finally the zone from 200 to 230°C where another relaxation process takes place, showing and increase in the signal to higher frequencies (α process). It is clear from the figures that both of the samples are in the optimal thermal treatment. The instant jump from one phase to the other shown by the sPEEK 100 is also observed here for the $FeSO_4$ 6% 120 and $FeSO_4$ 9% 55, but obviously shifted. This implies that the content of inorganic filler is able to modify the conditions at which the phase transition of the polymer occurs.

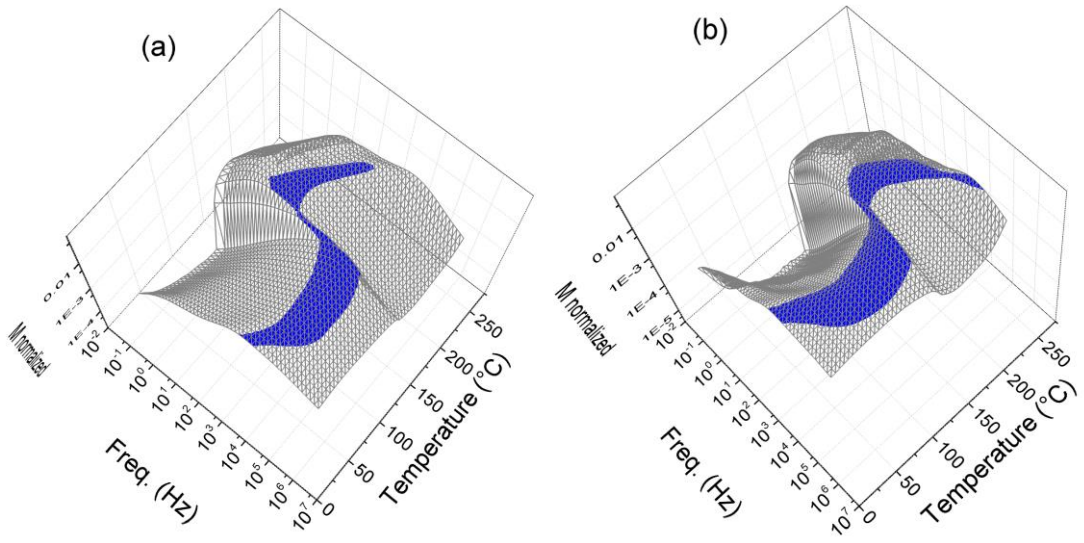

Figure 6.3 *3D plots of the imaginary part of the modulus obtained from the measurements of BDS of the $FeSO_4$ under two different thermal treatments (see chapter 4) a) 120°C and b) 55°C. The imaginary part of modulus is used because its ability to enhance the relaxation process in the sample.*

Although, it is important to remember that also the percolation threshold of the filler in the sPEEK phase needs to be reached in order to obtain the best conductivity that the hybrid membrane can deliver. For this it is necessary to measure the conductivity of the different compositions and find the one with the best performance. In Figure 6.4, the conductivity measurement of the different

compositions are shown and the results clearly state that the $FeSO_4$ 9% 55 gave the highest performance with respect to the proton conductivity. Once again the distinctive behavior of the segregated cluster explained in chapter 4 is also shown here. In the case of the $LiBPO_4$ this methodology was checked later, and it was found that the optimum for every membrane was always below 100°C. Since the conditions for the thermal treatment needs the membrane to have unlocked the sulfonic groups (which is the case under hydration state) and needs long times at certain temperatures to create the order in the inner phases of the sulfonated clusters, all this conditions could also be reach during the equilibration on the conductivity cell, as long as the optimal conditioning occurs below 100 °C and the equilibration process includes enough time and the right temperature for the optimization. The previous state described is the one you could achieve while equilibrating the membrane in a measurement cell under hydration conditions previous performing the conductivity measurements, since usually one measure from 55 to 100°C increasing 5 degrees between each measurements. (See chapter 4)

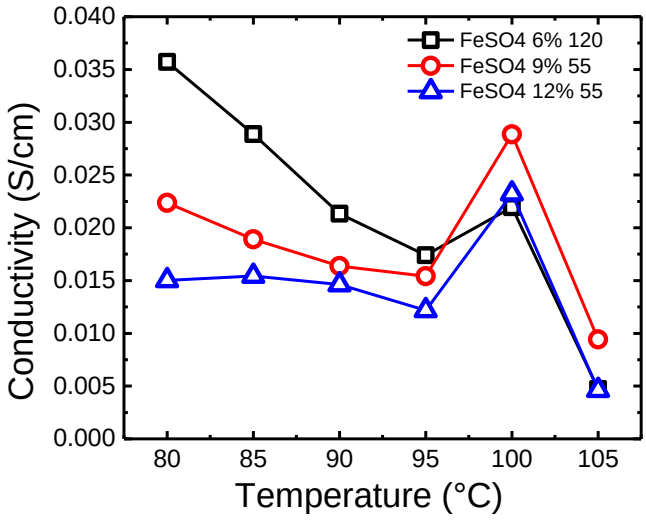

Figure 6.4 *Conductivity measurements from the $FeSO_4$ hybrid membranes at different compositions. Every composition was optimized using the procedure shown in chapter 4. The measurements were done using EIS in a 4 point probe cell with temperature controlled and 80% R.H.*

6.3.1.1. Optimization for the DND

By achieving the optimal conductivity for DND, the same procedure as above. The actual difference relies on the fact that the optimal point could not be reached, because as it happens with the $LiBPO_4$, it is below 55°C. In all the samples, the same trend was found. Figure 6.5 shows the 3D graphic of the BDS modulus measurement for the DND 1.5% 55. The double peak at high temperature is related to the interaction of the particle and the polymer which creates an interphase that has a different relaxation process parallel to the normal *Tg*.[6]

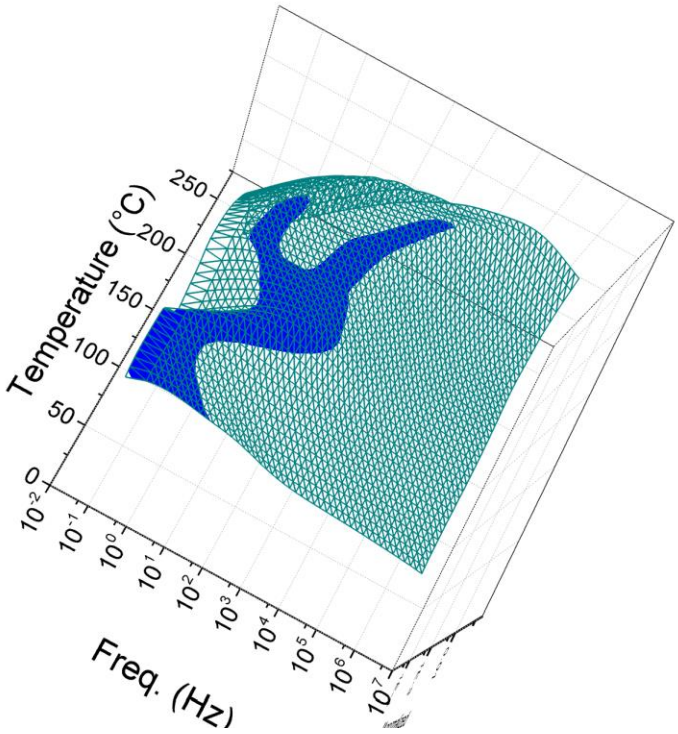

Figure 6.5 *3D plots of the imaginary part of the modulus obtained from the measurements of BDS of the DND 1.5% after thermal treatments (see chapter 4) at 55°C. The imaginary part of modulus is used because its ability to enhance the relaxation process in the sample.*

After these measurements all the thermal treatments where done at 55°C after which the conductivities where measured. No significant change in the conductivity was found in the range between 80 to 100°C. Therefore, measurements were performed at lower temperatures in order to obtain any changes in the conductivity at those temperatures which are less relevant for actual fuel cell operation. The results of this measurements are shown in the

Figure 6.6. The values for the conductivity at 100°C is higher for the DND 2% 55 but at low temperatures it is even higher for the DND 1.5%. From the previous TGA measurements it was clear that the DND 2% was able to introduce more water in the system than the DND 1.5% and that is possibly the reason for the higher conductivity of this sample at 100°C. The eventual higher conductivities at low temperatures are out of the scope of this chapter, and of the thesis in general. Nevertheless, it is possible that some interest could exist on the development on good conductivities at room temperature, but in the case of fuel cells, it will mean a very complicated water management and higher possibilities of platinum contamination with CO_2 in the electrodes.

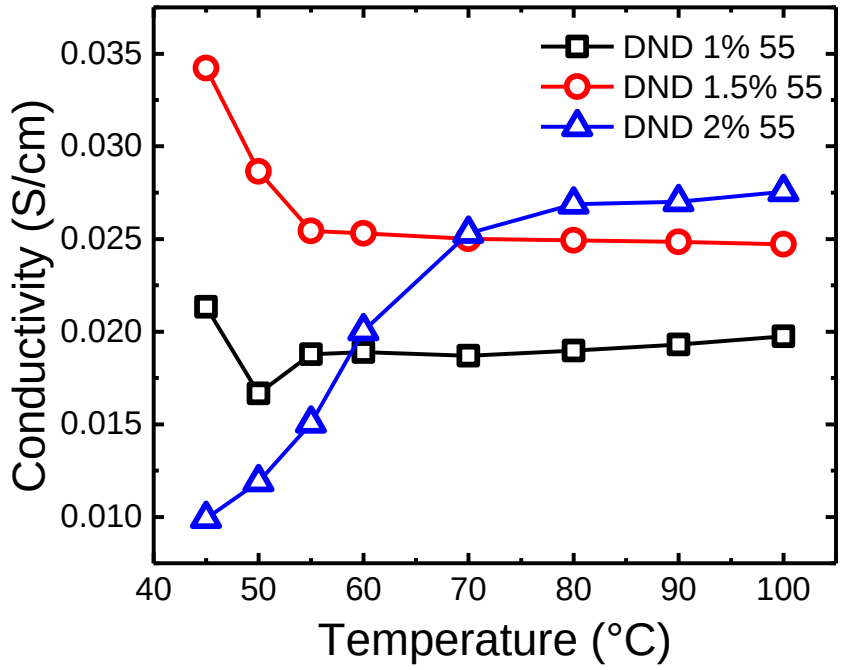

Figure 6.6 *Conductivity measurements from the DND hybrid membranes at different compositions. Every composition was optimized using the procedure shown in chapter 4. The measurements were done using EIS in a 4 point probe cell with temperature controlled and 80% R.H.*

Finally, a comparison between the best performing hybrid membranes was done together with the pristine sPEEK. In Figure 6.7 the results of the different conductivities can be observed. In the range of interest for this work, which is 100°C, there is a miniscule increase in the conductivity compared to sPEEK 100.

These inorganic compounds, even being able to increase the water content in the membrane after being optimized of its inner phase, could not succeed in increasing the overall proton conduction in the membrane. This could be due to various reasons. For instance, in the case of the DND, it could be that the water added by the filler was not enough to create a change in the mobility. For the $FeSO_4$, there was a significant amount of water in the membrane, as shown in the TGA results, apparently it was not accessible for proton conduction. It might also be so for $FeSO_4$ filler that the particle links to the sulfonic groups, and thereby deactivating the mechanism of the membrane for the water protonation, i.e. suppressing the proton donation to the system.

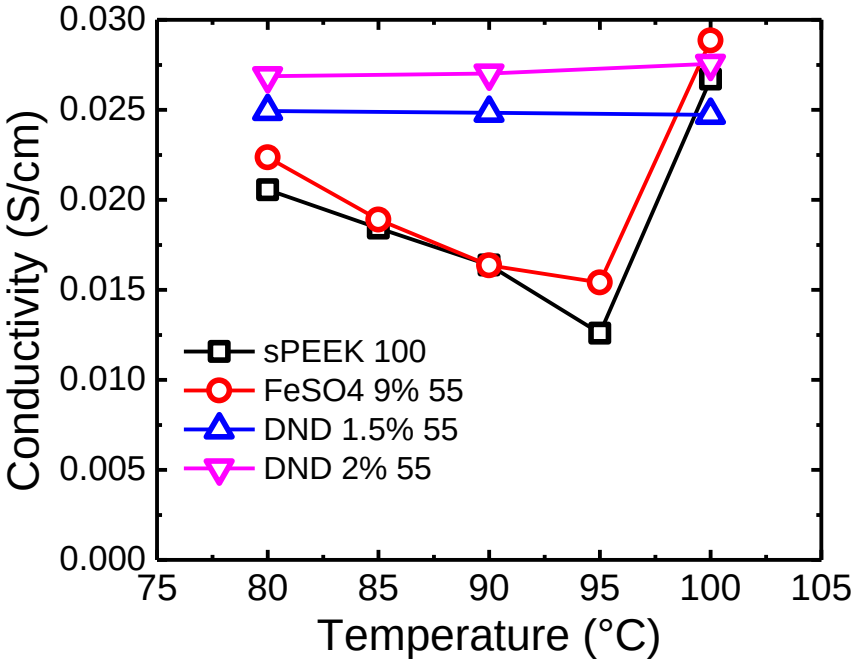

Figure 6.7 *Conductivity measurements comparing the hybrid membranes to sPEEK 100. Every composition was optimized using the procedure shown in chapter 4. The measurements were done using EIS in a 4 point probe cell with temperature controlled and 80% R.H. (try to work with other salts to see if it's related to the crystal structure of the water in the ionic crystal)*

6.4. Conclusion

The mobility of protons in a polymer electrolyte is dominated by different factors and all of them need to be present and tuned up to its best in order to succeed in enhancing the conductivity. In this case we were able to achieve a

percolation threshold, to optimize the inner phases of the sulfonated clusters, and to increase the water content. Unfortunately, some other factors were more important that could not be avoided. For the detonation nano-diamond, insufficient amount of water was available. For the $FeSO_4$, the water was in the membrane but it was not accessible for the proton conduction, hence, it was too strongly bound as a ligand to the iron ions. Besides, due to the interaction with the polymer, it might influence the deprotonation of the sulfonic groups and thereby reducing the number of available protons for conduction. These factors need to be further studied controlling all the different variables in the system, focusing on increasing the number of charge carriers, i.e. the protons, and increasing the mobility for them via well-defined and optimized conduction pathways.

6.5. Bibliography

1 Di Vona, M. *et al*. SPEEK-TiO2 nanocomposite hybrid proton conductive membranes via in situ mixed sol–gel process. *J. Membr. Sci.* **296**, 156-161 (2007).

2 Mikhailenko, S., Zaidi, M. & Kaliaguine, S. Sulfonated polyether ether ketone based composite polymer electrolyte membranes. *Catal. Today* **67**, 225-236 (2001).

3 Gomes, D., Buder, I. & Nunes, S. Novel proton conductive membranes containing sulfonated silica. *Desalination* **199**, 274-276 (2006).

4 Kreuer, K. & Portale, G. A critical revision of the nano-morphology of proton conducting ionomers and polyelectrolytes for fuel cells applications. *Adv. Funct. Mater.* **23**, 5390-5397 (2013).

5 Kalaitzidou, K., Fukushima, H. & Drzal, L. A Route for Polymer Nanocomposites with Engineered Electrical Conductivity and Percolation Threshold. *Materials* **3**, 1089 (2010).

6 Mikhailenko, S. D., Celso, F., Rodrigues, M. A. S. & Kaliaguine, S. Dielectric Measurements of Polymer Electrolyte Based Composites as a Technique for Evaluation of Membrane Homogeneity. *Electrochimica Acta* **136**, 457-465, doi:http://dx.doi.org/10.1016/j.electacta.2014.05.040 (2014).

Chapter 7 Interaction between sPEEK06 and Inorganic Nanoparticles and its effect on the increase of conductivity studied by BDS

This chapter tries to give an insight into how the interaction of the inorganic particles and its nature can affect the possible increase in the conductivity of sPEEK's based hybrid membranes used as electrolytes in fuel cells. Two techniques are selected in order to study this interactions, Differential Scanning Calorimetry and Broadband Dielectric Spectroscopy. With the use of these techniques, it is possible to follow the changes in the glass transition temperatures of the material under a set of conditions. The results are then used to better understand the reasons behind the differences between two inorganic fillers, $LiBPO_4$ and $FeSO_4$. In principle they showed the same characteristics, i.e. an increase in the membrane's water content, which has been proven to allow to increase the conductivity, but both fillers contribute to that by different means.

7.1. Introduction

The particle interaction in the hybrid polymers membranes has been studied to find a trend of how it affects the polymer behavior positively or negatively.[1-5] This interaction has an impact on the mechanical and electrical properties of the material,[5,6] making the understanding of these interactions of utmost importance to future design of materials used as electrolytes.

Throughout this dissertation, it has been claimed that, at least in the case of sPEEK, two glass transition temperatures are present in the polymer. This was observed if we heat the material up after being under the hydrated conditions of a working fuel cell. A transition at lower temperatures, which it is referred to as *Tg'*, created by breaking up the interaction between the sulfonic groups among the polymer chains , and, is the one that will affect the behavior of the electrolyte under working conditions of the fuel cell. In that respect, it is strange that in the literature, the studies are merely focused on the changes in the high temperature *Tg*.[7,8]

In the case of the hybrid membranes, the interaction of the particle with the polymer can change under different conditions. To recall a few, when there is water in the electrolyte, when there are channels left in the membrane by water extraction (what we take as *Tg'* conditions), or when only the *Tg* appear in the polymer (no thermal history in the material at low temperatures). The reason for this is simple. If there is any interaction of the inorganic particles with the sulfonic groups, it needs to be stronger that the interaction of these groups with the water in order to be able be maintained in hydrated conditions. In the other two cases there should be some compatibility between the surface of the particle and the sulfonic groups to obtain any changes.

The study of these interactions can be done through different measurements and then focusing on different properties.[5,6] In the case of DSC and BDS, usually

the glass transition temperature can be followed as well as the changes in the molecular dynamics related to interphases between the polymer and the particles. For the sPEEK, if there is an interaction of the inorganic particles with the polymer in the presence of water, a change in the temperature of *Tg'* should occur. Also if the water has been removed from the electrolyte this interaction should be present. The addition of particles linked to the sulfonic groups will imply an increment in the free volume of the chain of the polymer, becoming more rigid, and increasing the temperature needed to overcome this transition. On the other hand, if this interaction is not present, *Tg'* should stay at the same values.

In the case of the water in the polymer, this acts as a plastizacer. There is a saturation point in which the *Tg'* won't change more, but at lower concentrations, shifting of the *Tg'* to higher temperatures will mean that there is less water available in the membrane for proton conduction, either for creating the conduction pathway or for increasing the number of proton charge carriers via (de)protonation. In our case, we used DSC and BDS to follow the changes in the *Tg'* of two hybrid membranes as presented in the previous chapters concerning $LiBPO_4$ and $FeSO_4$. In both cases the water content of the membrane was increased, but only $LiBPO_4$ was able to increase the conductivity of the membrane to values close to Nafion, while $FeSO_4$ did not affect the conductivity of the membrane at all. Hence, with the use of DSC and BDS, we were able to reveal the reasons behind these different results.

7.2. Experimental

The preparation of the various materials does not differ from those reported in the previous chapters. In summary, the sPEEK used is the sPEEK0.6 (see Chapter 3), and the $LiBPO_4$ was prepared following the procedure explained in chapter 3.

The membranes were prepared as it was explained in Chapter 3, and the thermal procedure was the same one used in chapter 4. The measurement of DSC and BDS were carried out following the specifications presented in chapter 5

7.3. Results and Discussions

In order to determine the possible interactions of the inorganic particles with the polymers we are going to focus on two fillers, $LiBPO_4$ and $FeSO_4$. These fillers are able to increase significantly the water content in the sPEEK membranes, as it has been shown before in measurement done by TGA. These two fillers present an interesting behavior to study, since both of them increase the water content, but only the $LiBPO_4$ was able to increase the conductivity of the sPEEK. To understand the changes in the interaction, we will focus on the *Tg'*, as we believe this *Tg'* affect the parameters due to the temperature where it occurs, we will compare them with pristine sPEEK to understand what has changed in the polymer, as a consequence of the presence of the fillers.

In Figure 7.1, the DSC measurements for the three optimized samples are presented. The first heating after the thermal treatments are shown for the three samples. All of them present the same behavior as it was also shown in the previous chapters. From the figure we can see that the *Tg'* of the sPEEK and the $FeSO_4$ are at almost at the same value, whereas the *Tg'* of the $LiBPO_4$ appears to occur at higher temperatures, the transition its intense and more broad than for the other samples. The change in the behavior of the *Tg'* in the $LiBPO_4$ membranes, indicates that there is an impact on this transition as a consequence of the presence of the inorganic filler.

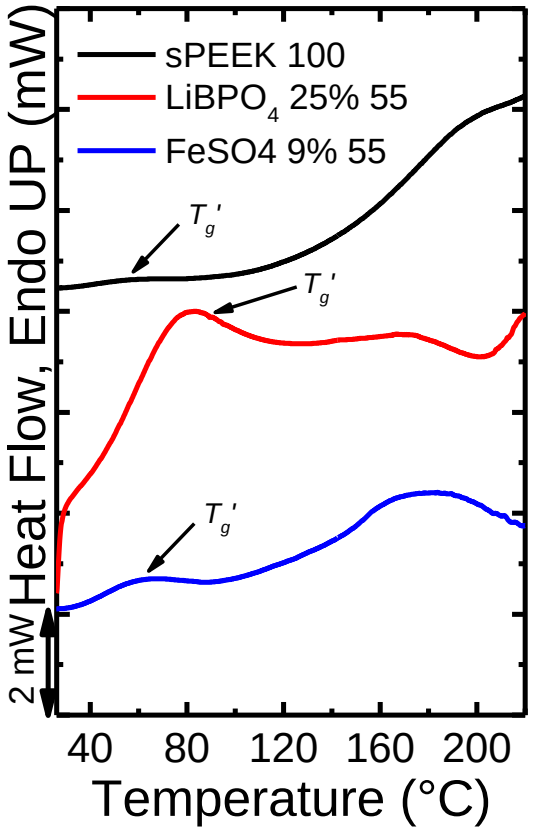

Figure 7.1 *First heating on dynamic DSC measurements for different membranes after applying the optimal thermal treatments for each sample.*

Figure 7.2 presents the results in a 3D graph of the relaxation processes observed in the samples. This graph is constructed by taking the loss modulus from the data obtained by BDS, which enhances the relaxation process so they can become more visible. In Figure 7.2a we show the sPEEK100 and the $FeSO_4$ 9% 55 and in Figure 7.2b we show also the $LiBPO_4$ 25% 55 together with the other two samples. The behavior of the sPEEK100 and the $FeSO_4$ 9% 55 are quite similar. The biggest difference is on the *a'*, which is the dielectric relaxation transition observed by BDS and directly related to *Tg'*. For the sPEEK100, the relaxation process is clearly visible, while for the $FeSO_4$ 9% 55 it is not observed. Actually it was not possible to fit the results according to the Havrileak-Negame equation. This could be due to the presence of water in the sample. We heated up the samples to 55°C in a vacuum oven to subtract the water but, from the TGA measurement, we observed that the water in the $FeSO_4$ has been strongly bound

since the temperature needed to go up above 200°C to see a final stabilization in weight loss.

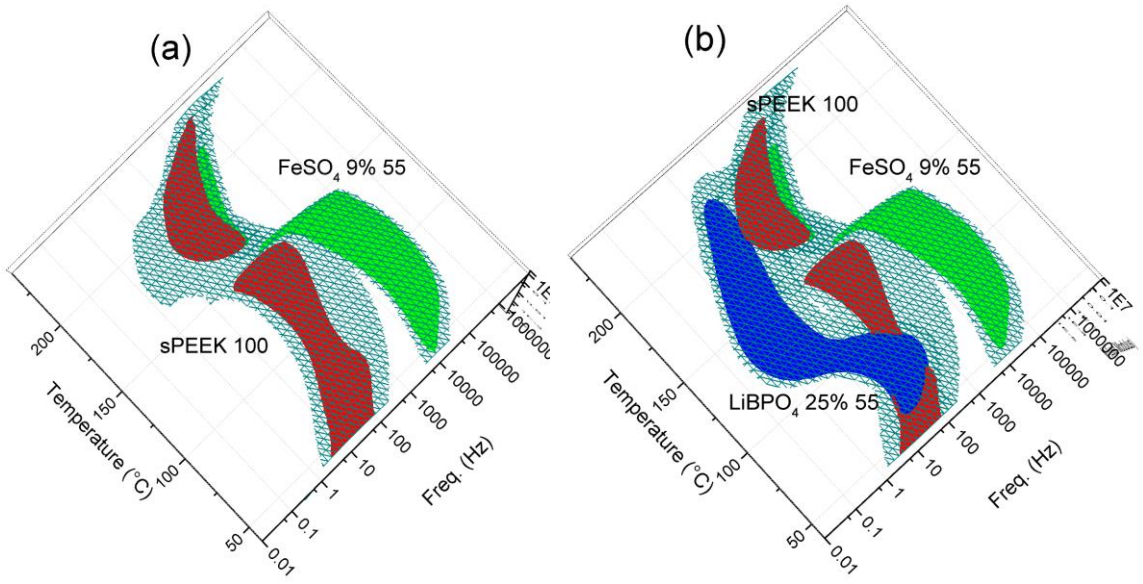

Figure 7.2 *3D images of the evolution of loss modulus as a function of temperature and frequency for a) $FeSO_4$ 9% 55 and sPEEK 100 and b) the two previous samples and $LiBPO_4$ 25% 55. The views from the top allow us to see the range at which the relaxation occurs so as to compare these between the samples.*

When the $LiBPO_4$ 25% 55 is incorporated in the figure we clearly observe that *a'* is present around the same values as in the sPEEK 100 but the dynamic restrictive process (a) actually starts at lower temperatures for the $LiBPO_4$ 25% 55 than for the other two samples. This is related to the fact that we could not reach the optimal treatment in the $LiBPO_4$, i.e. the change in the phase that creates the *a* relaxation (directly related to *Tg*), which always terminates at 150°C for all the samples. The rate at which this change occurs is dependent of the thermal treatment, as it was explained in Chapter 4. In the case of sPEEK and $FeSO_4$, they already are at the optimal value so here a direct jump from one phase to the other at 150°C is observed.

To this point we agree on the fact that there is no interaction between the particles and the sulfonic groups in the sPEEK at low temperatures. No change in the *Tg'* was observed. Also no interphase was detected by BDS. Since both fillers interact in the same way with the polymer and increase the water content: then

still the question remains what is the reason behind the low conductivity in the hybrid membranes with $FeSO_4$? To try to find out the answer, we go to Figure 7.3, which shows the DSC dynamic measurements of the different hybrid samples including the sPEEK, equilibrated at the same humidity and then sealed in hermetic pans. This strategy forces the water to stay in the polymer allowing us to observe the *Tg'* created by the water channels in the membrane. As we could expect from all the other results, the *Tg'* is the same for all the samples but one. $FeSO_4$ 9% 55 shows a higher *Tg'*, and the only possible explanation for this is that, even when all the membranes are equilibrated at the same water content, part of the water in the channel is not available for the sulfonic groups. Hence, the plastification effect is lower in this sample.

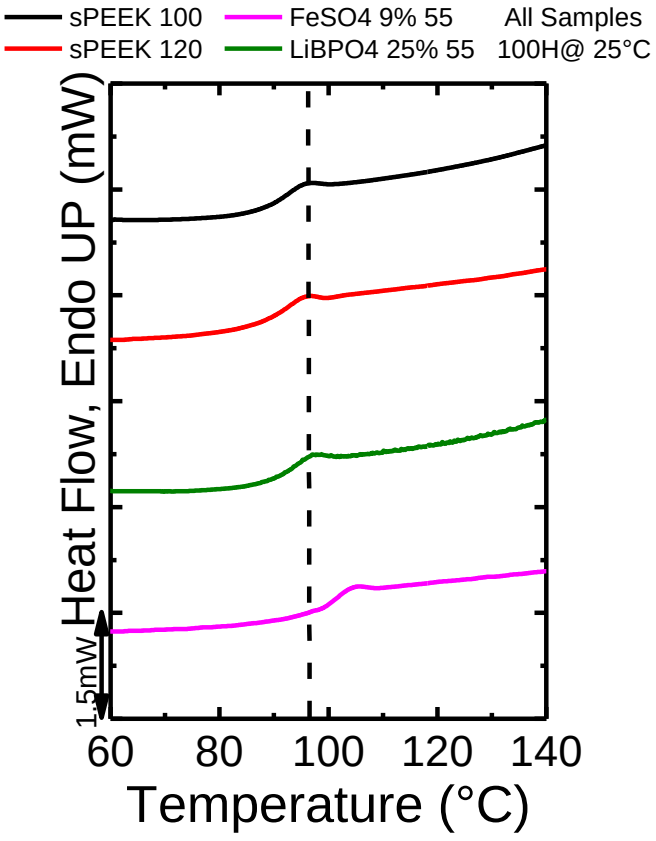

Figure 7.3 *Second heating of dynamic DSC measurement of samples stabilize at 100% RH at 25°C and encapsulated in sealed pans. The runs were performed at 5°C/min.*

The hydrated salts are known for creating stable bonding with water molecules, this is usually refer to as crystal water or hydrated crystals.[9]

Unfortunately, the exact configuration of this water and its accessibility from the surface of the particle is not well known. In order to shed some light over the results we obtained from the different samples using BDS and DSC, schemes of the possible structures we are observing in the measurement, are presented in Figures 7.4 to 7.7.

Figure 7.4 refers to the sPEEK structure explained earlier in Chapter 4. This is the structure left in the material after the thermal treatment and extraction of water. Figure 7.5 was already discussed in Chapter 5, where it was shown that the hydrated structure of the sPEEK has $LiBPO_4$ particles in it. The particles only add water to the channels and do not interact with the sulfonic groups.

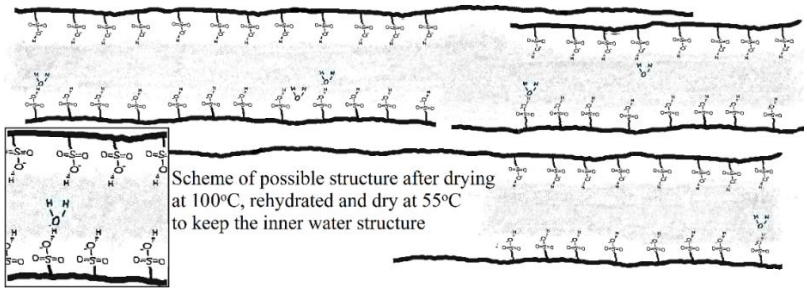

Figure 7.4 *Scheme of the proposed order in the inner phase of the sulfonated clusters of the polymer generated as a consequence of the thermal treatment applied at 100°C for the sPEEK 0.6.*

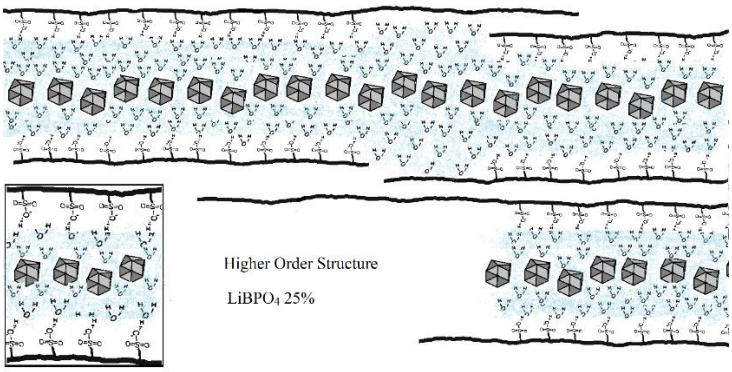

Figure 7.5 *Scheme of proposed model for the sulfonated clusters of the hybrid membrane of $LiBPO_4$ 25% 55 hydrated, there is no interaction of the particles with the sulfonic groups but an increase the water content because of the particles creating a bigger channel for the proton conduction.*

Finally, in Figure 7.6 we show the possible structures of the hydrated salt in the sPEEK channel. Here the particle it not interacting with the sulfonic groups,

and the additional water from the fillers present in the vicinity of the particle are not able to provide accessibility for protons to migrate in the channels. We added one last figure, Figure 7.7, where we depict the hybrid membrane $FeSO_4$ 9% 55, after being dried in a vacuum oven. It shows some water molecules still linked to the filler, which can be the reason for the low intensity in the relaxation at low temperatures.

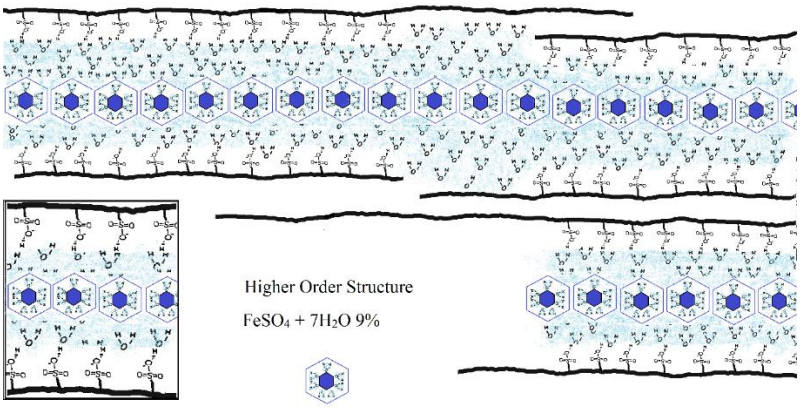

Figure 7.6 *Scheme of proposed model for the sulfonated clusters of the hybrid membrane $FeSO_4$ 9% 55 hydrated, in which there is no interaction between the particles and the sulfonic groups of the sPEEK and the water added from the particle is not available for the protons in the channels.*

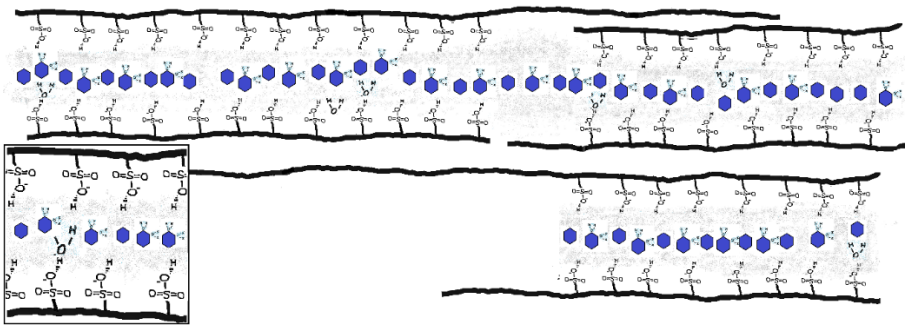

Figure 7.7 *Scheme of proposed model for the sulfonated clusters of the hybrid membrane $FeSO_4$ 9% 55 dried, in which there is no interaction between the particles and the sulfonic groups of the sPEEK and there is water left in the particle since the temperature used to remove it was not high enough. This water can show up in the BDS measurements at high frequencies making relaxations broader.*

7.4. Conclusion

Inorganic fillers are able to supply additional water in the electrolyte membranes used for fuel cells, but the fact that they are able to increase the water content of the membrane does not automatically results in a positive effect on the proton conductivity. BDS and DSC can be used as screening method for studying the interaction of the particle with the membrane and the availability of the water that it is being incorporated in the membrane. The different possible interaction of the particles with acidic groups can also be determined. In the case of $LiBPO_4$ and $FeSO_4$ no interaction with the sulfonic groups in the sPEEK was observed but, the fact that the water in the $FeSO_4$ was bond to the salt, in what is called crystal water, makes it inaccessible for proton conduction in the channels of the membrane, and as a result no increase in the conductivity was observed.

7.5. Bibliography

1 Tripathi, B. P. & Shahi, V. K. Organic–inorganic nanocomposite polymer electrolyte membranes for fuel cell applications. *Progress in Polymer Science* **36**, 945-979, doi:http://dx.doi.org/10.1016/j.progpolymsci.2010.12.005 (2011).

2 Zaidi, S. M. J., Mikhailenko, S. D., Robertson, G. P., Guiver, M. D. & Kaliaguine, S. Proton conducting composite membranes from polyether ether ketone and heteropolyacids for fuel cell applications *Journal of Membrane Science* **173**, 17-34 (2000).

3 Yang, Y., Zhang, H., Wang, P., Zheng, Q. & Li, J. The influence of nano-sized TiO2 fillers on the morphologies and properties of PSF UF membrane. *Journal of Membrane Science* **288**, 231-238, doi:http://dx.doi.org/10.1016/j.memsci.2006.11.019 (2007).

4 Chan, C.-M., Wu, J., Li, J.-X. & Cheung, Y.-K. Polypropylene/calcium carbonate nanocomposites. *Polymer* **43**, 2981-2992, doi:http://dx.doi.org/10.1016/S0032-3861(02)00120-9 (2002).

5 Chung, T.-S., Jiang, L. Y., Li, Y. & Kulprathipanja, S. Mixed matrix membranes (MMMs) comprising organic polymers with dispersed inorganic fillers for gas separation. *Progress in Polymer Science* **32**, 483-507, doi:http://dx.doi.org/10.1016/j.progpolymsci.2007.01.008 (2007).

6 Croce, F. *et al*. Role of the ceramic fillers in enhancing the transport properties of composite polymer electrolytes. *Electrochimica Acta* **46**, 2457-2461, doi:http://dx.doi.org/10.1016/S0013-4686(01)00458-3 (2001).
7 Sun, Y., Zhang, Z., Moon, K.-S. & Wong, C. P. Glass transition and relaxation behavior of epoxy nanocomposites. *Journal of Polymer Science Part B: Polymer Physics* **42**, 3849-3858, doi:10.1002/polb.20251 (2004).
8 Savin, D. A., Pyun, J., Patterson, G. D., Kowalewski, T. & Matyjaszewski, K. Synthesis and characterization of silica-graft-polystyrene hybrid nanoparticles: Effect of constraint on the glass-transition temperature of spherical polymer brushes. *Journal of Polymer Science Part B: Polymer Physics* **40**, 2667-2676, doi:10.1002/polb.10329 (2002).
9 Dunitz, J. D. The entropic cost of bound water in crystal and biomolecules. *Science* **264**, 670 (1994).

Chapter 8 Conclusions and Recommendations

This chapter presents all the conclusions that have been achieved throughout the work described in all the previous chapters. It aims to summarize the importance of the output of this research by presenting a correlation between all of the results obtained, showing how these new insights can help to further develop new hybrid polymer electrolyte, specifically based on sPEEK. In that regard, a set of ideas has also been proposed to get more in depth information related to certain types of behavior that have been observed in our results and the following steps that we believe should be taken.

Conclusions

The design of polymer electrolytes for fuel cells is a complex process. The characteristics of the materials and the variables that could affect the proton conduction were not completely clear at the start of this work and still, at this point, some of them, require further investigation.

Throughout this dissertation, we have investigated and tested variables that are certainly of relevance for the field of PEMFC. Based on the literature research done in chapter 2, we selected some of the methodologies to be used in the production and testing of the new hybrid membranes. The selection of the sPEEK with a 60% sulfonation degree was done based on multiple reported experiments published for degrees of sulfonation that will not affect the mechanical stability of the membrane. After preparation, it was confirmed by multiple thermal characterization methods, that the sulfonation process was successful and the stability of the membrane to temperature was good for values below 230°C. The capacity of the inorganic fillers to take up water above the threshold of 100°C was also confirmed.

At this point, the optimization of the inner structure of the sPEEK membrane was done. To the knowledge of the authors, no publication had address the existence of two glass transition processes occurring in sPEEK and how the lower T_g is the one present during the performance of the membrane under fuel cell conditions. The fact that the water in the membrane completely changes its internal morphology, changing the thermal properties of the matrix and, finally, that this internal morphology also presents an order, which can have a striking effects on the capacity of the membrane for proton conductivity. Our conclusions, after the studies done with DSC, EIS and BDS, are that these channels are of utmost importance for the proton conductivity, as they provide the proton's optimal

migration pathway from the anode to the cathode. To address this, we created a protocol that optimizes the channels in the sulfonated clusters of sPEEK. We also showed that it was possible to optimize these channels, even in the presence of inorganic fillers.

For $LiBPO_4$, we found that the particle was capable of positively affecting the proton conductivity capacity of sPEEK after the hybrid membrane's clusters were optimized via our thermal treatment protocol. The reason behind this improvement, we believe, is that the water present in the $LiBPO_4$ was available for the protons to move through. Because of this and the capacity of this inorganic filler to hold the water above 100°C, we have a high proton conductivity in our hybrid sPEEK/$LiBPO_4$ membranes at 100ºC. The content of $LiBPO_4$ also needed to be optimized, since a high amount can actually aggregate and disrupt the proton conductivity. We have proven that the optimal amount is reached at 25% in weight, for which we found conductivities of 0.1 S/cm at 100ºC and 80% R.H. (Nafion® shows a similar value under the same conditions). A major advantage of this membrane relies on the fact that the production of sPEEK and $LiBPO_4$ can be easily scaled to commercial production at low cost.

We demonstrated that inorganic fillers have a clear effect on the behavior of the material; this was based on particular interactions that depends on the filler. On one side, because they can increase the water content in the membrane, so you can have a change in the water uptake. Nevertheless, this does not mean that this water will be available for the protons to move. The nature of the interaction of the acidic groups with the inorganic particles is also important. These particles can block your acidic groups, diminishing the capability of water protonation. We showed this through DSC and BDS. It is clear that with the help of thermal treatments and different sample preparation, it is possible to achieve a better understanding of how the fillers interact with the polymer and what the nature of the water in the fillers is. For our studies, we used $FeSO_4$.7H2O and DND failure to increase conductivity and, $LiBPO_4$ success, as examples of how the aggregated

water and the particles interactions with the matrix have a major effect on the conductivity.

As our global conclusion, we would like to state that there are three main factors affecting the proton conductivity in a PEM:

- The order in the inner phase of the membrane needs to be optimized
- The water in the membrane needs to be enough
- The acidic groups in the polymer need to be able to protonate the water and make it a fast medium to move the positive charges.

These three main factors need to be tuned for every specific membrane that one wants to evaluate for use in a PEMFC. We propose and prove mechanisms in this research to tackle these three factors and address how to optimize them.

Finally, based on these conclusions we can state that the main objective of our research, the development of a new hybrid membrane, able to show a good proton conduction at 100°C, and viable for commercial upscaling, was accomplished for one of our selected materials.

We learned that the internal structure, present in the sPEEK, has a significant influence in the proton conductivity and found ways to improve it. This gave us and in deep understanding of the transitions of the material and the conditions under which, the sPEEK, operates inside a fuel cell. We discovered that the water added by inorganic fillers was not always available for the protons to move, and that the nature of the interactions of the fillers with the sulfonic groups were of high importance for the proton conductivity of the membrane.

Recommendations

Among the results we obtained, many things still need further analysis. We found a peculiar behavior in how the conductivity changes, as temperature rises, for all the samples that have passed through the thermal treatment. This behavior

can be related to the formation of specific clusters in the material at low temperature and humidity. This has been reported earlier to occur in sPEEK. In order to get a better insight in the internal structure, it would be necessary to run SANS/SAXS experiments on the samples, preferably in-situ.

Our measurements of the conductivity in the membranes were done under equilibrated conditions that mimic the actual fuel cell operation system in terms of heat and relative humidity. Still there are many characteristics related to this fuel cell operational process that are not being taken into account, such as pressure, electrode interface interactions, and life cycle of the membrane. These tests needs to be performed before introducing these novel membranes into commercial systems.

It was proven that BDS and DSC could help to determine the interactions of the particles with the polymers. This could be useful for other particles and other hybrid membranes. These interactions need to be better understood in order to be able to design new materials for electrolytes in all sorts of electrochemical devices.

Acknowledgments

In first place, I will like to thank my Promotor and Co-Promotor, Prof. Stephen Pickens and Dr. Erik Kelder, TUDelft and ADEM for giving me the opportunity of coming to the Netherlands for Venezuela and do my PhD in here. It has been a very challenging experience for me. We have been through many different situations but I have always felt your support.

Forward on, I will write my acknowledgments in Spanish since I will be addressing my family and friends.

Quiero agradecer a mi familia, a mi mamá y mi papá y a mi hermano por siempre apoyarme en todos mis proyectos. Desde que decidí empezar mis estudios de pregrado en la USB, mi master y luego venirme, lejos de ellos, a hacer mi PhD y mi vida al otro lado del charco. ¡Muchas gracias por siempre estar ahí, muchas gracias por siempre apoyarme! Los quiero mucho y siempre los tengo presentes.

Quiero agradecer a todos los amigos que hice en Delft y Rotterdam durante mi PhD. Empezando por Corrado y Esteban, las dos primeras personas que conocí al llegar a Holanda y los que me recibieron. Siempre recordare con cariño la oficina con Corrado, Esteban, David, Raphael y Julien. Ustedes hicieron mucho más fácil mi llegada a un país nuevo y a una vida nueva. Luego están todas las personas con las que salimos a pasar noches en Doerak y en Klooster, con las que fui a festivales y fiestas. Carolina, Nataly, Stefania, Damian, Miguel, Maria, Alicia (Soler), Alicia (Tang), a todos los demás que nos veíamos en tango algunas noches, a mis amigos de Griekse Olijf, a todos ustedes les debo que mi vida no fuera aburrida y solitaria en Delft. Mantengo todavía amistad con muchos de ustedes, aunque nos veamos de vez en cuando, siempre me siento como si nos hubiéramos tomado una cerveza el día anterior. ¡Muchas gracias! Here, i will make a small exception to mencion a friend that i made on DSM, and that also help me during my time there as well as with the translations to dutch needed for my thesis. Thanks a lot Lilian! You have been a very helpful and good friend in Chemelot and Resolve!

Quiero agradecerles a mis grandes amigas de la vida, a esas personas que llevan tanto tiempo en vida que ya son familia y que de una u otra forma siempre estamos ahí el uno para el otro. Melina, eres mi amiga más antigua, siempre hemos estado presentes, aunque ha habido mucho tiempo a la distancia… ¡Gracias! ¡Te quiero muchísimo!

Marcelia, tu especialmente has sido muchas cosas en mi vida en el tiempo que nos conocemos. Siempre hemos y estaremos ahí el uno para el otro. Esa promesa nunca la romperé, a pesar de haber tenido momentos difíciles nunca nos hemos fallado. Tu eres una de las cosas en mi vida de la cual siempre me puedo sentir seguro que tengo. ¡Te qui!

Por último, hay una persona que, aunque no lleva la misma cantidad de tiempo que las otras en mi vida, la ha impactado más allá de lo que yo podía imaginar. Camila, eres mi novia y mi amiga, mi roommate, eres mi confidente y mi apoyo, eres mi familia en Holanda y eso no tengo forma de agradecerlo. Espero que tu sientas eso mismo por mí, ¡te amo muchísimo!!!

Quiero hacer una mención especial a Nella, sin ella yo creo que esta tesis no hubiera sido posible. Eres una persona inmensa Nella, me apoyaste, me ayudaste, me enseñas, tuviste la paciencia de sufrir conmigo en la parte más importante de mi PhD y eso nunca lo voy a olvidar. Muchas gracias Nella y aunque yo sea muy **darks**, te lo digo nuevamente, ¡Te quiero! ¡Hay una mención especial a Alfredo por prestarnos a Nella en Holanda por casi 3 años!

Solo puedo terminar agradeciéndole a todos los demás que pasaron por mi vida, de una u otra forma durante mi doctorado y ahora mi trabajo en Holanda. Esta se ha vuelto una experiencia increíble en mi vida gracias a ustedes también y aunque, por alguna razón, ya no estemos en contacto o no nos veamos seguido, igual quiero que sepan que agradezco mucho haberlos conocido. Termino con una frase, para no perder la costumbre.

"Al andar se hace camino y al volver la vista atrás, se ve la senda que nunca se ha de volver a pisar…
Caminante no hay camino, se hace camino al andar"

"Cantares" - Joan Manuel Serrat

Curriculum Vitae

Miguel E. Córdova-Chávez was born in Caracas, Venezuela, did his Bachelor degree in Caracas, at Simon Bolivar University, in Material Science Engineering - Polymer technology and physics. After, he did a Master degree in Material Science – Polymer Characterization in the same university, working on physical properties of polymers. During the Master degree, he worked for the Simon Bolivar University as a Research Assistance and Teaching Assistance and did an internship for 4 months in Nottingham University, working on rheology and morphology of Block Copolymer's blends, as part of a Royal Society project.

He move to the Netherlands at the end of 2011 to start his PhD on Polymer Electrolyte Membranes for fuel cells. In 2015 he started working for TMC, doing a project at DSM Resolve as a Thermal Analysis Scientist, for 1 year and 8 months. At this moment, He is doing another project at Sabic, as a Thermal Analysis and Material Scientist, focus on the Properties-Structure relationship of Polyolefins.

Publication List

- ***Miguel Córdova***, *Arnaldo Lorenzo, Alejandro J. Müller, Paganiota Fragouli, Hermis Iatrou, Nikos Hadjicritidis, "Crystallization and physical ageing of Poly(2-vinyl pyridine)-b-poly(ethylene oxide) diblock copolymers, Macromol. Symp., 2010, 287, p. 101-106.*
- ***Miguel E. Córdova**, Arnaldo T. Lorenzo, Alejandro J. Müller, Léa Gani, Sylvie Tencé-Girault, Ludwik Leibler, "The Influence of Blend Morphology (Co-Continuous or Sub-Micrometer Droplets Dispersions) on the Nucleation and Crystallization Kinetics of Double Crystalline Polyethylene/Polyamide Blends Prepared by Reactive Extrusion", Macro. Chem. Phys., 2011, 212, p. 1335-1350* ***(Selected as the Issue Cover)**.*
- ***Miguel E. Córdova**, Arnaldo T. Lorenzo, Alejandro J. Müller, Jessica N. Hoskins, Scott M. Grayson, "A Comparative Study on the Crystallization Behavior of Analogous Linear and Cyclic Poly(ε-caprolactones)" Macromolecules (Comm. To Ed.), 2011, 44, p. 1742-1746.*
- *María Teresa Casas, Jordi Puiggalí, Jean-Marie Raquez, Philippe Dubois,* ***Miguel E. Córdova**, Alejandro J. Müller, "Single crystals morphology of biodegradable double crystalline PLLA-b-PCL diblock copolymers", Polymer, 2011, 52, p. 5166-5177.*
- *R.A. Pérez,* ***M.E. Córdova**, J.V. López, J.N. Hoskins, B. Zhang, S.M. Grayson, A.J. Müller, "Nucleation, crystallization, self-nucleation and thermal fractionation of cyclic and linear poly(ε-caprolactone)s", Reactive and Functional Polymers, Volume 80, July 2014, Pages 71–82.*
- ***M.E. Cordova-Chavez**, M. Hernandez, S. J. Pickens, E. M. Kelder, "Optimization of proton conducting sPEEK membranes through a thermal treatment methodology monitored by dielectric spectroscopy" Manuscript to be submitted.*
- ***M.E. Cordova-Chavez** , S. J. Pickens, E. M. Kelder, "Fabrication and Characterization of High Conductivity Membranes of sPEEK 0.6/$LiBPO_4$ for Fuel Cells Working at 100°C" Manuscript to be submitted.*
- ***M.E. Cordova-Chavez** , S. J. Pickens, E. M. Kelder, "DSC and BDS Used as a Tool to Identify the Interaction Nature and Effects of Inorganic Fillers on Sulfonated Polymer Matrix" Manuscript in preparation.*